Winter 1-1-2012

Hydrodynamics, Mixing, and Mass Transfer in Bubble Columns with Internals

Mohamed Hamed
Washington University in St. Louis

WASHINGTON UNIVERSITY IN ST. LOUIS

School of Engineering and Applied Science

Department of Energy, Environmental, and Chemical Engineering

Dissertation Examination Committee:

Milorad Duduković, Chair
Muthanna Al-Dahhan, Co-chair
Pratim Biswas
Berthold Breman
Guy Genin
Cynthia Lo
Palghat Ramachandran

Hydrodynamics, Mixing, and Mass Transfer in Bubble Columns with Internals

by

Mohamed Hamed

A dissertation presented to the Graduate School of Arts and Sciences of Washington University in partial fulfillment of the requirements for the degree of

Doctor of Philosophy

December 2012

Saint Louis, Missouri

Table of Contents

List of Tables

List of Figures

Nomenclature

a	Specific interfacial area, cm^2/cm^3
C	Phase concentration, mol/cm^3
C_D	Drag coefficient, -
C_{inj}	Gas tracer injection concentration, mol/cm^3
c'	Fluctuating concentration, mol/cm^3
c	Parameter in the hold-up profile to allow non-zero hold-up at the wall
D	Column diameter, cm
D_{Free}	Modified column diameter in the presence of internals, cm
D_g	Axial dispersion coefficient of the gas phase, cm^2/s
D_L	Axial dispersion coefficient of the liquid phase, cm^2/s
D_m	Molecular diffusivity, cm^2/s
D_{rr}	Local radial turbulent diffusivity, cm^2/s
$\overline{D_{rr}}$	Cross-sectional averaged radial turbulent diffusivity, cm^2/s
D_{zz}	Local axial turbulent diffusivity, cm^2/s
$\overline{D_{zz}}$	Cross-sectional averaged axial turbulent diffusivity, cm^2/s
$\overline{D_{Tylor}}$	Cross-sectional averaged Taylor-type diffusivity, cm^2/s
d_b	Mean bubble size, cm
d_t	Tube diameter, cm
$\boldsymbol{g}$	Gravitational acceleration, cm^2/s
H	Henry's constant, -
H_D	Dynamic liquid height, cm
H_S	Static liquid height, cm
k	Radial exchange term, cm^2/s
k_L	Gas-Liquid side mass transfer coefficient, cm/s
k_La	Overall volumetric mass transfer coefficient, s^{-1}
K_T	Empirical constant
L	Dynamic liquid height, cm
ℓ	Mixing length, cm (Chapter 3)
$\bar{l}$	Cross-sectional averaged mixing length, cm (Chapter 4)

$\overline{l_{eddy}}$	Mean eddy size
m	Power law exponent in the radial gas holdup profile
n_t	Number of internals
OA	Fraction of the area occupied by internals
Pe	Péclet number, -
P	Pressure, dyne/cm^2
R	Column radius, cm
Re	Reynolds number,-
r	Radial coordinate, cm
S	Surface renewal rate, 1/s
t	Time coordinate, s
t_e	Exposure time, s
u	Phase velocity vector, cm/s
u	Local phase velocity, cm/s
u_b	Bubble rise velocity, cm/s
u'	Local fluctuating phase velocity, cm/s
U_g	Superficial gas velocity based on the free cross-sectional area of the column, cm/s
U_L	Superficial liquid velocity based on the free cross-sectional area of the column, cm/s
$\sqrt{\overline{u'^2}}$	Root mean square of fluctuating phase velocity, cm/s
z	Axial coordinate, cm

Greek symbols

ρ	Phase density, g/cm^3
ε_g	Overall gas holdup,-
$\varepsilon_g(r)$	Local gas holdup,-
$\widetilde{\varepsilon_g}$	Parameter used in the gas holdup profile
ε_L	Overall Liquid holdup
ϵ	Energy dissipation rate, cm^2/s^3
ξ	Dimensionless radius (r/R)

τ^m	Molecular shear stress, dyne/cm^2
τ^t	Turbulent shear stress, dyne/cm^2
τ_P	Residence time of the gas phase in the plenum, s
μ^m	Molecular dynamic viscosity, cP
μ^t	Turbulent dynamic viscosity, cP
v^m	Molecular kinematic viscosity, cm^2/s
v^t	Turbulent kinematic viscosity, cm^2/s
λ	dimensionless radial position at which the downward liquid velocity is maximum
Γ	Source term in the convection-diffusion equation

Subscripts

CM	Cup Mixing Average
g	Gas phase
(i)~(iv)	Measurement in the gaseous tracer technique
in	Reactor inlet
L	Liquid phase
m	Ensemble-averaged
out	Reactor outlet
P	Plenum
r	Radial
rec	Recirculation
s	Slip
z	Axial

List of Abbreviations

1-D	One Dimensional
2-D	Two Dimensional
3-D	Three Dimensional
ADM	Axial Dispersion Model
BTL	Biomass To Liquid
CARPT	Computer Automated Radioactive Particle Tracking
CFD	Computational Fluid Dynamics
CSTR	Continuous Stirred Tank Reactor
CT	Computed tomography
CTL	Goal To Liquid
CSA	Cross-Sectional Area
DO	Dissolved Oxygen
EXP	Experimental data
GTL	Gas-To-Liquid
F-T	Fischer-Tropsch
LES	Large Eddy Simulations
PFR	Plug-Flow reactor
PIV	Particle Image Velocimetry
RTD	Residence Time Distribution
TCD	Thermal Conductivity Detector
WUSTL	Washington University in Saint Louis

Acknowledgments

First and Foremost, Thanks and praises to GOD for his Kindness and Blessing. Thanks for giving me Faith to believe in myself and guidance to overcome my weakness. Thanks for granting me patience through the hard times and thankfulness through the good times.

I wish to express my deep gratitude and thanks to my advisors Prof. M. Duduković and Prof. M. AL-Dahhan. Prof. Al-Dahhan was the first one to introduce me to WUSTL and to encourage me to pursue my Ph.D. at this great University. His ideas and enthusiasm have always inspired me to solve critical issues in my research and overcome many experimental obstacles and his critical review of my work greatly improved my skills. His technical and non-technical advice was invaluable to me in my professional and personal life. I also would like to thank him for helping me to attend different conferences from which I gained valuable experience.

Prof. Dudukovic has restructured my approach towards solving research problems in a more scientific way. His critical comments and suggestion added more insight and better perspectives to this work. His efforts in organizing regular meeting with my sponsors and ensuring the extension of my fund were the main reasons this work continued in an efficient and convenient manner. I want to thank him not only for advising me on my research work, but also for teaching me discipline, believing in my ideas, and sincerely advising me on my future professional life.

I want to extend my thanks to all my committee members. Prof. P. Ramachandran introduced me to the world of multi-phase systems in his transport phenomena course and has always provided enlightening ideas and suggestions during my CREL meeting presentations. Dr. Breman gave me a rare experience to get the industrial perspective on my work and pointed out several interesting papers and Thesis to read which opened my mind to new horizons and aspects of the hydrodynamics and mixing in bubble columns. His insightful questions and comments always encouraged me to develop a better understanding of the topic of my research. Prof. Biswas has provided very critical comments in my proposal regarding the internals' design, which brought up new perspectives to this work. I

also would like to thank him for the great help he offered as the department chair during the transfer of Prof. AL-Dahhan to ensure a smooth transition for me and for the efforts he made to secure my fund until my graduation. Prof. Genin brought-up helpful fundamental questions during my proposal which I seriously considered later in my work. In addition, he provided corrections to some of the historical misconceptions regarding the F-T process. Prof. Lo has added some nice aspects to the overall F-T process in bubble columns through our discussions during my proposal. Again, I thank them all for their time and for serving on my committee.

As I am writing this acknowledgement, I am finally seeing the result of the hard work I did during the peak years of my youth and also feel a great sense of gratitude to all those who have influenced it during these years. The first of those who supported and helped me along my journey is my lab-mate, college-mate, basketball-mate, room-mate, and my lifetime friend Dr. Ahmed Youssef. On the technical side, he taught me all the experimental aspects of operating bubble columns since day-1 in my research; he showed me how to construct and operate the 4-point optical probe; he constructed several probes for me during my experiments, and he advised me on many issues regarding my research. The discussions we had on different scientific matters, his encouragement for me since my first year in college back in Egypt, his sincere help in the courses I took during my first year at WUSTL were invaluable and unforgettable. On the social side, he greatly facilitated my move to USA and had been always there for me in different matters. He truly made my life during my Ph.D journey much more convenient and fun. For all that, and much more, THANKS Ahmed!

This work would have not been possible without the continuous financial support of the Bubble Column Consortium [Eni, Italy; Sasol, South Africa; Statoil, Norway; and Johnson-Matthey, UK]. I would like to extend my thanks to Dr. Gary Combes of Johnson-Matthey, Nicola Manchini and Fabrizio Bondenzani of Eni, Dag Schanke of Stat-Oil, and Dr. Breman of Sasol for their comments and suggestions that added value to this work and provided me with the needed industrial perspective on different parts of my research.

I wish to express my deep gratitude to Dr. S. Mohedas and Dr. R. Lemoine of Rentech for the chance they gave me to work on the modeling of a pilot scale slurry bubble column. The 4-month-internship I had at Rentech broadened my industrial experience and introduced me to many new aspects of the F-T process and bubble column operation. Thanks to Dr. R. Lemoine for introducing me to Aspen Custom Modeler program and for the long interesting discussion we had on the modeling of bubble columns.

I am proud to be a part of the Chemical Reaction Engineering Laboratory (CREL) and to have contributed to adding to the literature of this great Lab. Being a part of this lab has helped me enhance my skills in many different ways. The annual CREL report helped me to enhance my writing and team work skills. The weekly CREL meetings and the annual CREL meeting were challenging opportunities which greatly improved my presentation skills. I am thankful for all my CREL mates; Dan Combest, Evgieny Redekop, Mehmet Morali, and Vesna Havran for all the enjoyable discussions we had on different scientific and non-scientific issues. Thanks for sharing with me the best time of my day, the half-an-hour-mid-day coffee break which keeps us working until late night. Special thanks to Mehmet Morali for the long enlightening discussions we had on bubble columns and for introducing me to the gas tracer technique which I used later in my work, and to Dr. Dan Combest for validating my 2-D model using OpenFoam. I am deeply grateful for all the previous CREL students who worked on bubble columns especially, Dr. S. Kumar, Dr. S. Degaleesan, Dr. J. Chen, Dr. P. Gupta, Dr. J. Xue, Dr. B. Ong, Dr. L. Han, and Dr. A. Youssef. Although I never personally met them, but the efforts, ideas, and recommendations they provided in their Theses greatly helped me to further develop my work. Thanks for all the senior CREL students; Dr. R. Varma, Dr. R. Jevtic, Dr. S. Nayak, Dr. Z. Kuzeljevic, Dr. S. Mueller, and Dr. B. Henriques for all the nice time we spent together and for the great example they set for me to follow.

I want to extend my thanks to Rose Baxter, our Energy, Environmental, and Chemical Engineering Department secretary. Her timely responses to all my questions and emails resolved all my paper-work issues. Thank you Rose for all that, and for being so friendly and calm whenever I approach you with any concerns. I am very thankful for the Technical

writing center for reviewing my manuscripts and presentations. Special thanks to Seema Dahlheimer for all the time she spent with me to review my Thesis. Thanks for WUSTL libraries for bringing me all the references that I needed in a timely manner.

Warm and special thanks are due to my family: Dr. Ezzat, Dr. Azza, Yosra, and Tarek for their emotional support and encouragement throughout the years. Thanks for all their calls and visits that inspired and motivated me to carry on. Finally, thanks to my lovely wife, Nihal, who stood by my side during the ups and downs, for believing in me and for supporting my ideas and dreams. She was always the breath of fresh air that sailed me through my long Ph.D. Journey.

As I leave WUSTL, I hope I left good memory and I have transferred some knowledge to my successors, so they shall create new knowledge.

"If anyone travels on a road in search of knowledge, God will cause him to travel on one of the roads of Paradise. The angels will lower their wings in their great pleasure with one who seeks knowledge. The inhabitants of the heavens and the Earth and (even) the fish in the deep waters will ask forgiveness for the learned man. The superiority of the learned over the devout is like that of the moon, on the night when it is full, over the rest of the stars. The learned are the heirs of the Prophets, and the Prophets leave no monetary inheritance, they leave only knowledge, and he who takes it takes an abundant portion". Prophet Muhammad Peace be upon Him.

Mohamed Hamed

Washington University in St. Louis

December 2012

To Dad, Mom, Sis, Bro, Son, and Soul-mate

ABSTRACT OF THE DISSERTATION

Hydrodynamics, Mixing, and Mass Transfer in Bubble Columns with Internals

by

Mohamed Hamed

Doctor of Philosophy in Energy, Environmental and Chemical Engineering

Washington University in St. Louis, 2012

Bubble columns and slurry bubble columns are considered reactors of choice for a wide range of applications in the chemical, biochemical, and petrochemical industries. Most of the chemical applications of bubble columns include exothermic processes and hence they require some means of heat removal to maintain a steady process. The most practical means for heat removal in these reactors is the utilization of vertical cooling internals since they provide high heat transfer area per reactor volume. However, the effects of these internals on the reactor performance are poorly understood in the open literature. This causes the design of the internals to be based on empirical rules not on the applications of fundamentals.

The main objective of this study is to enhance the understanding of the effects of vertical cooling internals on the gas hydrodynamics, gas mixing, and mass transfer. In addition, this study attempts to develop and validate models that can simulate the radial gas velocity profile and axial gas mixing in the presence and absence of internals. Finally, this work aims to validate all the observed experimental results and models in larger columns with and without internals to have a better understanding of the scale-up effects in the presence of internals. This is accomplished by carrying out experiments in a lab-scale 8-inch bubble column and a pilot-scale 18-inch bubble column in the absence and presence of internals. The studied % occluded area by internals (~ 25%) is chosen to match the % occluded area used in the Fischer-Tropsch synthesis. The radial gas velocity profiles are measured using the 4-point optical probe and are used to validate the 1-D gas velocity model developed by Gupta (2002). Gar tracer techniques are used to study the effect of internals on the

overall axial gas mixing and mass transfer. A 2-D model, that considers the radial variations of the gas velocity and gas holdup, is developed and used to analyze the tracer data allowing the estimation of the turbulent diffusivities of the gas phase. The 2-D model along with the axial dispersion coefficient model developed by Degaleesan and Dudukovic (1998) are used to determine the contribution of different mixing mechanisms to the overall axial gas mixing.

The main findings of the current work can be summarized as follows:

- The effect of internals and column diameter on the gas velocity profile, gas mixing, and mass transfer is assessed. The presence of internals causes:
    - An increase in the center-line gas velocity.
    - A significant decrease in axial gas mixing.
    - A decrease in the gas-liquid mass transfer coefficient.
- The increase in column diameter causes:
    - Enhancement of the gas circulation.
    - An increase in axial gas mixing.
- The model developed by Gupta (2002) to predict radial gas velocity profiles is validated at different operating conditions in the presence and absence of internals.
- A 2-D convection-diffusion model is developed and proven useful in interpreting gas tracer data and simulating the overall axial gas mixing in the presence and absence of internals.

Chapter 1 - Introduction and Objectives

Bubble columns and slurry bubble columns are multiphase reactors in which gas is introduced via a sparger into a liquid or slurry contained in a vertical cylindrical column. Usually there are one or more reactants in the gas phase, while products and/or additional reactants are in the liquid phase. In slurry bubble columns, solids are typically fine catalyst particles. A schematic diagram of a typical slurry bubble column is shown in Figure 1.1. Bubble columns offer numerous advantages such as good heat and mass transfer characteristics, absence of moving parts and thus reduced wear and tear, ease of operation, and low operating and maintenance cost. However, there are considerable issues associated with their proper design and scale-up. This is due to the complexity of the flow structure inside these reactors and the intense operating conditions needed to achieve high productivity.

Three types of flow patterns have been observed in bubble columns: homogeneous (bubbly), heterogeneous (churn-turbulent), and slug flow. Researchers have reported the occurrence of a slug flow regime only in small diameter columns. Depending on the operating conditions, the homogeneous and heterogeneous regimes can be separated by a transition regime. The homogeneous flow regime generally occurs at low to moderate superficial gas velocities. It is characterized by the presence of uniformly sized small bubbles traveling vertically with minor transverse and axial oscillations. There is practically no coalescence and break-up between the bubbles, resulting in a narrow bubble size distribution. The gas holdup distribution is radially uniform, and the size of the bubbles depends mainly on the nature of the gas distribution and the physical properties of the liquid and gas phases. Heterogeneous flow occurs at high superficial gas velocities. The formation of larger bubbles traveling at high velocities enhances the rate of bubble coalescence and break-up, resulting in a wide bubble size distribution and a non-uniform gas holdup profile. This consequently leads to bulk gas and liquid circulation, where the large bubbles churn through the liquid in the column center, while small bubbles circulate with the liquid in the wall region. Homogeneous and heterogeneous flow regimes have entirely different hydrodynamic characteristics, which result in different mixing as well as heat and mass transfer rates. In

bubble columns applications that require high volumetric productivities, the operation is most often in the heterogeneous regime.

Bubble column reactors have been used in the chemical, petrochemical, biochemical, and pharmaceutical industries for various processes (Carra and Morbidelli, 1987, Deckwer, 1992, and Fan, 1989). Examples of such chemical and petrochemical processes are the partial oxidation of ethylene to acetaldehyde, wet-air oxidation (Deckwer, 1992), liquid phase methanol synthesis (LPMeOH), Fischer-Tropsch (F-T) synthesis (Wender, 1996), and hydrogenation of maleic acid (MAC). In the biochemical industry, bubble columns are used for cultivation of bacteria, cultivation of mold fungi, production of single-cell proteins, animal cell culture (Lehmann et al., 1978), and treatment of sewage (Diesterweg, 1978). In the metallurgical industry, they can be used for leaching of ores.

1.1 Bubble Columns and the Energy Problem

The Gas-to-Liquid (GTL) technology is considered one of the most promising solutions to the current energy problem. This technology is based on the generation of liquid fuels from synthetic gas using the F-T process as follows:

$$CO + H_2 \rightarrow -CH_2 - + H_2O. \tag{1.1}$$

The primary reaction, which is highly exothermic, involves contacting a mixture of carbon monoxide and hydrogen (syngas) over fine solid catalysts to produce hydrocarbons and water. The F-T process typically produces sulfur-free and aromatic-free liquid fuels, and can use many different sources to produce syngas, including natural gas, coal, and agricultural wastes. Since Franz Fischer and Hans Tropsch invented the original F-T process for GTL conversion, many refinements and adjustments have been made. Currently, the abundant reserves of coal, the uncommitted reserves of natural gas, and the renewable resources of biogas and biomass are the three major syngas sources. Their conversion processes to liquid fuels are called CTL (Coal-to-Liquid), GTL, and BTL (Biomass-to-Liquid), respectively.

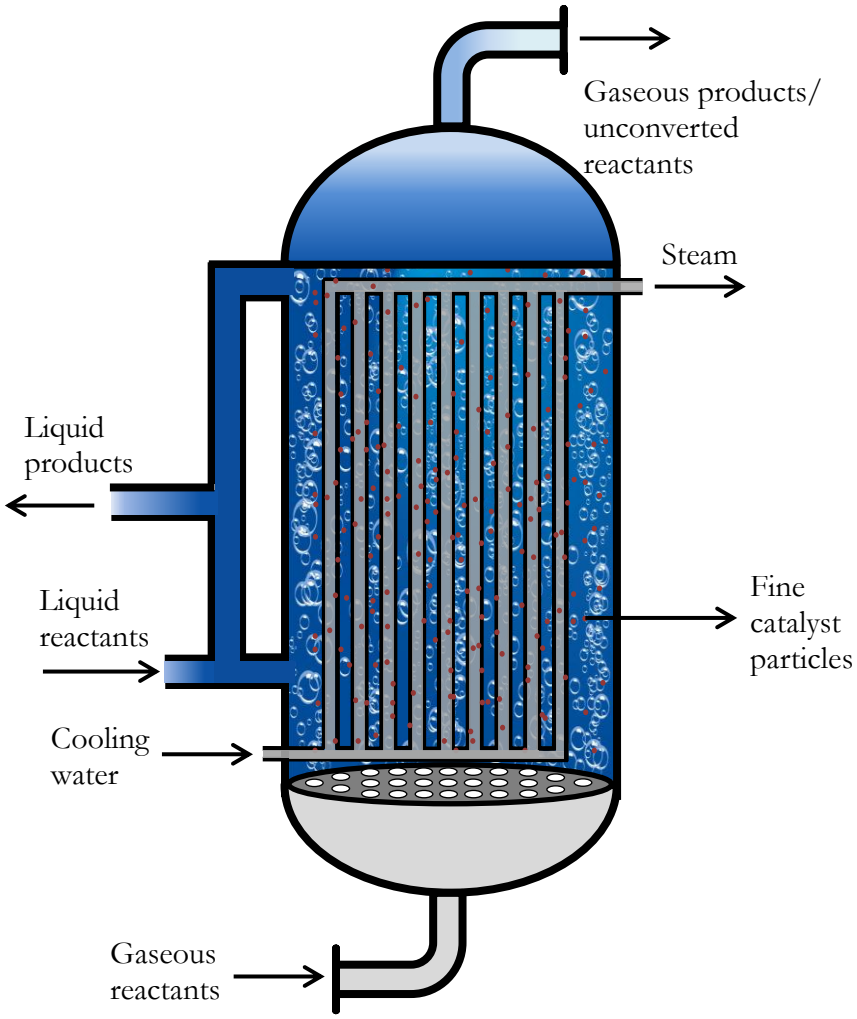

Figure 1.1 - A schematic diagram of a slurry bubble column with internals

Bubble columns are considered the reactors of choice for the F-T process. In the last 30 years, there have been major accomplishments in expanding the operation of the F-T process to a commercial scale by different companies like Sasol, PetroSA, and Shell. However, there are still considerable reactor design and scale-up issues associated with such energy conversion processes in bubble columns. The successful commercialization of bubble column reactors is crucially dependent on the proper understanding of their hydrodynamics and scale-up principles.

1.2 Internals for Heat Removal

Most applications of bubble columns, as shown in Table 1.1, include exothermic chemical reactions which require some means of heat removal in order to maintain a steady process.

In some bubble column applications like F-T synthesis, it is essential to control the temperature profile within the column since it significantly affects reaction selectivity. In addition, maintaining a rather uniform temperature distribution is crucial to prevent over-heating of the catalyst. These are considered central issues in the design and safe operation of commercial-scale slurry bubble column reactors. These considerations become more critical for highly exothermic processes such as the F-T synthesis.

Table 1.1 - Applications of Bubble Columns

Products	Feed	ΔHr, kJ/mol	Temperature, °C
Acetaldehyde	Ethylene, Oxygen	-243.00	120-130
Acetone	Propene, Oxygen	-255.00	110-120
Ethyl Benzene	Benzene, ethylene	-113.00	125-140
Benzoic Acid	Toluene, Air (or Oxygen)	-628.00	110-120
n-, iso-butyraldehyde	Propene, Hydrogen, Oxygen	0.80	90-120
Cumene	Benzene, Propene	-113.00	35-70
Cyclohexane	Benzene, Hydrogen	-214.00	200-225
Cyclohexanol, Cyclohexanone	Cyclohexane, Air	-294.00	125-165
1,2 - Dichloroethane	Ethylene, Chlorine, Oxygen	-239.00	170-185
Acetic Acid	Acetaldehyde, Oxygen	-294.00	50-70
Acetic Acid, Methyl ethyl ketone	n-Butane, Air	-1270.00	180.00
Vinyl Acetate	Ethylene, Ethyl Acid, Oxygen	-176.00	110-130
Wet air oxidation of sewage sludge	Sewage sludge, air	-435.00	200-300
Fischer-Tropsch synthesis	Hydrogen, Carbon Monoxide	-210.00	250-290
Methanol synthesis	Hydrogen, Carbon Monoxide	-91.00	220-270

Different methods can be used for heat removal in bubble columns, including direct heat transfer, indirect heat transfer through the reactor wall or cooling internal installations, and indirect heat transfer through an external heat exchanger (Steiff and Weinspach, 1978). Cooling internals provide a practical means for heat removal in slurry bubble columns, since they eliminate the need to use external heat exchangers or expensive slurry pumps.

Generally, bubble column reactors can be equipped with two types of internals: horizontal internals, such as perforated plates (trays) or horizontal tube bundles, and vertical internals. Horizontal internals are usually used to control the flow behavior to achieve higher productivities, since their insertion reduces the overall liquid back-mixing (Westerterpet al, 1987, Mashelkar, 1970, Palaskar et. al., 2000, Nosier, 2003, and Alvaré and Al-Dahhan, 2006). In addition, the presence of horizontal internals increases mass transfer (Kawasaki,

1994) due to the decrease in the average bubble size caused by enhanced bubble break-up. Vertical internals are preferred as means of heat removal because they provide higher heat transfer area per reactor volume.

Unfortunately, the design of vertical internals is still based on strictly protected proprietary know-how which embodies empirical rules, not on application of fundamentals. To date, no systematic method has been reported which dictates how to choose different parameters involved in designing vertical heat internals in bubble columns. Despite the lack of systematic studies on internals, some guidelines regarding their design can be extracted from the pieces of information currently available in the literature. In what follows, these guidelines will be summarized. The design of internals requires the choice of three main parameters:

1. Tube diameter.
2. Tube configuration (including geometrical configuration, pitch, and inter-tube gap).
3. The ratio of occluded cross-sectional area (CSA) by internals (total CSA of internals/CSA of reactor).

Generally, the tube diameter and the number of tubes are determined by an iterative procedure to optimize the conversion and selectivity of the desired process. Typically, commercial F-T bubble columns have tubes which are 3-5 inches in diameter (Hawthorne et al., 2006). The choice of the number of tubes and tube diameter is usually governed by:

- The exothermicity of the process, which determines the rate of heat generation.
- The desired volumetric productivity.
- The heat transfer characteristics of the process (overall heat transfer coefficient), which dictates the needed surface area.
- The reactor diameter.
- The percentage covered CSA with internals, which should be chosen based on the required hydrodynamic, mixing, and thermal characteristics of the flow.

Based on the experimental data in the available literature, the geometric configuration of internals does not seem to affect the gas holdup. Yamashita (1987) and Youssef (2010) showed that the overall gas holdup was not affected by the geometric configurations of internals for bubble columns operating in the churn turbulent regime. In addition, Youssef

(2010) showed that the percentage occluded CSA by internals is the major parameter that characterizes the internals' effect, and he claimed that, for a fixed percentage of occluded CSA by internals, the choice of the geometrical configuration is a matter of convenience, as long as internals are evenly distributed across the column cross section.

The knowledge of the effect of the occluded CSA by internals is crucial to the process of designing internals. Therefore, this work will concentrate on quantifying the effect of internals using the occluded column CSA as a parameter. One of the main goals of this work is to provide experimental information and models that, along with the work of previous researchers, will enhance the fundamental understanding of the effect of the internals occluded CSA on the hydrodynamics, mixing, and mass transfer in bubble columns. Ultimately, this will provide a more scientific approach to the design of internals and a better prediction of the performance of bubble columns equipped with internals.

1.3 Motivation

Despite the potential applications for bubble columns equipped with internals, there is a lack of qualitative and quantitative understanding of the effect of these internals on hydrodynamics, mixing, and mass and heat transfer in bubble columns at different operating conditions, as indicated in recent reviews (Dudukovic et al., 2002 and Jakobsen et al., 2005). Not only is a firm theoretical basis lacking, but there are very few experimental data available in the presence of internals, mainly caused by the complexity that the design and installation of internals add to the experimental setups.

The presence of internals is expected to significantly alter the hydrodynamics, mixing patterns, and mass and heat transfer inside the reactor. It is likely that the large number of vertically oriented boundaries of the heat exchanger tubes would affect the flow field and transport on the local scale as well as on the reactor macro-scale (Larachi et al., 2006). However, the quantitative description as to how this happens is not currently available. We suspect that the presence of vertical tube bundles will lead to a change in the macro-scale circulation pattern in the column, hindrance of radial bubble motion, bounding of the eddy size, and altering of the bubble size distribution, which would consequently affect the

mixing behavior in both phases as well as mass and heat transfer rates. However, no data to support these assertions are currently available, nor has a firm theoretical basis been outlined.

The effect of internals has been addressed only in very few studies in the available literature. These studies focused on the effect of internals on the overall gas holdup (Fair et al., 1962, Pradhan et al., 1993, and Youssef, 2010), bubble dynamics (Chen et al., 1999 and Youssef, 2010), liquid mixing (Chen et al., 1999 and Forret et al., 2003), and heat transfer (Korte, 1987 and Schlüter et al, 1995). To the best of the author's knowledge, no studies have reported the effect of vertical internals on the gas velocity profiles, gas phase mixing and mass transfer in bubble columns or slurry bubble columns. This is mainly due to the difficulties involved in the measurements of these quantities in the presence of internals, especially at high superficial gas velocities. The speed of the gas phase places a stringent demand on the use of rapid and accurate measurement systems to measure the bubble velocities and the residence time distribution (RTD) of the gas phase. Consequently, the absence of reliable experimental data has led to the absence of accurate models to predict gas velocities and simulate gas mixing in bubble columns. The presence of internals is anticipated to affect gas phase mixing, as they will decrease the axial and radial eddy diffusivities of the liquid phase as shown by Chen et al. (1999) and will also lead to the enhancement of the overall liquid circulation (Chen et al., 1999 and Forret et al., 2003). Both of these phenomena directly affect the extent of gas mixing in bubble columns (Joshi, 1982 and Lefebvre et al., 2004). Furthermore, the decrease in the bubble size (Youssef, 2010) and enhancement of liquid circulation in the presence of internals is anticipated to influence the gas velocity profile. Therefore, there is a need to investigate the effect of internals on the gas velocity profiles and gas phase mixing in bubble columns. The simultaneous investigation of the gas phase mixing and the gas phase hydrodynamics will allow better understanding of the effects of the gas hydrodynamics on gas phase mixing.

In addition to the absence of experimental data and models for predicting gas velocity in the presence of internals, gas velocity itself has been poorly studied even in the absence of internals. There are almost no gas velocity models that can predict the gas velocity profiles in bubble columns. The only attempt to simulate gas velocity was done by Gupta (2002), who

never validated his model predictions with experimental data. The absence of models to predict gas velocity hinders our ability to fully understand the hydrodynamic picture inside bubble columns and leads to a poor understanding of the effect of different fluid dynamic parameters on the gas phase hydrodynamics and the gas phase mixing. Thus, there is a need for the development and validation of models that can predict the gas velocity.

Various models have been developed for simulating reactor scale gas mixing in bubble columns, including the plug flow model (Stern et al., 1983, van Vuuren and Hydenrych, 1985, and Herbolzheimer and Iglesia, 1994), the axial dispersion model (Towell and Ackermann ,1972, Field and Davidson, 1980, Mangartz and Pilhofer, 1981, Kulkarni and Shah, 1984, Joseph et al., 1984, and Wachi and Nojima, 1990), the slug and cell model (Myers et al. 1987), two-bubble class models (Shetty et al., 1992, Modak et al., 1993, and Kantak et al., 1995), compartmental models (Kawagoe et al., 1989 and Gupta, 2002), and the pure convective mixing model (Hyndman and Guy, 1995). All these models, with the exception of Gupta's model, considered only one mixing mechanism to be dominant in spite of the fact that both convective mixing and turbulent dispersion contribute to the overall axial gas phase mixing, as indicated by Joshi (1982). Moreover, these models were all developed for bubble columns without internals, and their applicability in the presence of internals has never been verified. It is important to develop a mixing model that better describes the physical phenomena of gas phase mixing in bubble columns by taking into account all the hydrodynamic and turbulent factors that affect gas mixing, such as the radial gas holdup profile, radial velocity profile, and turbulent mixing parameters, in addition to the physical presence of internals.

In view of the work done in bubble columns with internals, the mass transfer characteristics will most likely be influenced by their presence. On one hand, the increase in the interfacial area of bubbles (Youssef, 2010) and in the rate of bubble breakup in the presence of internals will enhance the overall volumetric mass transfer coefficient, k_La. On the other hand, the reduction in the turbulent intensity, including turbulent kinetic energy (Larachi et al., 2006) and fluctuating velocity (Chen et al., 1999 and Forret et al., 2003), in the presence of internals may lead to a decrease in the liquid-side mass transfer coefficient, k_L. Hence, it is

important to study the poorly understood effect of internals on k_L and k_La in bubble columns with internals.

1.4 Objectives

The major thrust of this work is to advance the understanding of the gas hydrodynamics, gas phase mixing and gas-liquid mass transfer in bubble columns with internals. In addition, this work aims to develop and validate fundamental hydrodynamic models that allow the prediction of gas velocity profiles and the simulation of the gas phase mixing in bubble columns with internals. In order to achieve these goals, the following objectives are set for this work:

- Investigate and quantify the effect of internals on the radial gas velocity profile, the overall axial gas phase mixing, and the overall volumetric mass transfer coefficient at different operating conditions and reactor scales.
- Validate a 1-D model to predict the gas velocity profile at different operating conditions and reactor scales in the presence and absence of internals.
- Develop and validate a 2-D gas mixing model that can quantify the contributions of different mixing mechanisms on the overall axial gas mixing, and then use this model to relate the global mixing parameters to the local hydrodynamic and turbulent mixing parameters at different operating conditions and reactor scales.

The above objectives will be pursued by performing experiments in two bubble columns 8 and 18 inches in diameter, to study the effect of column scale, using three different percentages of occluded cross-sectional area by internals (0 %, 5 %, and 22 %) to investigate the effect of internals.

As mentioned earlier, the ratio of the occluded CSA by internals will be used as the main parameter to characterize the effect of internals. All the previous studies on internals have recommended the use of this parameter (Bernemann, 1989, Chen et al., 1999, Forret et al., 2003, and Youssef, 2010) to characterize the effect of internals, which is well justified in view of the experimental evidence presented by Yamashita (1987) and Youssef (2010), as long as the internals are distributed uniformly across the CSA area of the column.

1.5 Thesis Structure

This thesis consists of the following chapters:

- Chapter 1 introduces bubble column reactors and their use in the F-T process, highlights the importance of internals in bubble columns as a means of heat removal, and presents the motivation for and objectives of this study.
- Chapter 2 includes a brief literature review relevant to the work done in this thesis.
- Chapter 3 reports the results of the investigated gas phase hydrodynamics in the lab-scale 8-inch and the pilot-scale 18-inch bubble columns with and without internals and validates the 1-D gas velocity model developed by Gupta (2002).
- Chapter 4 discusses the impact of internals on gas phase mixing supported by a 2-D convection-diffusion model that quantifies the contribution of different mixing mechanisms to the overall axial gas mixing in bubble columns.
- Chapter 5 highlights the effect of internals on mass transfer in bubble columns.
- Chapter 6 presents conclusions and recommendations for future work on bubble columns.

Figure 1.2 shows a schematic diagram of the Thesis structure and explains the relation between the different chapters of the Thesis.

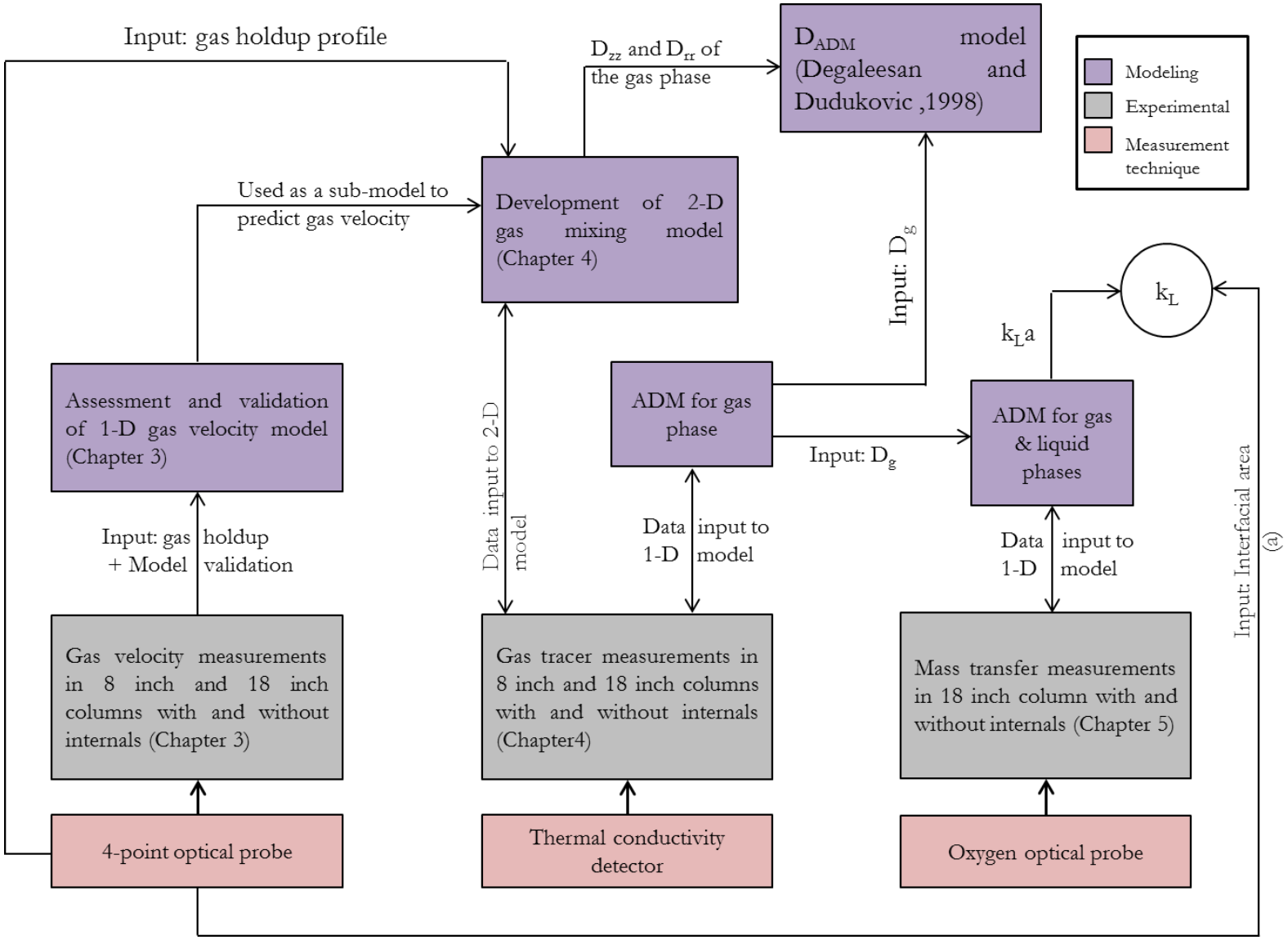

Figure 1.2 - A schematic diagram of the Thesis structure

Chapter 2 - Background

This chapter focuses on the critical analysis and review of the literature pertinent to the present work. Firstly, the current status and findings on bubble columns with internals are highlighted. Secondly, the experimental and modeling work done on the gas velocity profile is discussed. Thirdly, the experimental and modeling research done on gas phase mixing is presented. Finally, some of the important experimental studies on mass transfer in bubble columns are reviewed.

2.1 Internals

In the last decade there had been extensive research on bubble and slurry bubble columns. Unfortunately, most of these studies have not accounted for the presence of vertical internals for many reasons, as discussed in Chapter 1. The presence of vertical internals is expected to alter the flow pattern, mixing, and heat and mass characteristics, and hence, their effect should be considered in the design and scale-up of bubble columns. This section presents a brief background on the previous work done on the effect of vertical heat internals in bubble columns.

The effect of vertical internals on the hydrodynamics and mixing behavior of bubble columns has been addressed systematically in no more than five studies in the open literature. These studies focused mainly on investigating the effect of internals on the overall gas holdup and the radial gas holdup profile, bubble dynamics, liquid velocity profiles, liquid mixing, and heat transfer. The first systematic attempt to study the effect of internals was carried out by Bernemann (1989), who investigated the effects of different configurations and occluded CSA by internals (10%-19%) on the liquid velocity profile and liquid mixing in two bubble columns, 8 and 18 inches in diameter. Bernemann (1989) found that the increase in the occluded CSA by internals increased the steepness of the liquid velocity profile and increased the overall axial liquid mixing.

Chen et al. (1999) investigated the effect of the occluded CSA by internals on the radial gas holdup profiles, time-averaged liquid velocity profiles, turbulent stresses and eddy diffusivities (radial and axial) in an 18-inch diameter bubble column with and without internals (5% occluded CSA) at 12 cm/s. They concluded that the presence of the 5% occluded CSA by internals slightly enhanced liquid circulation patterns, confirming Bernemann's (1989) findings. The presence of internals was found to decrease turbulent stresses and eddy diffusivities. This effect was more pronounced in the radial direction than in the axial direction.

Forret et al. (2003) studied the effect of internals on liquid back-mixing in a 1 m diameter bubble column with and without internals (22% occluded CSA). They concluded that internals caused an enhancement in the large-scale liquid mixing and a decrease in the axial fluctuating liquid velocity. This decrease is in line with the findings of Chen et al (1999). In their work, they used a 2-D model which accounts for the radial variations of the liquid velocity and the gas holdup profiles and found that the ratio of D_{zz}/D_{rr} increased in the presence of internals. This finding is consistent with the work of Chen et al. (1999) who found that the decrease in the turbulent diffusivities in the presence of internals is more significant in the radial direction.

Larachi et al. (2006) used a two-fluid transient 3-D CFD model to simulate five pilot-scale configurations of internals with different percentages of occluded CSA in 19 cm, 91 cm, and 100 cm inner diameter bubble columns. CFD simulations showed that internals affect the liquid gross flow structures and sharply decrease the liquid kinetic turbulent energy.

Youssef (2010) focused on investigating the effect of internals on the gas holdup profiles, bubble dynamics including gas-liquid interfacial area, bubble chord length, and bubble velocity distributions, and liquid mixing in 8-inch and 18-inch diameter bubble columns. In his study, he used configurations of internals that mimic the ones used in methanol synthesis (5% occluded CSA) and the F-T process (22% occluded CSA). He found that the presence of internals enhanced the bubble break-up, causing a decrease in the bubble chord length and an increase in the interfacial area. The decrease in the bubble sizes caused an increase in the overall gas holdup and a flattening of gas holdup profiles. In addition, the overall axial

liquid mixing increased in the presence of internals, further supporting the work of Bernemann (1989) and Forret et al., (2003). Figure 2.1 shows the different configurations of internals used by the above-mentioned studies. All the superficial gas velocities used in these studies were based on the free CSA of the column.

Other work on internals includes the work of Yamashita (1987), who studied the effect of the configuration of internals on the overall gas holdup. His work showed that the overall gas holdup is not affected by the arrangement of the vertical tubes; rather it is sensitive only to the number of tubes and their outer diameter (i.e., the occluded CSA is the main controlling parameter). This finding was also supported by the work of Youssef (2010). Korte (1987) studied the effect of vertical internals on the heat transfer coefficient using 13 different configurations in two different columns, 19.6 cm and 45 cm in diameter. Korte (1987) found that in the presence of internals, the heat transfer coefficient increased steeply with increasing the superficial gas velocity up to 20 cm/s, and then leveled off. The effect of internals on the heat transfer coefficient was found to depend on their configuration. Later, Schlüter et al. (1995) confirmed this finding in three bubble columns, 19, 29, and 45 cm in diameter, using different configurations of internals. In general, Korte (1987) and Schlüter et al. (1995) showed that the effect of internals on the heat transfer coefficient is insignificant compared to the effects of column diameter and liquid viscosity on the heat transfer coefficient.

In summary, the work done on internals has focused on addressing their effects on bubble dynamics, liquid mixing, and heat transfer. However, the description and quantification of their effect on the gas velocity profile, gas phase mixing and mass transfer rate is still lacking in the open literature. In addition, no attempt has been made to develop phenomenological models to describe the performance of bubble columns with internals. The development of such models will greatly improve the fundamental understanding of internals on the hydrodynamics, mixing, and mass transfer in bubble columns.

Configuration of internals used by Bernemann (1989)

Copied from Youssef et al (2012)

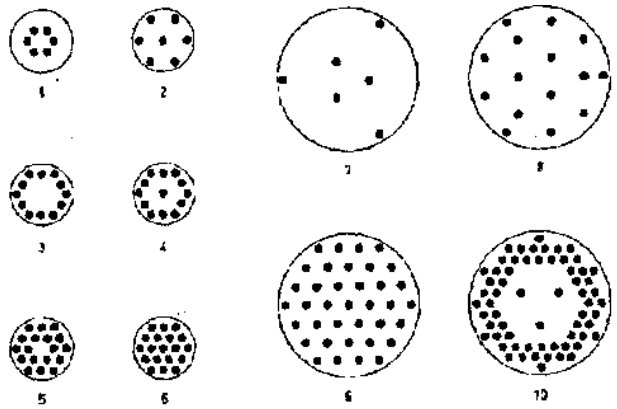

Bundle configuration #	1	2	3	4	5	6	7	8	9	10
# tubes	6	7	12	13	18	19	6	15	37	63
Relative free CSA	0.90	0.88	0.79	0.77	0.69	0.67	0.98	0.95	0.89	0.81
Relative wall surface area	1.79	1.52	2.18	2.32	2.97	3.11	1.33	1.83	3.06	4.50
Pitch (mm)	40	70	40	40	40	40	-	120	70	40
Tube diameter	25 mm									

Configuration of internals used for the 3-D CFD simulation

Configuration	No internals			Full internals	Scattered internals	Star	C-Star
Column diameter	Laboratory	Laboratory	Pilot	Pilot	Pilot	Pilot	Pilot
Column diameter (cm)	19	19	91	100	100	100	100
Aspect ratio	10	10	11	10	10	10	10
Internals number	0	0	0	253	31	121	132
Internals diameter (cm)	—	—	—	2.5	2.5	2.5	2.5
Triangular pitch (cm)	—	—	—	5.7	17.1	5.7	5.7

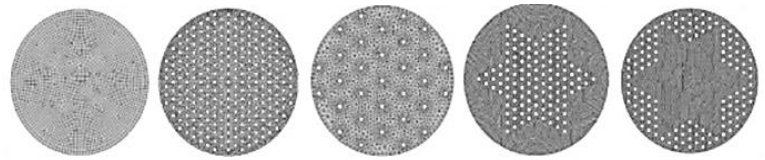

(a) (b) (c) (d) (e)

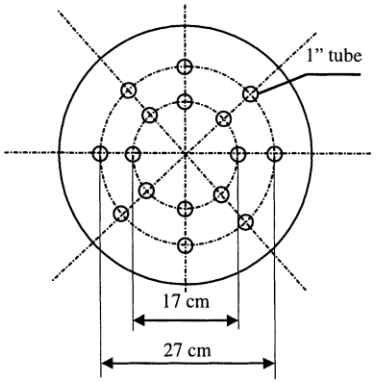

Configuration of internals used by Chen et al (1999). Copied from Chen et al (1999)

Two bundles of 1" aluminum tubes (1/16" in thickness) located at two different radial positions are: r/R of 0.39 and 0.61 respectively

Configuration of internals used by Korte (1987). *Copied from Youssef et al (2012)*

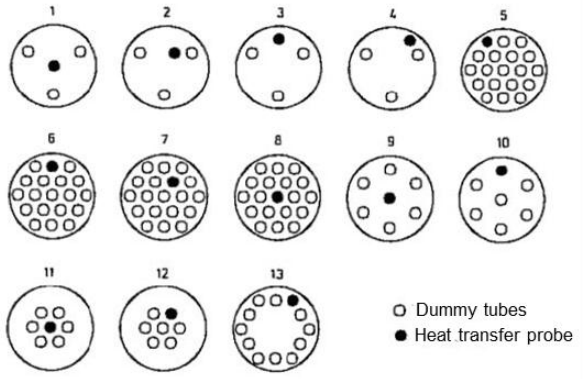

Figure 2.1 - Configuration of internals used by different researchers

2.2 Gas velocity profiles in bubble columns

In bubble columns, the gas introduced at the bottom of the reactor through the sparger forms bubbles that rise preferentially along the center of the column, entraining some of the liquid in that region in the bubbles' wakes. This movement induces gas and liquid recirculation, where the liquid is dragged by the large gas bubbles along the column center and descends at the wall, dragging downwards the small bubbles that are entrained in the wall region. As a result, the actual velocity of the gas bubbles becomes a function of the liquid velocity, the bubble size and shape, and the physical properties of gas and liquid phases. Most of the work done on the gas phase velocity concentrated on measuring and modeling the rise of single bubbles in a quiescent liquid. However, the extension of the developed models and results has not been verified in accelerating or moving liquids. The absence of these experiments limits our ability to model the gas velocity profiles in bubble columns and understand the nature and magnitude of different forces affecting the gas phase in bubble columns. This section presents a brief review on the experimental and modeling work on bubble velocities.

2.2.1 Experimental Studies on Gas Velocity

Most of the work done on bubble velocities in bubble columns has been concerned with the rise bubble velocity of isolated bubbles. Wu (2007) presented a detailed review of the developed correlation for estimating the single bubble rise velocity. Generally, the single bubble rise velocity is a function of liquid properties, including density, surface tension, and viscosity and of the operating conditions including pressure and temperature. The effect of liquid properties on the rise bubble velocity decreases as the bubble size increases, which causes the rise velocities of large bubbles to be insensitive to the liquid properties (Fan, 1989). However, the continuous bubble coalescence and breakup in in bubble columns causes the behavior of bubble swarms to be more complex than that of isolated single bubbles.

Deen et al. (2000) measured the simultaneous bubble and liquid velocities in a rectangular bubble column using the Particle Image Velocimetry (PIV) technique at 5 mm/s superficial

gas velocity. He showed that in the homogenous regime, the trend of the gas velocity profile qualitatively matched the liquid velocity profile. Unfortunately, the extension of his technique to measure bubble velocities in bubble columns operating at high superficial gas velocities is not feasible. The only systematic and complete work on the gas velocity profiles in bubble columns under a wide range of superficial gas velocities was done by Xue (2004) who measured the gas velocity profiles for an air-water system in a 6-inch bubble column at superficial gas velocities ranging from 3 to 60 cm/s at different pressures (0.1-1 MPa) using a 4-point optical probe. Xue (2004) showed that the trend of gas velocity profile is similar to that of the liquid velocity profile, where bubbles move upwards in the central region and move down in the wall region. This was evident both in the homogenous and heterogeneous regimes. Xue (2004) also showed that the increase in pressure causes an increase in the steepness of the gas velocity profile (an increase in the center-line gas velocity and a decrease in the near-wall velocity) mainly due to the enhancement of liquid circulation at higher pressure in spite of the decrease in bubble chord length at high pressures. Wu (2007) studied the effect of solids loading on the gas velocity profiles, and found that the gas velocity increases with the increase in solids loading, but the difference becomes negligible at higher superficial gas velocities. It should be emphasized that in all these studies, the average gas velocity at a certain radial location was assumed to be equal to the average velocities of the bubbles moving upwards and downwards at this location. Notably, the PIV technique and the 4-point optical probe measure the absolute velocity of bubbles and, hence, the mean bubble velocity or gas velocity at a certain radial location represents the actual gas velocity which is the sum of the liquid and slip velocities at this location. The actual gas velocity is of course different from the superficial gas velocity, U_g, and is usually defined globally (reactor-average) as: U_g/ε_g. More experimental work is needed to further study the effects of different operating conditions on the gas velocity profiles such as the physical properties of the liquid and gas phases, column diameter and internals. Finally, more insight in the flow behavior in bubble columns can be gained by developing fundamental models to predict the gas velocity profiles under different operating conditions in bubble columns.

2.2.2 Modeling of gas phase hydrodynamics

The fundamental modeling of the velocity profiles of the gas and liquid phases in bubble columns is typically based on two approaches: Eulerian-Eulerian and Eulerian-Lagrangian. The Eulerian-Eulerian approach involves solving the fundamental Navier-Stokes equation for gas and liquid phases based on the interpenetrating fluid model which views both phases as coexisting and being continuous. Typically the Reynolds Averaged Navier-Stokes (RANS) solvers are used and this requires numerous closures. Simplified models based on assumed gas holdup profiles, gas-liquid drag and correlations for turbulent viscosity and /or mixing length have also been employed for estimation of the liquid velocity profiles. This approach of modeling had been pursued by several research groups for the last 50 years (Ueyama and Miyauchi, 1979, Svendsen et al., 1992, Jakobsen et al., 1996, Sokolichin and Eigenberger, 1994, Ranade, 1992, Grienberger and Hofmann, 1992, Geary and Rice, 1992, Kumar et al. 1995, and Gupta, 2002). The liquid velocity data developed using the Computer Automated Radioactive Particle Tracking (CARPT) technique and the gas holdup profiles obtained using Computed tomography (CT) allowed the validation of some of these models in the homogeneous and heterogeneous regimes provided that the correct gas holdup profile and turbulent closure are chosen (Kumar, 1994 and Degaleesan, 1997). This approach can be extended to calculate the velocity profile of the gas phase by solving the gas momentum equation. In this case, the bubble size is needed to calculate the interfacial drag force between the gas and liquid phases. However, the absence of experimental data of the gas velocity profiles and bubble size hindered different authors from extending this Eulerian-Eulerian approach to model the gas velocity. The only attempt to model gas velocity using this approach was done by Gupta (2002). The main motivation for the development of his gas velocity model was to use it as an input sub-model to a compartmental gas and liquid mixing model. Although the compartmental model developed by Gupta (2002) was validated using gas RTD data, the predicted gas velocities were never validated using gas velocity data in bubble columns. The formulation of Gupta's model, which will be used in this work to simulate gas phase velocity profile, is given in section 2.2.3.

The other approach in the fundamental modeling of gas-liquid flows is the Eulerian-Lagrangian approach. In this formulation, the individual bubbles of the gas phase are tracked

by writing a force balance for each bubble (Lapin and Lubbert, 1994 and Delnoij et al., 1997). The Lagrangian motion of bubbles is coupled with the momentum balance (Eulerian) equation for the liquid phase via the source interaction term and the volume fraction of the gas. This method requires as an input the bubble size, and has so far only been attempted for bubbly flows where there are uniform bubbles without mutual interaction. Eulerian-Lagrangian models do not require turbulence modeling since they are, at present, applied to cases of low gas velocities. For high gas velocities, this approach may not be feasible due to the large number of bubbles that need to be tracked along with multiple and complex bubble interactions and sizes. The solution of these fundamental equations, given the complexities involved regarding various closures and computational resources (for 3-D calculations), remains a subject of current research. Progress in this area requires reliable experimental information to validate these models (average bubble size, phase velocities, holdup profile and turbulence stresses) and can provide insight into mechanisms that drive the flow. Sokolichin et al. (1997) showed that, provided that the gas phase equations are discretized adequately, both the Euler-Euler method and the Euler-Lagrangian method give the same results in bubbly flows.

There is an increasing use of Computational Fluid Dynamics (CFD) as an engineering tool for predicting the flow behavior in various types of equipment on an industrial scale. Although the tools for applying single-phase flow CFD are widely available, application of multiphase CFD remains complicated from both a physical and a numerical point of view. Although some of the developed CFD codes (e.g.: Krishna et al., 2000 and Larachi et al., 2006) were successful in predicting the qualitative flow behavior in bubble columns for the homogeneous regime, the validity of these codes to the churn-turbulent regime is still questionable. This is mainly due to the incomplete understanding of the different interfacial forces at high volume fractions and the absence of experimental data to validate the CFD predictions. Furthermore, the application of CFD to model practical reactive systems, such as the F-T process, implies the use of 20-30 species transport equations, which is very difficult to achieve in a realistic time-frame. Hence, most CFD applications to bubble column design are limited to describing the fluid dynamics from which relevant information can be passed to the models describing species transport.

In light of the previous discussion on different modeling approaches, it is clear that simple yet fundamental models that can capture the physics of the flow are needed to design and scale up bubble column reactors. Detailed compartmental models (Gupta, 2002) and 2-D models (Degaleesan, 1997) are good examples of these models. This work attempts to extend the 2-D model developed by Degaleesan (1997) to simulate the gas phase mixing. These models can be easily extended to include reaction terms and ultimately provide practical means for modeling reactive systems at intense operating conditions.

2.2.3 The 1-D Gas-Liquid Recirculation Model

One-dimensional recirculation models are based on solving the 1-D continuity and momentum balance equations, which are simplified versions of the two-fluid model equations (Ishii, 1975). The two-fluid model treats the general case of modeling each phase as a *separate fluid in continuum* with its own set of governing balance equations. In general, each phase has its own velocity, temperature and pressure. In this model, the gas and liquid phases are coupled using interfacial forces that generally arise due to the relative motion between individual phases. The 1-D recirculation models are usually applied to the fully developed section of bubble columns with aspect ratios (L/D) larger than 5, where experimental evidence indicates the presence of 1-D profiles for the liquid (Devanathan, 1991) and gas phases (Xue, 2004). The fundamental Navier-Stokes equation for the gas and liquid phases can be written as (Gupta, 2002):

Continuity Equations:

$$Liquid - Slurry: \frac{\partial \varepsilon_l}{\partial t} + \nabla.(\varepsilon_l \boldsymbol{u_l}) = 0 \tag{2.1}$$

$$Gas: \frac{\partial \varepsilon_g}{\partial t} + \nabla.\left(\varepsilon_g \boldsymbol{u_g}\right) = 0 \tag{2.2}$$

Momentum Equations:

$$Liquid - Slurry: \rho_l \varepsilon_l \left[\frac{\partial \boldsymbol{u_l}}{\partial t} + \boldsymbol{u_l}.\nabla \boldsymbol{u_l}\right] = \rho_l \varepsilon_l \boldsymbol{g} - \varepsilon_l \nabla p - \nabla.(\varepsilon_l \tau_l) - (\boldsymbol{M_d} + \boldsymbol{M_{Lift}}) \tag{2.3}$$

$$Gas: \rho_g \varepsilon_g \left[\frac{\partial \boldsymbol{u_g}}{\partial t} + \boldsymbol{u_g}.\nabla \boldsymbol{u_g}\right] = \rho_g \varepsilon_g \boldsymbol{g} - \varepsilon_g \nabla p - \nabla.\left(\varepsilon_g \tau_g\right) + (\boldsymbol{M_d} + \boldsymbol{M_{Lift}}) \tag{2.4}$$

In the momentum balance equations, τ_l and τ_g are the stress tensors representing the normal and shear stresses in the liquid and gas phases, respectively. M_d is the drag force that arises due to the relative velocity between the two phases, and M_{lift} is the lift force acting on

the gas phase due to the presence of a shear flow field. Other axial and radial forces also exist, like the Basset, virtual mass, turbulent dispersion, Magnus, and wall lubrication forces. However, these forces are usually neglected in the modeling of practical gas-liquid flows due to the lack of understanding of these forces at high gas volume fraction and the small magnitude of these forces compared to the drag and lift forces.

The drag force that results from the motion of bubbles, acts in a direction opposite to that of the motion of bubble and is related to the slip velocity, liquid density, and drag coefficient. The mathematical representation of the drag force can be obtained by making a force balance on a spherical bubble:

$$M_d = \frac{6\varepsilon_g \varepsilon_l}{\pi d_b^3} F_d \tag{2.5}$$

$$F_d = \frac{1}{8}\rho_l \pi d_b^2 C_D \left|\boldsymbol{u_l} - \boldsymbol{u_g}\right| (\boldsymbol{u_l} - \boldsymbol{u_g}) \tag{2.6}$$

where, C_D is the drag coefficient and d_b is the bubble diameter. The lift force will not be discussed here, since the main concern of the model is to obtain the axial velocities of the gas and liquid phases. The reader is referred to Rafique et al. (2003) for an excellent review on the origin and mathematical representation of the different interfacial forces in bubble columns.

In the well-developed region of the column, experimental evidence shows that the flow of the liquid and gas phases are axisymmetric in the time-averaged sense with only the axial velocities being non-zero (Devanathan, 1991, Degaleesan, 1997, and Xue, 2004). Hence the liquid and gas velocity profiles can be represented by a single radial profile in the fully developed region. These assumptions are well justified in view of the experimental data in available bubble columns, including gas holdup profiles data obtained using CT (Kumar, 1994) and the 4-point optical probe (Xue, 2004), liquid velocity profiles measured with CARPT (Devanathan, 1991 and Degaleesan , 1997), and gas velocity profiles obtained using the 4-point optical probe (Xue, 2004). Based on these assumptions:

- The equations of continuity for the gas and liquid phases are satisfied.
- At steady state conditions, the left hand side of the gas and liquid momentum equations becomes zero.

- Due to no net flow condition in the radial and azimuthal directions, the pressure is assumed to be independent on the radial and azimuthal coordinates and the pressure gradient term in the momentum equations reduces to $\frac{dp}{dz}$.

Hence, the liquid and gas momentum equations reduce to:

$$Liquid - Slurry: 0 = -\rho_l \varepsilon_l g - \varepsilon_l \frac{dp}{dz} - M_d - \frac{1}{r}\frac{d}{dr}\left(r\varepsilon_l\left\{\tau_{l,rz}^m + \tau_{l,rz}^t\right\}\right) \tag{2.7}$$

$$Gas: 0 = -\rho_g \varepsilon_g g - \varepsilon_g \frac{dp}{dz} + M_d - \frac{1}{r}\frac{d}{dr}\left(r\varepsilon_g\left\{\tau_{g,rz}^m + \tau_{g,rz}^t\right\}\right) \tag{2.8}$$

In the above equations, the superscripts "m" refers to molecular (viscous) contributions, while "t" refers to turbulent contributions. The molecular and turbulent stresses in the gas and liquid phases are defined as:

$$\tau_{l,rz}^m = -\mu_l^m \frac{du_l}{dr} \; and \; \tau_{g,rz}^m = -\mu_g^m \frac{du_g}{dr} \tag{2.9}$$

$$\tau_{l,rz}^t = \rho_l \overline{u'_{l,r} u'_{l,z}} \; and \; \tau_{g,rz}^t = \rho_g \overline{u'_{g,r} u'_{g,z}} \tag{2.10}$$

Since the gas viscosities are much smaller than the corresponding liquid viscosities ($\mu_g^m \ll \mu_l^m$) and the gas densities are much smaller than liquid densities ($\rho_g \ll \rho_l$), the molecular and turbulent shear stresses in the gas phase can be neglected compared to those in the liquid phase. Therefore, upon the addition of the simplified liquid and gas momentum equations, one obtains:

$$0 = -(\rho_l \varepsilon_l + \rho_g \varepsilon_g) g - \frac{dp}{dz} - \frac{1}{r}\frac{d}{dr}\left(r\varepsilon_l\left\{\tau_{l,rz}^m + \tau_{l,rz}^t\right\}\right) \tag{2.11}$$

In order to solve this equation to obtain the liquid velocity profiles, two inputs are required:

1 **The gas holdup profile**: although gas holdup profiles have been extensively studied in bubble columns, there are no satisfactory models that can confidently predict it under a wide range of operating conditions. As a result, most researchers (Ueyama and Miyauchi, 1979, Rice and Geary, 1990, Kumar, 1994, Burns and Rice, 1997, Degaleesan, 1997, and Gupta, 2001) assume a certain form for the gas holdup profile and fit their gas holdup data to that form and use it as an input to the 1-D model.

2 **A closure for the turbulent stresses**: the simplest and most common approach used in the modeling of liquid velocity is the closure of the turbulent stresses in terms of turbulent kinematic viscosity (Miyauchi and Shyu, 1970, Ueyama and Miyauchi, 1979, Kojima et al., 1980, Riquarts, 1981, Sekizawa et al., 1983, Kawase and Moo-young 1989). The turbulent kinematic viscosity can be further closed in terms of a turbulent mixing length (Clarck et al., 1987, Devanathan, 1991, Geary and Rice, 1992, Kumar, 1994, and Gupta, 2001).

It should be noted that starting from Equation (2.11), several versions of the 1-D model appear in the literature for predicting the liquid velocity profile (Ueyama and Miyauchi, 1979, Clark et al., 1987, Anderson and Rice, 1989, Rice and Geary, 1990, Luo and Svendsen, 1991, Kumar et al. 1994, and Gupta, 2001). The variations among these models arise from the different boundary conditions and closure models used for the Reynolds shear stress, based on Prandtl's mixing length or the eddy viscosity shear stress. A detailed comparison of the existing approaches to study liquid recirculation in bubble columns using the 1-D recirculation model has been performed by Kumar (1994). His study demonstrated the deficiency of literature correlations for eddy viscosity and mixing length in satisfactorily predicting the 1-D liquid velocity profiles under a wide range of operating conditions. Kumar (1994) estimated the mixing length from the experimental measurements of Reynolds shear stress and liquid velocity gradient, based on which a functional form for the mixing length profile was proposed. He showed that the mixing length correlation based on data evaluated in a 19 cm diameter column can be used, along with the measured holdup profile, to predict the liquid velocity profile in larger diameter columns, up to 30 cm. His model was successfully tested for superficial gas velocities ranging from 2 cm/s to 12 cm/s. In what follows, the solution procedure of Gupta (2002) will be discussed briefly.

The axial pressure drop is obtained in terms of the dimensionless radial position at which the downward liquid velocity is maximum, which is usually estimated by an iterative process by closing the liquid phase mass balance as:

$$2\int_{\xi=0}^{\xi=\lambda}\varepsilon_l(\xi)u_l(\xi)\xi d\xi + 2\int_{\xi=\lambda}^{\xi=1}\varepsilon_l(\xi)u_l(\xi)\xi d\xi = U_l \qquad (2.12)$$

where λ is the dimensionless radial position at which the downward liquid velocity is maximum and ξ is the dimensionless radial coordinate (r/R). The boundary conditions used for the solution are typically:

$$u_l|_{\xi=0} = 0\,, and\ \left.\frac{du_l}{d\xi}\right|_{\xi=0} = 0 \tag{2.13}$$

The knowledge of the axial liquid velocity profile along with the axial pressure drop allows the solution of the gas momentum equation, which reduces to:

$$u_s(\xi) = u_g(\xi) - u_l(\xi) = \sqrt{\frac{4d_b(-\frac{dp}{dz} - \rho_g g)}{3C_D\rho_l(1-\varepsilon_g(\xi))}} \tag{2.14}$$

where the drag coefficient, C_D, is a function of slip velocity and bubble diameter, and hence an iterative method is needed to solve for the gas velocity profile. The average bubble diameter can be obtained by an iterative scheme by closing the overall gas phase mass balance as:

$$2\int_{\xi=0}^{\xi=\lambda} \varepsilon_g(\xi)u_g(\xi)\xi d\xi = U_g. \tag{2.15}$$

This approach can also be used to estimate the bubble size distribution, provided that a form for the bubble size distribution is assumed. Gupta's model allows the calculation of the gas velocity profile while ensuring that the gas phase continuity is satisfied. In addition, the model also predicts the average bubble diameter; however, the predicted bubble diameter is strongly affected by the drag coefficient used.

2.3 Gas Phase Mixing

The complex flow structure in bubble columns causes non-idealities in the mixing behavior of the gas and liquid phases. Both turbulent dispersion of gas bubbles and non-uniform gas velocity profiles result in axial mixing of the gas phase. On the reactor scale, the 'overall axial gas mixing' is assessed by the dimensionless variance of the RTD curve at the reactor outlet. Alternatively, the overall axial gas phase mixing can also be quantified using the Péclet number (Pe) which is inversely proportional to the dimensionless variance. The Péclet number is a dimensionless number that represents the ratio between the rate of advection of a tracer by the flow and the rate of dispersion of that tracer. Hence, any condition that

causes an increase in the dimensionless variance of the RTD curve of the gas phase or a decrease in the axial gas Péclet number will cause an increase in the overall axial gas mixing.

All the studies done on gas mixing in bubble columns were mainly interested in measuring and modeling the overall axial gas mixing since it can adversely affect the reaction rates and product selectivity (Deckwer, 1976 and Deckwer and Schumpe, 1993). The investigation of gas phase mixing has received significantly less attention than liquid phase mixing, partly due to the technical problems involved in determining reliable gas RTD data. The speed of the phenomena places a stringent demand on the realization of a reproducible input signal, and the fast response requires a rapid and accurate detection of the local or mixing cup gas concentration. Thus, the collection and analysis of experimental data pose problems, particularly in accounting for the extra dispersion caused by the end effects and sampling lines, especially at high gas flow rates. As a result, the experimental data and correlations reported in the literature reveal considerable scatter, much of which is attributed to the experimental techniques used to acquire the data.

The proper way to collect the RTD data at the reactor outlet from which one can quantify the extent of the overall axial gas mixing, is to measure the gas concentration at different radial locations (at the reactor outlet) and calculate the cup mixing average from these different radial positions. However, most researchers did not discuss the way by which they averaged their RTD data. This may not be a critical issue in bubble columns, since the gas phase is well mixed in the radial direction, causing the tracer responses measured at different radial locations to be nearly the same. The main issue that has not been addressed in the literature is the effect of the reactor height on the extent of the gas phase mixing (i.e. the dimensionless variance of the RTD curve). Levenspiel and Fitzgerald (1983) showed that the dimensionless variance of a tracer is directly proportional to the square of the reactor height if the axial mixing is dominated by dispersion, while it is directly proportional to the reactor height if the mixing is mainly caused by convection. However, since the overall axial gas mixing is a result of both phenomena, the dependence of the dimensionless variance of the gas phase on the reactor height is unknown. In reactive systems, this dependence is further complicated due the fact that the contribution of the different mixing phenomena (dispersive and convective mixing) changes with the reactor height due to the shrinkage of

the gas phase and the consequent change in the gas and liquid hydrodynamics. The main obstacle that hinders our ability to develop a better understanding of the gas mixing phenomenon is the absence of local axial RTD curves of the gas phase, since the current available techniques, except for the radioactive gas tracer technique, do not allow the measurement of the gas tracer concentration in a multiphase system. Until this phenomenon is better understood, one should look at the findings of different researchers carefully and only consider the qualitative reported trends.

2.3.1 Experimental Studies on Gas Phase Mixing

Table 2.1 summarizes the gas phase mixing studies in bubble columns and slurry bubble columns published in the available literature. Most of these studies focused on the effect of superficial gas velocity and column diameter on the extent of gas phase mixing. It is evident from these studies that the axial gas mixing increases with increasing the superficial gas velocity and increasing the column diameter. Kantak et al. (1994) studied the effect of liquid properties on the gas phase mixing. They found that the axial gas phase mixing decreased with decreasing surface tension and increasing liquid viscosity. The effect of the physical properties of the gas phase on the extent of the axial gas phase mixing was found to be negligible. Han (2007) reported the effect of pressure and solid loading on axial gas phase mixing, where he concluded that the gas phase mixing decreased with increasing pressure and decreasing solids loading.

A more critical look at the work on gas phase mixing indicates that all the conditions that cause a decrease in turbulence in bubble columns will cause a decrease in the extent of the axial gas phase mixing, even if this decrease in turbulence is coupled with an increase in gas and liquid circulation. For instance, the increase in pressure which enhances the circulation of gas (Xue, 2004), solids (Rados, 2003), and liquid (Ong, 2003) and decreases turbulent intensity (Ong, 2003) causes an overall decrease in the gas phase mixing. Moreover, the increase in solids loading, which increases turbulence (Han, 2007), causes an overall increase in the axial gas phase mixing in spite of the decrease in the circulation of solids (Rados, 2003), which also indicates a decrease in the liquid and gas circulation. This experimental evidence suggests that the extent of gas phase mixing is mainly controlled by turbulent dispersion rather than convective mixing within the range of operating conditions of these

reported studies, which were mostly at superficial gas velocities ranging from 10-30 cm/s (churn turbulent regime), solids loading ranging from 0-25% by volume, and operating pressures ranging from 0.1-1 MPa. This idea will be studied in more detail in this work by quantifying the contribution of different mixing mechanisms on the overall axial gas phase mixing.

2.3.2 Modeling of Gas Phase Mixing in Bubble Columns

In simulation studies, the gas phase mixing in bubble columns was usually modeled as plug flow (Stern et al., 1983, van Vuuren and Heydenrych, 1985, Herbolzheimer and Iglesia, 1994). However, several authors (Joseph et al., 1984, Shetty et al., 1992, and Kaštánek et al., 1993) showed that this assumption was inaccurate and that gas phase mixing cannot be neglected in bubble columns. The most common approach to modeling the non-ideal mixing behavior in bubble columns is the 1-D axial dispersion model (ADM). In this model, all the mechanisms leading to the longitudinal axial gas mixing are lumped into a single axial dispersion coefficient. The vast popularity of the model is due to its simplicity and ease of use. In addition, it contains only one unknown parameter: the axial dispersion coefficient (D_g). However, the validity of the axial dispersion model to describe two-phase flows with large degrees of mixing, such as those in bubble columns, is questionable (Myers, 1986 and Lefevebre et al., 2004) and the 'a priori' estimation of D_g is difficult because it is a complex and poorly understood function of the liquid and gas hydrodynamics. Despite its lack of a sound basis, the ADM still remains extremely popular, and numerous correlations for the gas and liquid axial dispersion coefficient in bubble columns have been developed over the years. A survey of the existing correlations for gas phase axial dispersion coefficients has been presented by Joshi (1982), Deckwer (1993), and Kaštánek et al. (1993). In the majority of published work, the axial dispersion coefficient (D_g), which quantifies the extent of the overall axial gas mixing was correlated as a function of superficial gas velocity (U_g) or actual gas velocity (U_g/ε_g) and of the reactor diameter. The validity of published empirical correlations is, however, limited to the experimental conditions of the particular studies, and data of other authors can rarely be accommodated. Available literature correlations for the axial gas dispersion coefficients are listed in Table 2.1.

Table 2.1 - Reported experimental studies on gas phase mixing in bubble columns

Author	System	D (cm)	SGV (cm/s)	D_g (m2/s)	Model used	Correlation
Carleton et al. (1967)	Air-H_2O (+rings)	7.6-30.5	3-6	0.1-1	ADM	
Towell and Ackerman (1972)	Air/ H_2O	40.6-106	1.62-3.4	0.02-0.14	ADM	$D_g = 19.7D^2U_g$
Pilhofer et al. (1978)	Air/ H_2O N_2/n-Propanol Air/glycol	10	1-20	0.003-1	ADM for gas and liquid phases + mass transfer	$D_g = 2.64U_s^{3.56}$
Field and Davidson (1980)	Air/water	320	4.5 – 5.5	1-8	ADM	$D_g = 56.4D^{1.33}(U_g/\varepsilon_g)^{3.56}$
Mangartz and Pilhofer (1981)	Air / H_2O N_2/n-Propanol Air/glycol	10	1.5-10	0.01-1	ADM for gas and liquid phases + mass transfer	$D_g = 50D^{3/2}(U_g/\varepsilon_g)^3$
Kulkarni and Shah (1984)	Air-sulfite solution	7.5	0.14-1.3	0.001-0.5	ADM for gas and liquid phases + mass transfer	-
Joseph et al. (1984)	Air- H_2O	30.5	3-7	0.1-1	ADM	-
Shah et al. (1985)	N_2- H_2O N_2- H_2O-glass beads	10.8	9-30	-	Small bubbles: CSTR Large bubbles: Plug flow	-
Molerus and Kurtin (1986)	Air- H2O -Alcohol	19	10-50	-	3 parameter zero-shifted log-normal distribution	-
Kawagoe et al. (1989)	Air- H_2O Air-CMC (aq) Air-Na_2SO_4 (aq)	15.9 29.0	2.7-9.5	0.001-0.5	Two region class mixing model Core: ADM Annular: ADM	
Wachi et al. (1990)	Air/ H_2O	20-50	2.9-45.6	0.02-5	ADM	$D_g = 20D^{3/2}U_g$
Shetty et al. (1992)	Air- H_2O	15-25	1-16	0.001-0.5	Small bubbles: ADM Large bubbles: plug flow	-
Modak et al. (1993)	Air- H_2O	29	3-25	-	Single & Two bubble class models	-
Kantak et al. (1995)	Air- (H_2O , alcohols, & CMC solutions)	15 -25	1-18	0.005-0.35	Small bubbles: ADM Large bubbles: plug flow	-
Hyndam and Guy (1995)	Air-Argon- H_2O	20	3.7-9.4	-	Log-Normal bubble velocities distribution for bubbles population (purely convective model)	-
Han (2007)	Air-C9C11-FT catalyst	16.2	3-30	0.05-0.35	ADM	-

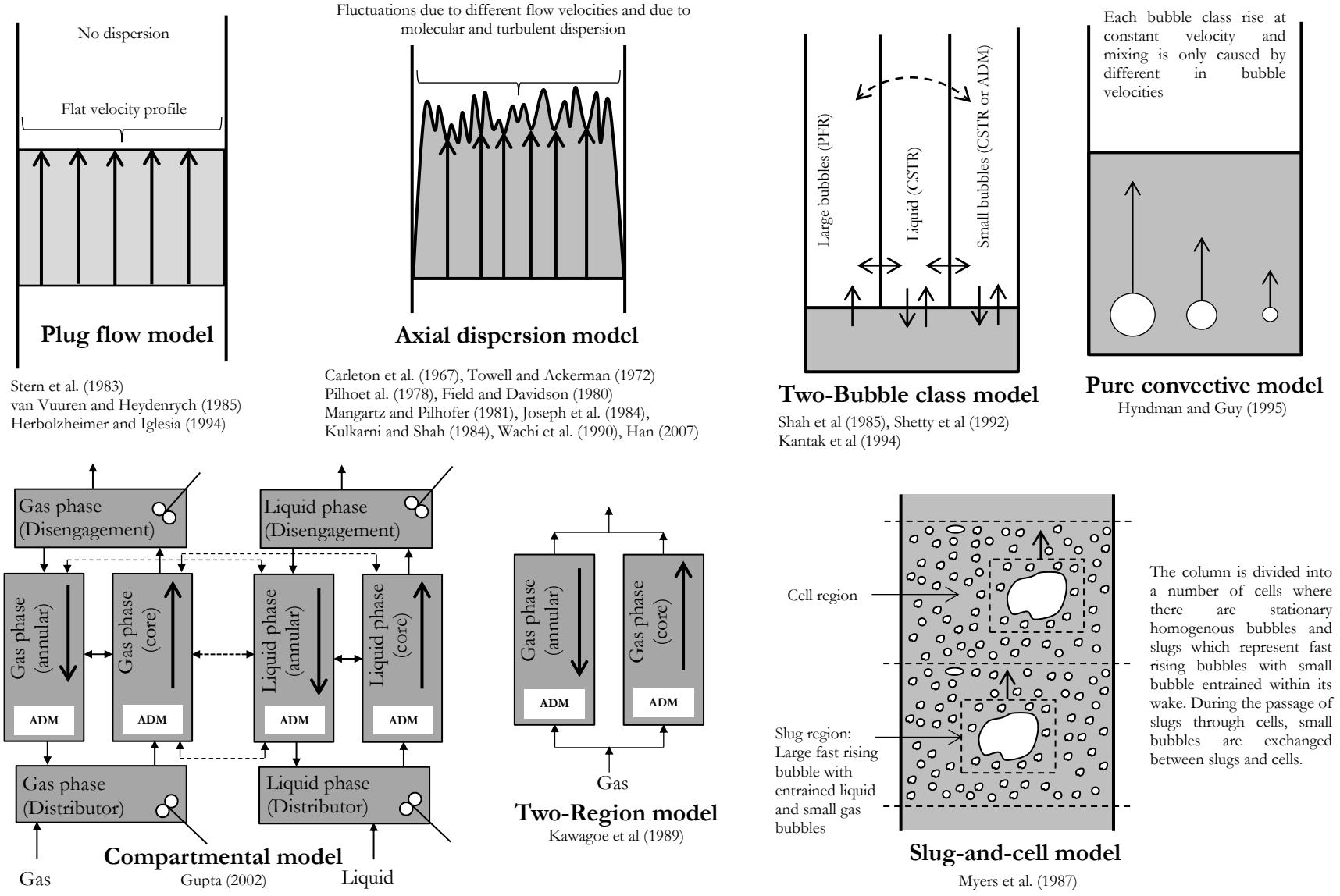

Figure 2.2 - Different models used for gas phase mixing

Several phenomenological models that attempted to capture the physics of the gas phase mixing have been proposed in the literature. Two bubble class models (Shah et al., 1985, Shetty et al., 1992, and Kantak et al., 1995) assumed that bubbles may be separated into small bubbles driven by liquid motion, and large bubbles which rise in a plug flow manner independent of liquid motion. This model is a superposition of a convective mechanism (transport at two velocities) onto a dispersive mechanism where each bubble class is treated separately with no interaction between bubble classes. Meyers et al. (1987) introduced the slug and cell model, where he divided the bubble column into gas rich slugs, which consist of large fast-rising bubbles with any small bubbles and liquid entrained in the wake, and gas lean cells, which consist of a series of stationary pseudo-homogenous dispersions of small gas bubbles in liquid. Hyndman and Guy, (1995) suggested a pure convective model to describe gas phase back-mixing assuming a superposition of many bubbles in plug flows, where bubbles rise at constant velocity along the column axis and mixing is caused solely by the differences in bubble velocities. Kawagoe et al. (1989) adopted the use of a two-region model, where the bubble column was divided into a core region, in which bubbles move upwards, and a wall region, where bubbles moved downwards. Each region was modeled separately using an axial dispersion model and had its own axial dispersion coefficient, where no interaction was assumed between different regions. Gupta (2002) developed a more detailed compartmental model to simulate liquid and gas phase mixing, where he assumed that bubbles move upwards in the core region and downwards in the wall region with interaction between the two regions. Although Gupta's model accurately describes the physical picture of gas phase mixing emerging from numerous experimental studies, his model requires many mixing input parameters for the different reactor compartments. In order to overcome this problem, Gupta (2002) developed a method to estimate these parameters based on the experimental data of CARPT and CT and using the radial gas holdup profile as an input to the model. Figure 2.2 shows a schematic representation of the concept of each of these models.

Some of the previously mentioned models were criticized by different authors. Kaštánek (1993) and Lefebvre et al.(2004) questioned the applicability of the bi-modal (two-bubble class) models to describe gas phase mixing in bubble columns since the experimental measurements of bubble behavior reported in the literature (Xue et al., 2004 and Lefebvre et

al., 2004) did not show a bi-modal distribution of the bubble size population. Furthermore, the two-bubble class model fails to explain the increase in the extent of the axial gas phase mixing with the increase in superficial gas velocity, because it assumes that the increase in the fraction of large bubbles will cause the gas mixing behavior to approach plug flow, contradicting the reported experimental data. Finally, the pure convective models are not physically valid because the dispersive mechanism contributes greatly to the gas phase dispersion. This claim has been confirmed by many experimental studies as shown in the previous section.

In order to accurately model gas phase mixing, one needs to understand the dominant mixing mechanism of the gas phase. This can only be accomplished if the contribution of different mixing mechanisms can be quantified and related to the macro-mixing of the gas phase using physically based models.

2.4 Mass Transfer

The gas-liquid mass transfer, in particular the liquid side gas-liquid mass transfer, can be the limiting step in reaction systems performed in bubble columns (Deckwer, 1992). Although the mass transfer may not be controlling in some cases, the volumetric gas-liquid side mass transfer was found to be reduced significantly in larger columns (Vandu and Krishna, 2004) and hence becomes a concern during reactor design and scale-up. Therefore, the knowledge of mass transfer rates in bubble columns is essential for determining of the maximum overall rates that can be supported in the heterogeneous flow regime.

In bubble columns application, the species concentration in the gas films are high enough to prevent partial pressure of the liquid in the gas phase from imposing any resistance to transport (Behkish, 2004), and hence the gas-side mass transfer resistance can be safely neglected (Deckwer, 1992). Consequently, the main resistance to the rate of mass transfer in bubble columns is the gas-liquid mass transfer. The total mass transfer flux depends also on the available interfacial area. Therefore, the estimation of the overall volumetric mass transfer coefficient, k_La, at different process conditions necessitates the knowledge of the

effect of operating conditions and equipment configuration and scale on the gas-liquid mass transfer coefficient, k_L, and the interfacial area.

The effect of various parameters on k_L and k_La has been extensively studied in the literature (Voyer and Miller, 1968, Akita and Yoshida, 1973, Deckwer and Zoll, 1974, Vermeer and Krishna, 1981, Letzel and Krishna, 1999, Vandu and Krishna, 2004, etc). These studies have focused on measuring the global (i.e. reactor average) mass transfer parameters including k_La, interfacial area, a, and k_L at various operating conditions and physical properties of the gas and liquid phases. However, all of these studies were carried out in columns without internals. Generally, these studies showed that there are a number of parameters that are directly related to mass transfer, including gas holdup, interfacial area, turbulent intensity, bubble size and bubble rise velocity. These parameters are complex functions of the physical properties of the gas and liquid phases, gas sparger, reactor geometry, and the operating conditions, including pressure, temperature, and superficial gas velocity, as shown in Figure 2.3. The general applicability of individual pieces of information collected from the open literature on mass transfer studies is rather limited, and the recommendations presented by respective authors must be viewed with caution. This is a result of the complex nature of gas-liquid systems, which causes the relationships between the phenomena of bubble coalescence and break up in bubble swarms and the pertinent fundamental hydrodynamic parameters of bubble columns to remain poorly understood.

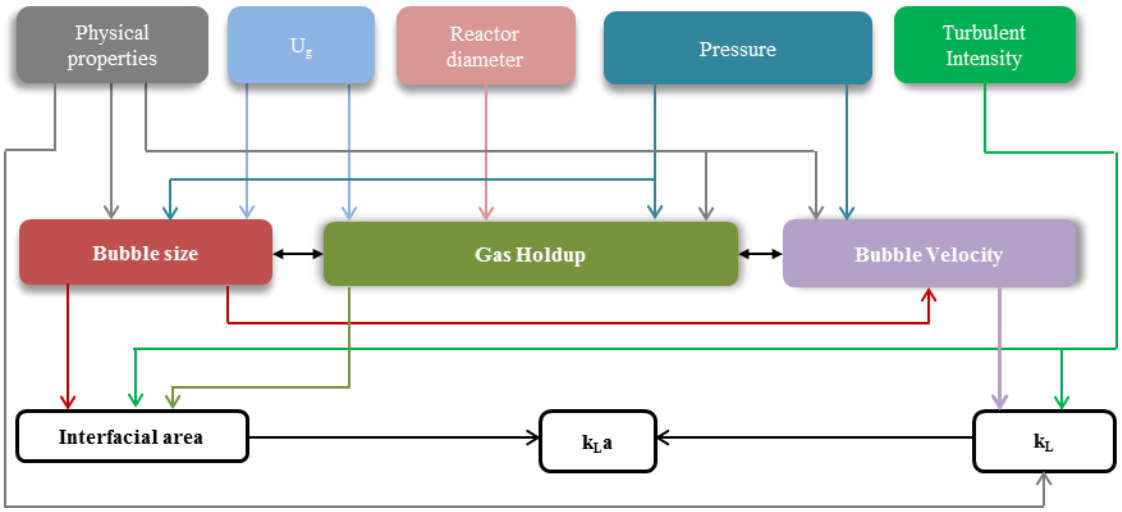

Figure 2.3 - Relationship between different parameters that affect k_L and k_La

Experimental techniques used for measuring mass transfer in bubble columns include chemical and physical methods. Chemical methods were introduced by Danckwerts (1966) and propagated by Alper et al. (1980 and 1984). These methods are not currently used to determine mass transfer coefficients, since they are subject to many uncertainties and may even alter the system's physicochemical properties leading to the estimation of k_La values specific to the system used but not pertinent to the system of interest. Physical methods are more popular; however, they require the knowledge of the hydrodynamic and mixing behavior at same operating conditions to accurately quantify the values of k_La. Deckwer (1992) showed that the assumption of ideal flow patterns (CSTR and PFR) for the quantification of mixing in both phases leads to the estimation of erroneous values of k_La. For instance, the assumption of CSTR for the liquid phase leads to the estimation of minimum concentration difference between the equilibrium concentration and the actual liquid phase concentration, leading to the estimation of the maximum values of k_La. In contrast, the assumption of PFR for the liquid phase leads to an underestimation of the value of k_La. In addition, the tracer response curves used for k_La calculations are sensitive to the extent of mixing in the gas phase, which is usually neglected during mass transfer measurements. This is one of the reasons why different k_La data and correlations exhibit significant scatter among different studies, as shown in Figure 2.4. As a result, it is important to account for the mixing in both phases during the measurements of the k_La. This can be achieved by experimentally quantifying the hydrodynamic and mixing parameters at the same experimental conditions used for k_La measurement.

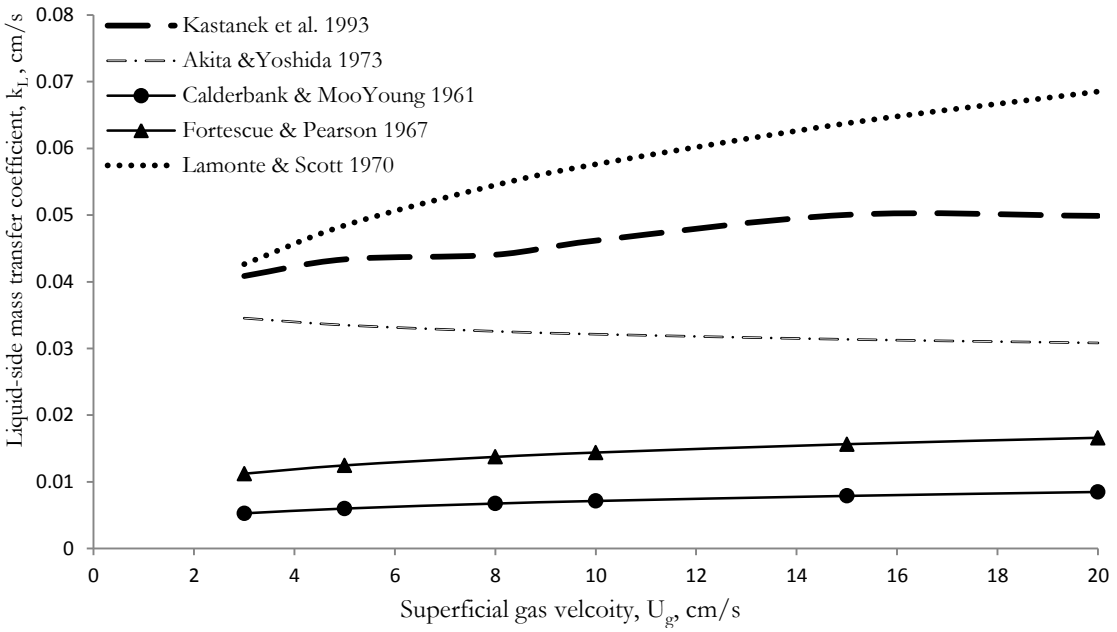

Reference	Correlation
Kastanek et al., 1993	$k_L a = 1.3 * 10^{-3}(\frac{\rho_L^{0.75} D_L^{0.5} g^{1.15}}{\sigma^{0.6} \rho_g^{0.15} \nu_g^{0.25} \nu_L^{0.785}}) \varepsilon_g^{0.35} (1 - \varepsilon_g)^{0.65} u_g^{0.65}$
Akita & Yoshida , 1973	$k_L a = 0.6 \left(\frac{\rho_L}{d_b \, \mu_L} \right)^{0.5} (\frac{g D^2 \rho_L}{\sigma})^{0.62} (\frac{g D^3 \mu_L^2}{\rho_L^2})^{0.31} \varepsilon_g^{1.1} \frac{d_b}{D^2}$
Calderbank & MooYoung, 1961	$k_L = 0.13 (g u_g)^{0.25} \mu_L^{-5/12} \rho_L^2 D_L^{2/3}$
Fortescue & Pearson, 1967	$k_L = 1.46 \sqrt{\frac{D_m \sqrt{\overline{u^2}}}{\overline{l_{eddy}}}}$
Lamonte & Scott, 1970	$k_L = 0.4 \sqrt{\frac{D_m}{(\nu_m / \epsilon)^{0.5}}}$

Figure 2.4 - Predictions of the liquid-side mass transfer coefficient, k_L, in the 8-inch column by different correlations

Numerous correlations have been proposed for the prediction of k_La in bubble columns. The vast majority of these correlations are empirical; however, some theoretical attempts have been also proposed (Higbie, 1953, Danckwerts, 1952, Kawase et al., 1987, and Kaštánek et al., 1993). The reader is referred to Kaštánek et al. (1993) for a more comprehensive review on the different models used to quantify k_L and the interfacial area. Generally, most of the available k_La correlations are still partially empirical and may be not be applicable to all systems and conditions, and hence the validity of some of these theories and correlations should be examined in the presence of internals. Chapter 5 of this work will discuss the validity of these correlations using some of the developed k_La data in the presence of internals.

Chapter 3 - Modeling of Gas Phase Velocity in Bubble Columns

This chapter focuses on the investigation of the effect of internals on gas hydrodynamics at different conditions and on the development of a hydrodynamic model that predicts the gas velocity profile in bubble columns. The experimental data obtained in a laboratory scale and a pilot scale bubble columns operating under a wide range of conditions were used to validate the developed model predictions.

3.1 Introduction

Numerous models have been developed in the literature to simulate bubble column hydrodynamics. Most of them have focused on predicting the time-averaged liquid velocity profile (Ueyama and Miyauchi, 1979, Geary and Rice, 1992, and Kumar, 1994). Comparatively, little attention has been given to the prediction of gas velocity profiles (Gupta, 2002) mainly due to the scarcity of experimental data available for validating the model predictions. The absence of models that can predict the gas velocity profiles hinders our ability to understand the complete hydrodynamic picture in bubble columns, especially the mechanism and magnitude of gas phase mixing and their effects on the final conversion and productivity. Therefore, it is important to develop fundamentally based hydrodynamic models that predict the gas velocity profiles in bubble columns and to validate these models at different operating conditions.

3.2 Research Objectives

This work aims to advance the state of knowledge and improve the understanding of the gas phase hydrodynamics in multiphase reactors, especially bubble column reactors. With this overall objective in mind, the following specific tasks were set:

- Investigate the effect of superficial gas velocity, internals, and column scale (diameter) on the gas velocity profile in bubble columns.

- Asses a 1-D hydrodynamic model to simulate the time-averaged gas phase velocity profiles in bubble columns and examine the effect of various closure correlations of mixing length and turbulent viscosity on the predicted gas velocity profile using the developed model.
- Validate the model predictions using the experimental data obtained at different superficial gas velocities and at different scale (effect of column diameter and internals).

3.3 Gas Velocity Experiments

Table 3.1 lists the experimental conditions used in this work. Originally, two sets of internals were investigated with: 5% and 22% occluded CSA. However, the 5% configuration had a negligible effect on the gas hydrodynamics compared to that in columns with no internals, as was shown by Youssef (2010), and hence these results are not discussed here. The configurations of the 5% and 22% internals in the 8-inch column are shown in Figure 3.1.

Table 3.1 - Experimental conditions of the gas velocity measurements

Exp #	D (cm)	Internals	U_g (cm/s) *Based on the free CSA*	H_D (cm)
1	19.00	No Internals	20	190
2	19.00	No Internals	30	190
3	19.00	No Internals	45	190
4	45.00	No Internals	20	267
5	45.00	No Internals	30	267
6	45.00	No Internals	45	267
7	19.00	22 % Internals	20	190
8	19.00	22 % Internals	30	190
9	19.00	22 % Internals	45	190

In the 8-inch and the 18-inch columns, the superficial gas velocity, U_g, ranged from 20 to 45 cm/s covering the churn turbulent regime which is the regime of interest for chemical industrial processes that require high productivities such as F-T synthesis. In addition, in all the experiments presented in this work, the superficial gas velocity was based on the free cross-sectional area of the column in order to accurately account for the effect of internals. In all experiments, the gas phase, compressed air, was introduced at the bottom of the

column through a perforated plate with holes arranged in triangular pitch, with a total free area of 1.09%, while tab water was used as the liquid phase in a batch mode.

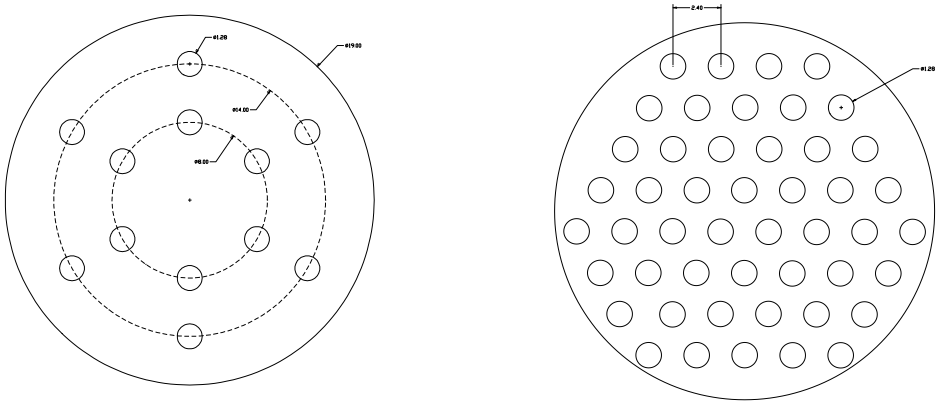

5% occluded area
Circular pitch: 2 concentric bundles of 4 and 7 cm radius (12 rods)
(Same as MeOH synthesis)

22% occluded area
Triangular pitch = 2.4 cm (48 rods)
(In the range of percentage of Fischer-Tropsch Synthesis)

Figure 3.1 - Configuration of internals in the 8-inch column

In this work, the 4-point optical probe was used to measure the radial gas velocity profile at different operating conditions. The details of how the gas velocity profile is obtained from the 4-point optical probe and the validation of the optical probe technique were shown by Xue (2004). In summary, the 4-point optical probe measures the instantaneous velocity vector of individual bubbles, their chord length and interfacial area. The 4-point optical probe can be placed facing downwards to measure the bubble dynamics of bubbles moving upwards, and facing downwards to measure the bubble dynamics of bubbles moving downwards. The probe data can then be analyzed to calculate the axial components of individual bubble velocities. In this work, the axial velocity of the gas phase at a given radial location is assumed to be equal to the mean axial bubble velocity at that location, defined as the time-averaged axial velocity of bubbles moving upwards and downwards. This assumption has been used by Deen et al., (2000) who measured the individual bubble velocities using PIV technique and averaged them to get the axial gas velocity profile. Later, Deen et al. (2001) employed a 3-D CFD model based on the Large Eddy Simulation (LES) in an Euler-Euler framework to simulate bubble columns. In their simulations, they showed that they were able to predict the axial gas velocity and the axial gas velocity fluctuations. This presents strong evidence that the average axial velocity of individual bubbles represents

the ensemble-averaged gas velocity in the Euler-Euler two-fluid model (Drew and Passman, 1998) used in the modeling of bubble columns. Moreover, Sokolichin et al. (1997) showed that the Lagrangian motion of the dispersed gas bubbles can be represented by the Eulerian approach if the gas phase equations were adequately discretized.

3.3.1 Results

The effect of superficial gas velocity based on the free cross-sectional area, U_g, on the time-averaged gas velocity profile in the laboratory scale 8-inch column is shown in Figure 3.2. In the column center, gas flows upward at velocities much higher than the liquid velocities (Kumar, 1994 and Degaleesan, 1997). In the region close to the wall, gas flows at much lower velocities, and in some extreme cases it can move downwards similar to the liquid velocity profile. Figure 3.2 also shows that the increase in U_g causes an increase in the gas circulation (proportional to the difference between the center-line gas velocity and the near-wall gas velocity), which is the same trend reported by Xue (2004) and Wu (2007). Many authors have reported the same effect of U_g on the liquid velocity profile (e.g: Degaleesan, 1997 and Ong, 2003), which suggests that the liquid velocity profile has a strong effect on the gas velocity.

In order to understand the effect of different operating conditions on the gas velocity profile, one should analyze the components of the local gas velocity. The gas velocity at any given location depends on two main factors: the local liquid velocity, u_l, and the local slip velocity, u_s, at that location:

$$u_g(r) = u_l(r) + u_s(r). \tag{3.1}$$

The slip velocity is a function of a number of variables including local gas holdup, drag, bubble diameter, pressure drop, and gas and liquid physical properties. Gupta (2002) derived an expression for the local slip velocity from the gas momentum equation as:

$$u_s(r) = \sqrt{\frac{4d_b(-\frac{dp}{dz} - \rho_g g)}{3C_D\rho_l(1-\varepsilon_g(r))}} \tag{3.2}$$

where, d_b is the average bubble diameter, $\frac{dp}{dz}$ is the axial pressure drop, C_D in the drag coefficient, and $\varepsilon_g(r)$ is the local gas holdup.

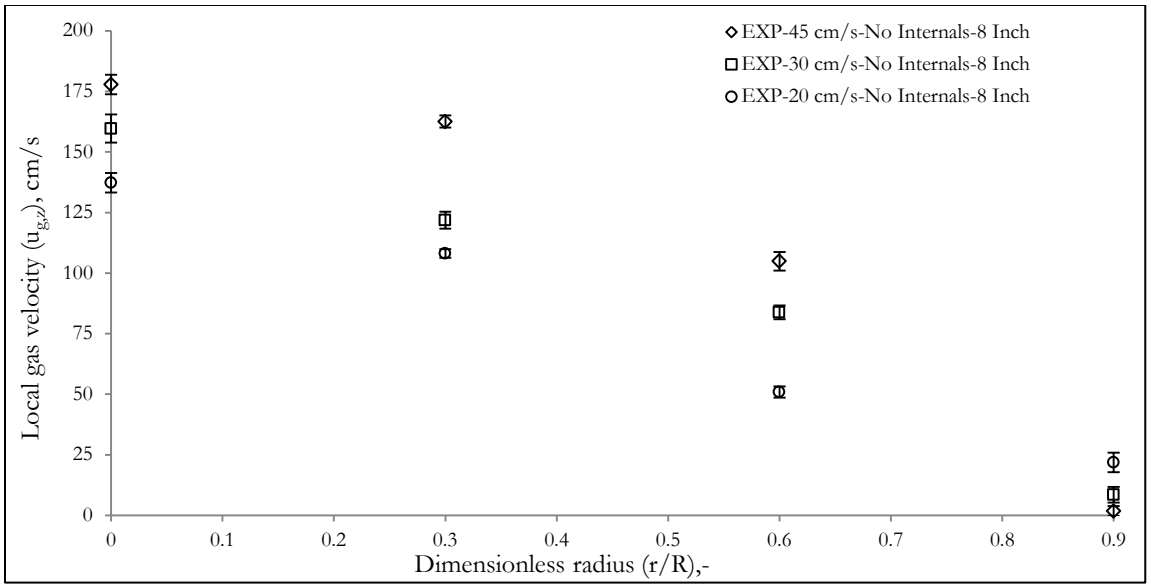

Figure 3.2 - Effect of superficial gas velocity (based on free cross-sectional area) on the gas velocity profile

The increase in the superficial gas velocity leads to an increase in the liquid velocity, an increase in the bubble size and an increase in the gas holdup. All these effects cause an increase in the gas velocity profile, as evident from Equation (3.2). Section 3.4 provides more details on the effects of different variables on the gas velocity profile using the developed gas velocity model.

The presence of internals was found to affect the shape of the gas velocity profile in bubble columns. Figure 3.3 shows that the presence of internals that occupy 22% of the cross-sectional area causes an increase in the centerline gas velocity, while there is a much lesser effect at the other radial positions. A similar trend was also reported for the liquid velocity profile by Bernemann (1989), Chen et al. (1999), and Forret et al. (2003), where the presence of internals was found to increase the steepness of the liquid velocity profile. The increase in the liquid velocity in the column center reported by other researchers is most probably caused by the observed increase in the centerline gas velocity in the presence of internals which is mainly due to the decrease in turbulent intensity in presence of internals (Chen et al., 1999, Forret et al., 2003, and Larachi et al., 2006). However, this effect is not straightforward, since the presence of internals also causes a decrease in the average bubble size, which one might expect to decrease gas velocity. The experimental results show that the effect of the decrease in turbulent intensity outweighs the decrease in bubble diameter

only near the column center, leading to an overall increase in the centerline gas velocity, whereas both effects seem to balance at the other radial positions.

Figure 3.4 shows the effect of the column scale on the radial gas velocity profile. It can be clearly seen that the increase in the column diameter increases the steepness of the gas velocity profile, where the gas velocity increases in the column center and decreases near the column wall. In addition, Figure 3.4 illustrates that in the 18-inch column the gas starts to flow downwards in the wall region. These are expected results, although they have never been reported in literature, since the increase in the column diameter allows the formation of large bubbles that churn at higher velocities than in smaller diameter columns.

The results shown in this section provide needed information on the time-averaged profile of the axial radial gas velocity that has not been studied systematically in the literature. The experimental data demonstrate that the gas velocity profile is significantly affected by the liquid velocity profile, turbulence, and column scale. The next section presents a simulation of the gas velocity profile in bubble columns using a simple but fundamentally based hydrodynamic model that takes into account all the previously mentioned variables. The experimental data presented in this section are used later to validate the model prediction.

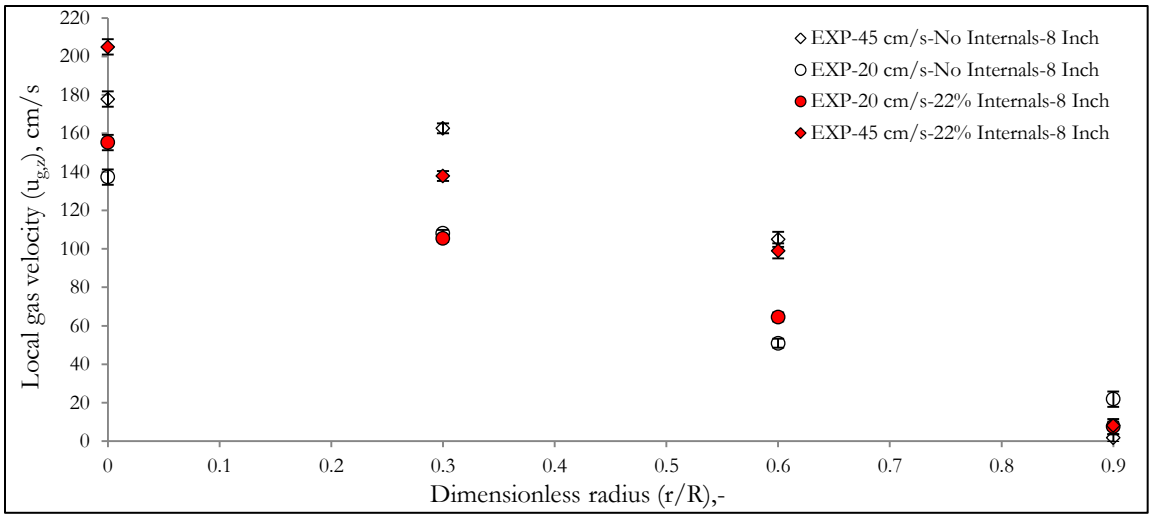

Figure 3.3 - Effect of internals on the gas velocity profile at different superficial gas velocities (based on the free cross-sectional area)

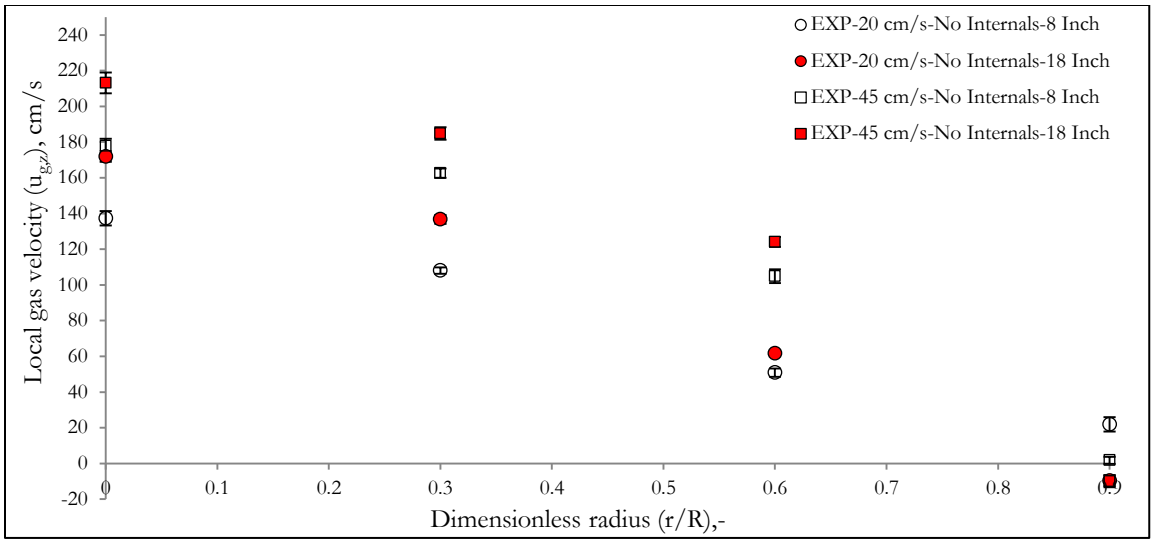

Figure 3.4 - Effect of column scale on the gas velocity profile at different superficial gas velocities (based on the free cross-sectional area)

3.4 The 1-D Gas Recirculation Model

A steady state 1-D two-fluid model is implemented to examine the ability of the existing correlations for eddy viscosity and mixing length, which are used in conjunction with the developed model to predict the experimentally measured gas velocity data obtained using the 4-point optical probe. The details of the model derivation are given in Gupta (2002) and are reviewed in Chapter 2.

In summary, the 1-D gas phase model is derived from the Euler-Euler two-fluid representation of the 1-D momentum balance equation for the gas and liquid phases (Drew and Passman, 1998). The liquid phase turbulence is closed either in terms of a turbulent viscosity correlation or a mixing length correlation. A number of investigators have reported similar approaches for modeling the liquid velocity profile (Ueyama and Miyauchi, 1979, Luo and Svendsen, 1991, Geary and Rice, 1992, and Kumar, 1994). In Gupta's model, the momentum equations were extended to calculate the radial profiles of the time-averaged axial gas and liquid velocities. Furthermore, the model predicts the average bubble diameter by solving the mass balance equation of the gas phase. Figure 3.5 is a simplified diagram of the model. The model developed by Gupta (2002) was primarily used as a sub-model to

predict the radial gas velocity profile for a mechanistic gas mixing model; however, the predicted gas velocity was never validated using gas phase velocity data in bubble columns.

The 1-D liquid-gas recirculation model requires as input the gas holdup radial profile and an eddy viscosity or mixing length correlation. The radial gas holdup profile was measured using the 4-point optical probe and fitted to the gas holdup equation developed by Kumar (1994) as follows:

$$\varepsilon_g(\xi) = \frac{\widetilde{\varepsilon_g}(m+2)}{m}(1 - c(\xi)^m) \tag{3.3}$$

The fitted parameters ($\widetilde{\varepsilon_g}$, c, and m) were used as input parameters to the 1-D liquid-gas recirculation model.

Figure 3.6 shows a typical experimental and fitted radial gas holdup profiles using equation (3.3) for experiments 1 to 3 as defined in Table 3.1. As shown in this figure, the empirical expression shown in equation (3.3) fits the radial gas holdup well.

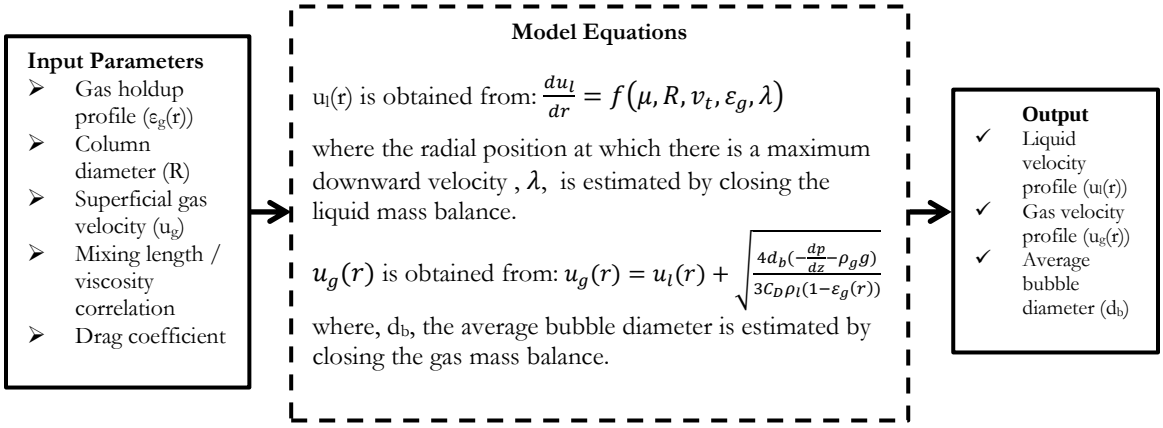

Figure 3.5 - Simplified diagram of the gas velocity model

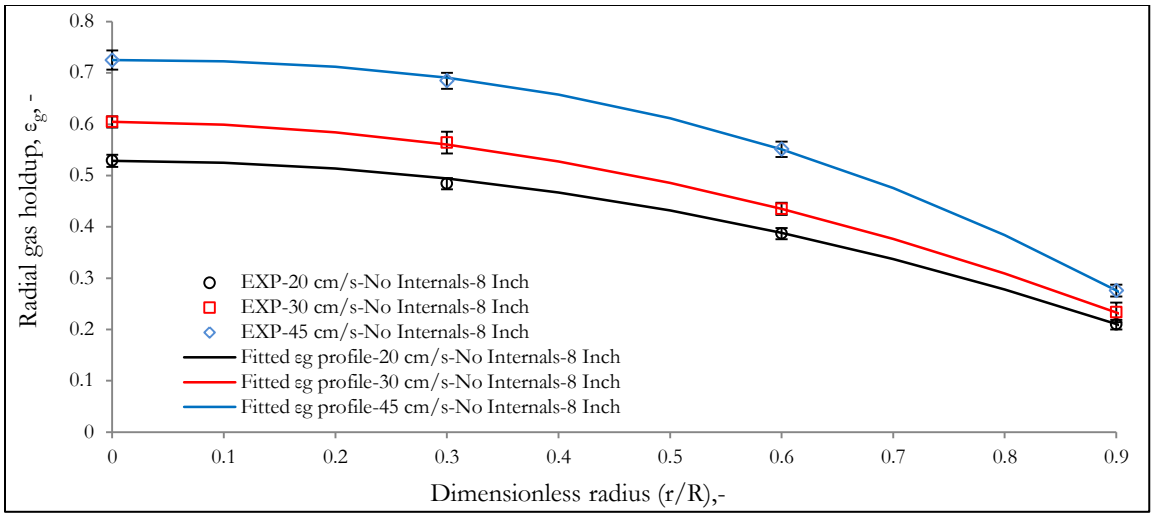

Figure 3.6 - Fitted holdup profiles for experiments 1 to 3

In this work, the drag coefficient (C_D) correlation developed by Tomiyama et al. (1995) was used:

$$C_D = \max\left[\frac{24}{Re_b}\left(1 + 0.15Re_b^{0.685}\right), \frac{8}{3}\frac{Eo}{Eo+4}\right] \tag{3.4}$$

where, $Eo = g(\rho_L - \rho_g)d_b^2/\sigma$, is the Eötvös number based on the bubble diameter and the liquid surface tension, and $Re_b = d_b|u_l - u_g|/v_L^m$ is the bubble Reynolds number. Notably, the use of other drag coefficient formulations will not affect the predicted gas velocity profile. This is because when the model closes the gas phase mass balance by iterating for d_b, it is actually iterating for the ratio d_b/C_D because C_D is a function of d_b (Equations 2.14 and 2.15). This means that the change in the value of C_D will only affect the predicted value of d_b but not the ratio d_b/C_D and hence, the gas velocity profile is not affected. Consequently, the use of any drag formulation that is based on the average bubble diameter will yield the same gas velocity profile and will only affect the predicted average bubble diameter or the predicted bubble size distribution.

3.4.1 Effect of turbulent viscosity and mixing length closures

The choice of a proper mixing length scale and turbulent viscosity correlation in bubble columns has been a topic for research for the last 50 years as these two approaches dominated the attempts to close the Reynolds stresses. The first approach is to propose a certain form for the turbulent kinematic viscosity, v_t, and use experimental data for the local

liquid velocity to fit an empirical constant in this form. Based on this approach, the shear stress is expressed as:

$$\tau_{l,rz}(\xi) = -\frac{\rho_l(v^m+v^t)}{R}\frac{du_{l,z}}{d(\xi)} \tag{3.5}$$

The second approach is to use the Prandtl mixing length theory to represent the turbulent viscosity and use the experimental data for the local liquid velocity to estimate the value of the mixing length. Based on this approach, the shear stress is expressed as:

$$\tau_{l,rz}(\xi) = -\frac{\rho_l v^m}{R}\frac{du_{l,z}}{d(\xi)} - \frac{\rho_l \ell^2}{R}\left|\frac{du_{l,z}}{d(\xi)}\right|\frac{du_{l,z}}{d(\xi)} \tag{3.6}$$

Different researchers in the field developed numerous correlations for the turbulent viscosity. The differences in the predicted magnitudes of turbulent viscosity by these correlations vary by as much as a factor of 6. Most of the correlations assume that the turbulent viscosity is a function only of column diameter (Miyauchi and Shyu 1970, Kojiima et al. 1980, Sekizawa et. al. 1983, and Ueyama and Miyauchi 1981). A few other researchers included the superficial gas velocity (Kawase and Moo-Young 1989, Miyauchi et al. 1981, and Riquarts 1981). All these correlations imply that the kinematic viscosity is constant over the entire flow field. Table 3.2 lists the existing eddy kinematic viscosity correlations used in this work.

Table 3.2 - Eddy kinematic viscosity correlations

Researcher	**Eddy kinematic viscosity correlations**
Miyauchi and Shyu, 1970	$v^t = 0.050D^{1.8}\rho_l^{-1}$
Ueyama and Miyauchi, 1979	$v^t = 0.128D^{1.7}\rho_l$
Kojima et al., 1980	$v^t = 0.053D^{1.77}\rho_l^{-1}$
Miyauchi et al.,1981	$v^t = 0.160D^{3/2}\rho_l^{1/6}$
Riquarts, 1981	$v^t = 0.011D^{3/2}U_g^{3/8}v_{m,l}^{-1/8}g^{3/8}$
Sekizawa et al., 1983	$v^t = 0.265D^{1.5}$
Kawase & Moo-Young, 1989	$v^t = 0.0295D^{4/3}U_g^{1/3}g^{1/3}$

The mixing length approach has been used by some researchers. Clark et al. (1987) and Devanathan et al. (1990) recommended the use of a single-phase length scale as measured by Nikuradse (Schlichting, 1979). Geary and Rice (1992) advocated the use of two different length scales depending on the origin of turbulence generation. For bubble induced turbulence, they defined the following relation for the mixing length in terms of the bubble diameter:

$$\ell(\xi) = d_b \varepsilon_g(\xi)/\bar{\varepsilon}_g \quad (3.7)$$

The local variation in the mixing length is accounted for by the presence of the local void fraction, while $\bar{\varepsilon}_g$ acts as a normalizing factor so that the integral of the mixing length is equal to the bubble diameter. For wall generated turbulence, the authors suggested using Nikuradse's single phase correlation. According to Geary and Rice (1992), the bubble scale dominates in small columns, while the single phase mixing length scale dominates in larger columns.

Kumar (1994) proposed an empirical form for the radial profile of the mixing length and used data that covered a wide range of conditions in bubble columns to fit the proposed mixing length form as follows:

$$v^t = \frac{\overline{u'_{l,z}u'_{l,r}}}{du_{l,z}/dr} = \ell^2 \left|\frac{du_{l,z}}{dr}\right|, \text{ and} \quad (3.8)$$

$$\ell(\xi) = \frac{a(1-\xi)}{(\xi+b)^c} + d(1-\xi)^e. \quad (3.9)$$

Kumar (1994) showed that there is no universal turbulent viscosity or mixing length correlation that is able to predict liquid velocity data developed at different operating conditions and that all the existing correlations are still unable to predict the effects of scale-up on turbulent viscosity under a wide range of conditions. This was mainly attributed to the inconsistent nature of the data base used to develop these correlations.

In this work, Nikuradse's mixing length was used to establish the upper bound of the predicted gas velocity since it was developed for single phase turbulence, Kumar's mixing length was used since it was developed based on a wide range of data covering different column diameters and superficial velocities similar to the ones used in this work, and finally Joshi's mixing length was used due to its popularity among researchers in the field. Table 3.3 lists the existing mixing length correlations used in this work.

Researcher	Mixing length
Nikuradse (Schlichting, 1979)	$\ell(\xi) = (0.14 - 0.08(\xi)^2 - 0.06(\xi)^3)R$
Kumar **(**1994**)**	$\ell(\xi) = \frac{a(1-\xi)}{(\xi+b)^c} + d(1-\xi)^e$

Joshi (1980)	$\ell = 0.16R$

Table 3.3 - Mixing length correlations

In order to assess the predictive capabilities of different turbulent viscosity and mixing length closures, correlations shown in Tables (3.2) and (3.3) were used as input to the gas velocity model, and the predicted radial gas velocity profile was compared to the experimental data.

Figure 3.7 and Figure 3.8 show the predicted radial gas velocity profile for different turbulent viscosity and mixing length correlations for experiment 2 (as defined in Table 3.1). The significant variation of the predicted profiles for different turbulent viscosities with respect to the measured data is obvious from Figure 3.8. It is evident that the only kinematic viscosity correlations that match the experimental data within deviations comparable to a reasonable experimental error are the ones developed by Kawase and Moo-Young (1989) and Riquarts (1981). Notably, these correlations are the only ones that incorporate the effect of superficial gas velocity in their estimates of turbulent viscosity. All the other correlations, which are a function of the diameter only, always lead to an over-prediction of the gas velocity. This indicates that they under-predict the value of the turbulent viscosity, most probably due to their failure to account for the extra bubble-induced turbulence at higher superficial velocities.

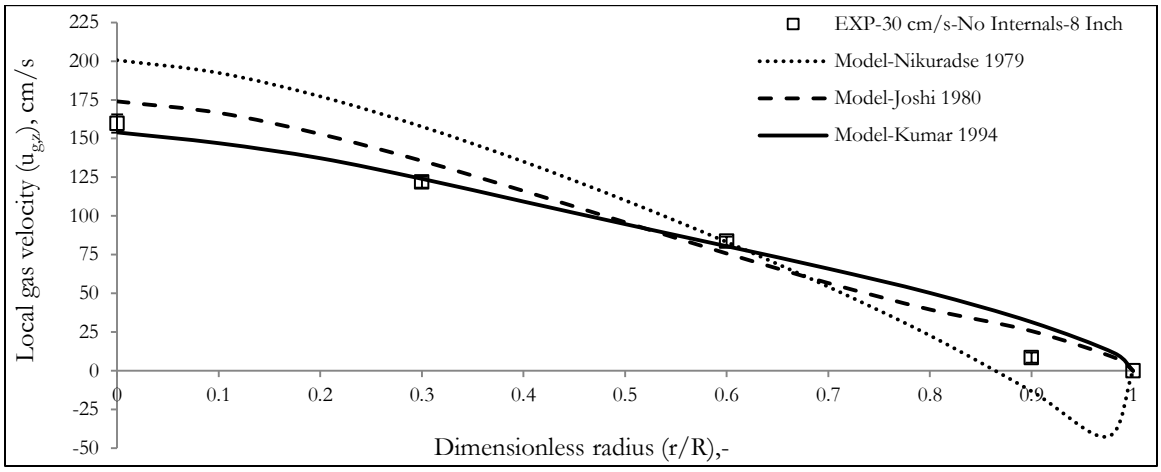

Figure 3.7 - Model predictions using different mixing length correlations

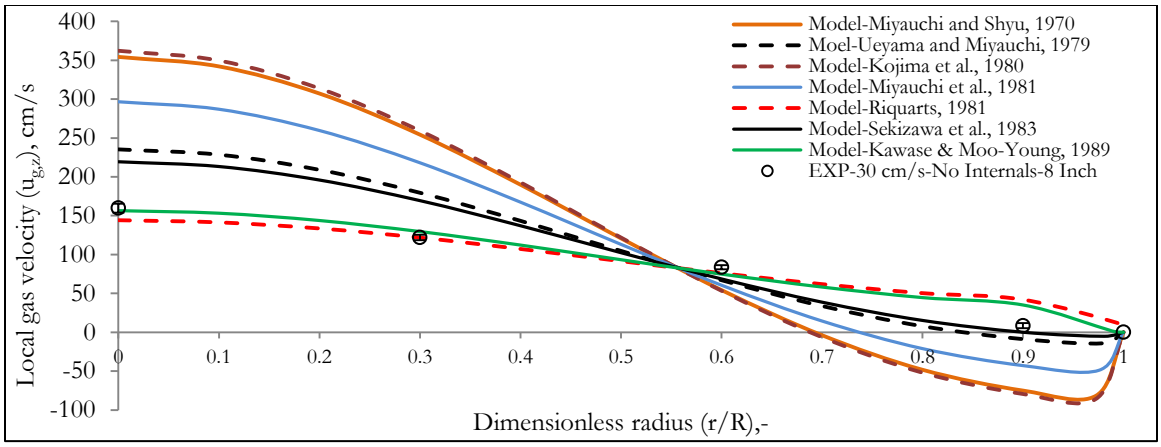

Figure 3.8 - Model predictions using different kinematic viscosity correlations

3.4.2 Effect of Internals

The presence of internals affects the liquid and gas velocity profiles because it affects gas holdup, bubble size and the turbulent intensity in the system (Youssef, 2010). Two competing factors affect the gas velocity profile in the presence of internals. On the one hand, the presence of internals causes an increase in the gas holdup, which decreases the area available for liquid flow causing an increase in the liquid circulation. The increase in the gas holdup also increases the area available for gas flow, which causes a decrease in the gas velocity. In addition, the presence of internals causes an increase in the shear stress in the bubble column, which increases the rate of bubble breakup leading to the formation of smaller bubbles that travel at slower velocities. On the other hand, the presence of internals decreases the turbulent intensity which causes an increase in the steepness of the gas and liquid velocity profiles. Several researchers have shown that the presence of internals increases the centerline liquid velocity and increases the steepness of the liquid velocity profile (Bernemann, 1989, Chen et al. 1999, and Forret et al., 2003). In this work, a similar trend was observed for the gas velocity profile, where the centerline gas velocity was found to increase in the presence of internals, as shown in Figure 3.3.

In order to simulate the effect of internals in the developed model, one needs to account for the decrease in the turbulent intensity caused by the presence of internals. Since the only parameter that quantifies the turbulent intensity in the current model is the mixing length, it

was proposed to modify the column diameter used in calculating mixing length, by multiplying the column diameter by the % free area:

$$D_{Free}^2 = D^2(1 - OA) \tag{3.10}$$

where OA is the fraction of the area occupied by internals and D_{Free} is the modified column diameter in the presence of internals, which will be used in the calculation of the mixing length correlations. This simple relation indicates that the mixing length being proportional to column diameter will decrease in the presence of internals, which is valid physically since the presence of internals will dampen the large turbulent eddies causing a decrease in the turbulent fluctuations, which are directly proportional to the mixing length from the Prandtl mixing length theory. This relation also assumes that the decrease in the turbulent intensity is proportional to the % occluded area by internals. This assumption was validated by the work of Bernemann (1989) on liquid velocity profiles. It is important to note that the objective of this work is to test the capability of the developed model to match the experimentally observed trends in the gas velocity profile in the presence of internals and not to find the best correlation that fits the data. The ability of the developed 1-D model to predict the gas velocity profile in the presence of internals is shown in Figure 3.9. Similar trends were also observed for all the other experiments in this work. The capability of the model to account for the presence of internals using the modified mixing length was investigated by comparing the model predictions to the experimental data at different superficial gas velocities, as shown in Figure 3.10

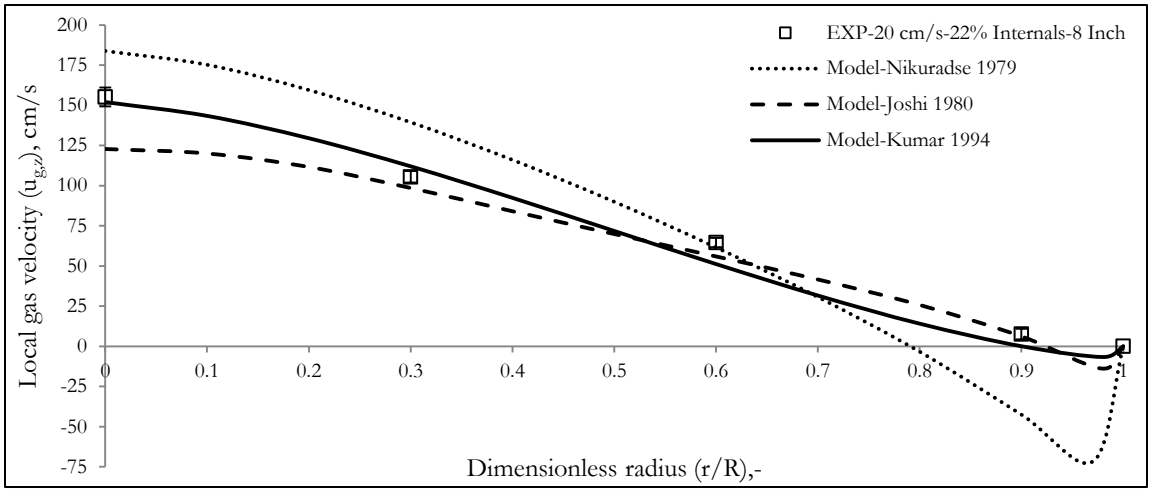

Figure 3.9 - Model predictions vs. experimental data in the presence of internals using different mixing length correlations

In addition to the prediction of the gas velocity profile, the model also provided some insight into the hydrodynamics of both phases, some of which were experimentally observed by other researchers. Based on the model simulations, the following effects are expected in the presence of internals:

- The pressure drop decreases due to the increase in the overall gas holdup (at the same superficial gas velocity).
- At the same superficial gas velocity, the model predicts a higher centerline liquid velocity and a steeper liquid velocity profile in the column with internals. These results qualitatively match the experimental results reported by Berneman (1989), Chen et al. (1999), and Forret et al., (2003) and the CFD model results of Larachi et al. (2006)). This effect is due to the decrease in the liquid holdup and turbulent intensity in the presence of internals. Unfortunately, no experimental data is available to quantitatively validate the predicted liquid velocities in this work.
- At the same superficial gas velocity, a decrease in the predicted average bubble diameter and in the average slip velocity is predicted in column with internals. This is due to the increase in the local liquid velocity profile which forces the model to predict smaller values for the slip velocity needed to satisfy the overall gas continuity.
- The drag coefficient is not affected significantly by the presence of internals. Although the decrease in the bubble diameter and in the slip velocity causes a decrease in the drag coefficient, the drag formulation of Tomiyama et al. (1995) used in this work is not a strong function of the slip velocity and of the bubble diameter, especially at high Eötvös numbers. While the presence of internals is expected to increase the drag on the bubbles due to the increased wall surface area, the drag also decreases due to the decrease in the bubble size. Based on model predictions, the net result seems to be an overall unaffected drag.

In summary, the model is able to match the experimentally observed trends in the gas velocity profiles in the presence of internals using the modified mixing length. Figure 3.10 shows the comparison between the model predictions and the experimental data for experiments 1, 3, 7, and 9.

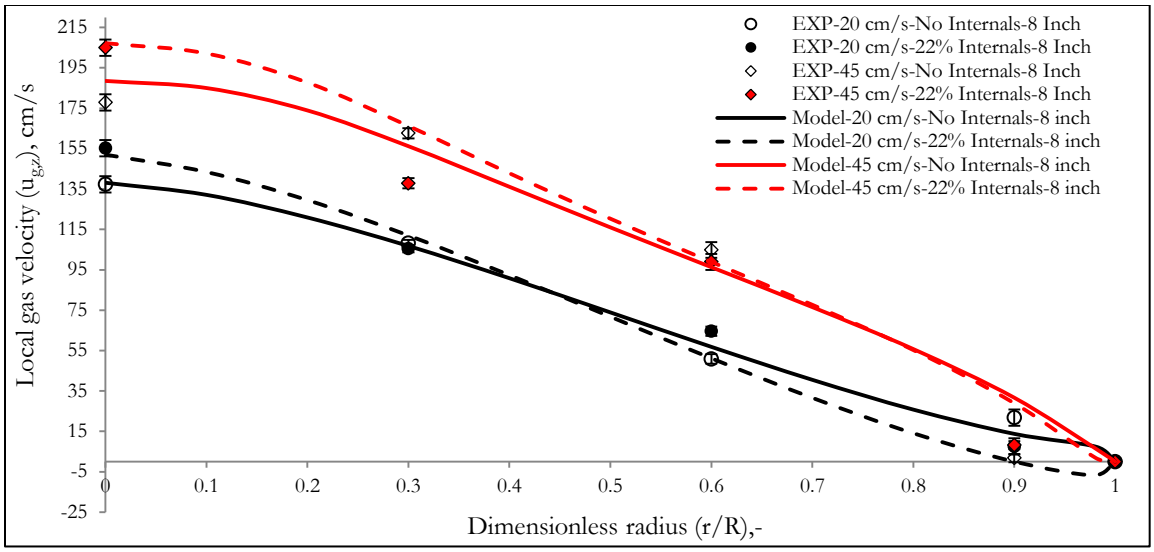

Figure 3.10 - Model predictions vs. experimental data in the presence of internals at different superficial gas velocities (based on the free cross-sectional area)

3.4.3 Effect of Scale

The column scale, within the two column diameters investigated in this work, was found to have a strong effect on the gas velocity profile, as shown in Figure 3.4. The available gas velocity data from columns of two different scales were used to further asses the capability of the developed model to account for the effect of scale on the gas velocity profile. Figure 3.11 shows the comparison between the experimental data and model predictions at 30 cm/s in the 18-inch column. Figure 3.12 shows the comparison between the model predictions and experimental data at different scales for different superficial gas velocities. It is evident from these figures that the model is able to capture the effect of scale. In fact, the model predictions fit the experimental data in the large-scale column better than in the small-scale column. The model also predicts an increase in the liquid circulation with the increase in the column scale, which was experimentally validated by many researchers in the field (Bernemann, 1989, Kumar, 1994, Degaleesan, 1997, etc). The increase in column diameter causes an increase in liquid circulation and in turbulent intensity. This consequently leads to the observed increase in gas circulation. Moreover, as mentioned earlier, the increase in the column diameter allows the formation of larger bubbles which churn at higher velocities in the column center.

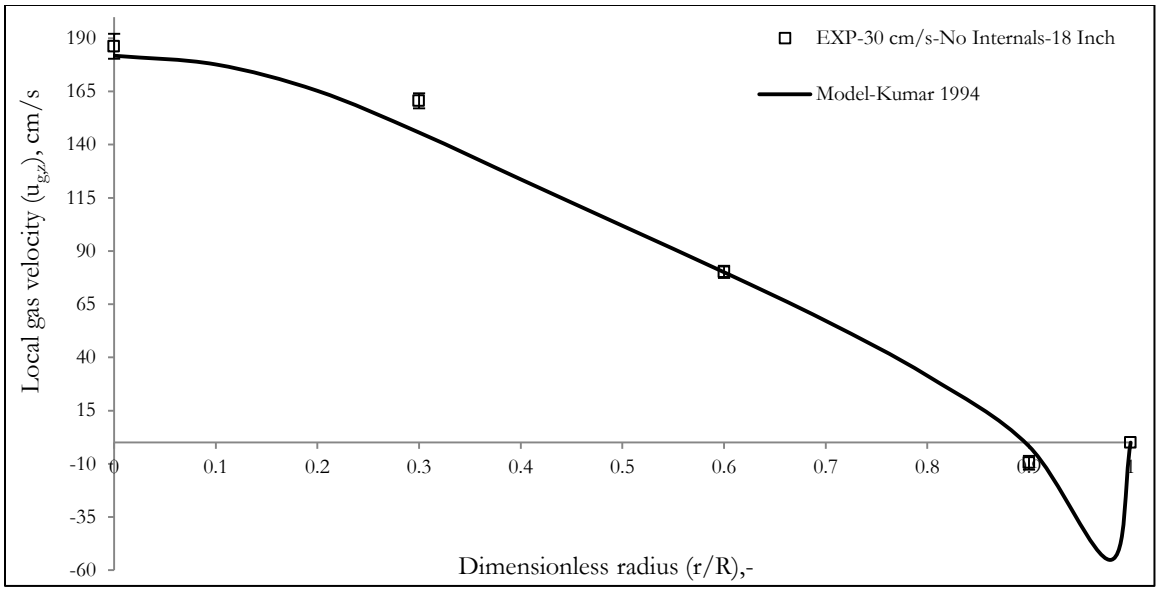

Figure 3.11 - Model predictions vs. experimental data in the 18 inch column

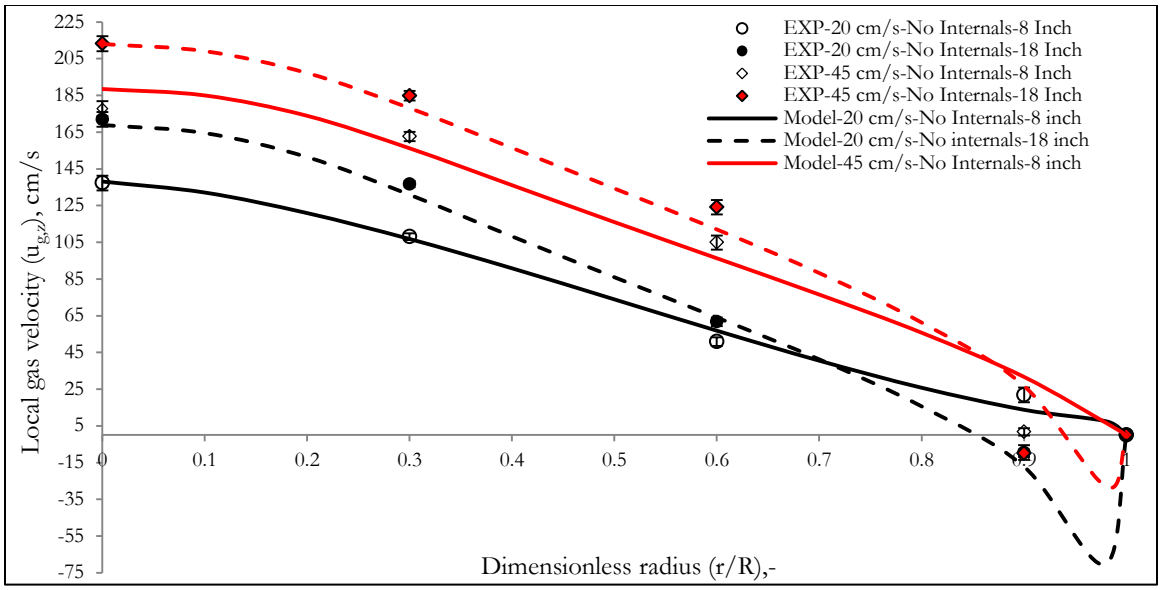

Figure 3.12 - Model predictions vs. experimental data in different scale columns at different superficial gas velocities (based on the free cross-sectional area)

3.5 Remarks

In this chapter, the effects of superficial gas velocity, internals, and column scale on the gas velocity profiles in bubble columns were investigated. It was shown that these variables have a strong effect on the gas velocity profile. In order to better understand how these variables affect the gas velocity profile, a gas velocity model that takes all these variables into account was assessed and validated using the available experimental data. This model was shown to

provide, for the first time, confident means for predicting the gas velocity profiles under different operating conditions in the churn turbulent regime. The main conclusions of this chapter can be summarized as follows:

- The experiments showed that the steepness of the gas velocity profile was affected by the superficial gas velocity, internals, and column diameter. The increase in superficial gas velocity caused an increase in the steepness of the gas velocity profile and an increase in gas circulation.
- The presence of internals was found to increase the centerline gas velocity, while the increase in the column diameter significantly enhanced gas circulation both in the presence and the absence of internals.
- Simulations using the 1-D gas velocity model provided good predictions of the gas velocity profile when a proper closure for turbulence was used in the model equations. The gas velocity model simulations indicated that the mixing length correlations were able to better predict the gas velocity profile, where Kumar's mixing length was found to be the best mixing length correlation to fit the gas velocity data in this study. The gas velocity model was capable of simulating the gas velocity profile at different operating conditions and different column diameters both in the presence and the absence of internals.
- The ability to predict the gas velocity profiles either in the presence of internals or for different column diameters enhances the understanding of the gas hydrodynamics and its effect on gas mixing and mass transfer, which will eventually improve the predictions of conversion and selectivity. In the next chapters, the importance of the knowledge of the gas velocity profile is illustrated by integrating the gas velocity sub-model predictions with a 2-D gas mixing model to predict the extent of gas phase mixing in bubble columns with and without internals.

Chapter 4 - Gas Mixing in Bubble Columns: Experiments and Modeling

In this chapter, the effect of superficial gas velocity, internals, and column scale on gas phase mixing is investigated using a well-developed gas tracer technique. The intent is to couple the experimentally obtained residence time distribution (RTD) of the gas phase at different conditions with the gas velocity profile measured at the same conditions to quantify the contribution of different mixing mechanisms to the overall axial gas mixing based on a 2-D convection diffusion gas mixing model.

4.1 Introduction

Gas phase mixing is one of the important hydrodynamic parameters to be considered in the scale-up of bubble columns, as it significantly affects reaction rates and product selectivity (Deckwer, 1976). The extent of gas phase mixing is a complex function of the superficial gas velocity, liquid phase properties, and reactor geometry. As mentioned earlier, there are no public records of gas tracer studies in bubble columns with vertical internals, and only very limited tracer studies in bubble columns in general have been reported. Previous work on the effect of internals has shown that their presence affects the hydrodynamics of liquid and gas phases, extent of liquid mixing, bubble dynamics, and turbulent intensity. All these effects are expected to significantly affect the extent of gas phase mixing. Therefore, this work addresses the effect of internals on the overall axial gas mixing. As mentioned in chapter 2, the extent of the overall axial gas phase mixing can be quantified by the dimensionless variance of the RTD curve of the gas phase at the column exit or by the corresponding value of the axial gas Péclet number (Pe) calculated at the column exit.

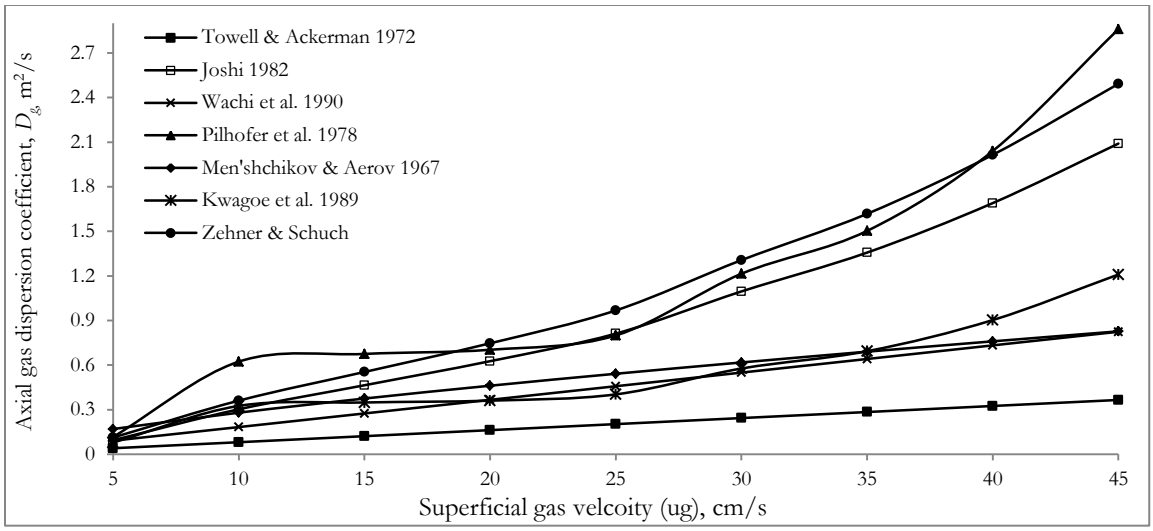

Figure 4.1 - Predictions of the axial dispersion coefficient, D_g, in the 8-inch column by different correlations

In addition to paucity of experimental data on gas phase mixing in bubble columns with internals, there is also a lack of fundamental understanding of the effects of different variables on gas phase mixing. This often leads to the development of correlations for gas phase mixing, which are not based on rational physical models. The net result is that such correlations are unreliable as can be clearly seen from the significant discrepancies in predictions of different correlations for the axial dispersion coefficient of the gas phase (D_g), especially at high superficial gas velocities (Figure 4.1). In order to accurately simulate the gas phase mixing, one needs to account for the dominant mixing mechanisms that control gas phase mixing and understand the effect of the change in operating conditions on these mechanisms. This work attempts to simulate the gas phase mixing using a 2-D convection diffusion model, which is expected to better quantify the effects of convective mixing and turbulent dispersion.

4.2 Objectives

The above brief overview indicates that there is a lack of understanding of gas phase mixing in bubble columns especially in the presence of internals. Therefore, the main objective of this chapter is to enhance this understanding by:

- Investigating the effect of vertical cooling internals on the extent of the overall axial gas phase mixing by measuring the values of the axial dispersion coefficient of the gas phase (D_g) and the corresponding axial gas Péclet numbers (Pe) at different

superficial gas velocities and different column scales (diameters) using a well-developed gas tracer technique.

- Developing a gas phase mixing model that accounts for the contribution of convective mixing and turbulent dispersion on the axial mixing of the gas phase and using this model to understand the effect of different operating conditions on the turbulent mixing parameters.
- Relating the axial gas dispersion coefficient to the key fluid dynamic parameters, determining these parameters experimentally, and establishing the effect of operating conditions on such parameters and on the axial gas dispersion coefficient.

4.3 Gas Phase Mixing Experiments

4.3.1 Experimental Setup

Table 4.1 shows the experimental conditions used in this work to study the effect of superficial gas velocity, internals, and column diameter on the gas phase mixing. In the 8-inch lab-scale column, the superficial gas velocity ranged from 5 to 45 cm/s, which covers both the homogenous and the churn turbulent regimes, while in the 18-inch pilot-scale column, the superficial gas velocity ranged from 20 to 45 cm/s covering only the churn turbulent regime. In all experiments, the gas phase, compressed air, was introduced at the bottom of the column, while tab water was used as the liquid phase in a batch mode at a constant dynamic height.

Table 4.1 - Experimental conditions of the gas tracer measurements

D_c (cm)	Internals (% CSA)	U_g (cm/s)	H_D (cm)
19.00 (8 inch)	No Internals & 22% Internals	5,10,15,20,25,30,35,40,45	190
45.80 (18 inch)	No Internals & 25% Internals	20,25,30,35,40,45	266

* All experiments were carried out at ambient temperature and pressure using air-water system

As mentioned in the previous section, in all the experiments done in this work, the superficial gas velocity, U_g, was calculated based on the free cross-sectional area of the column in order to address the effect of the internals accurately and eliminate the effect of the decrease in the cross-sectional area resulting from the presence of internals. Thus, the

area used to calculate the superficial gas velocity in the presence of internals was determined as follows:

$$Area = \frac{\pi}{4}(D^2 - n_t d_t^2) \tag{4.1}$$

where n_t is the number of tubes and d_t is the diameter of each tube.

4.3.2 Gas Tracer Technique

A well designed gas tracer technique was used to measure the residence time distribution (RTD) of the gas phase (Han, 2007). The gas tracer unit consists of a gas analyzer, gas pump, and a PC with data acquisition software. The gas analyzer is a GOW-MAC 20 series binary analyzer, which contains a flowing reference thermal conductivity detector (TCD). A GOW-MAC 59-300 pump was used to draw the gas sample out of the reactor to the TCD. The response from the TCD was amplified, converted to digital signals, and recorded as time-series data at a sampling frequency of 10 Hz.

The tracer technique used to measure the RTD in this study extends to the one developed by Han (2007). This technique offers an advantage over other gas tracer techniques since it yields an accurate estimation of the RTD of the gas phase because it accounts for the extra dispersion that occurs due to the non-ideal tracer injection and extra dispersion in the plenum, sampling lines, and analysis system. The gas tracer injection at the plenum inlet does not create a perfect delta function for an impulse injection (or an ideal step in the step change method) at the plenum outlet, which is the input boundary for the reactor, due to the mixing of the gas phase in the plenum. Similarly, due to the dispersion in the sampling lines, analytical components, and space above the dynamic liquid surface (disengagement zone), the response measured by the gas detection system does not represent the actual tracer response at the reactor disengagement level which is the gas outlet of the gas-liquid mixture in the reactor. In order to compensate for these extra dispersion effects, a convolution method was applied (Levenspiel, 1972) by which the response of the actual system of interest is convoluted with the response of the extraneous components to yield the measured response. Some studies have employed similar methods to account for the extra dispersion in the sampling lines and analytical system (Joseph et al., 1984, Wachi et al., 1990, Shetty et al., 1992, and Kantak et al., 1995). However, none of them accounted for the extra

dispersion in the plenum and the non-ideal tracer injection. Neglecting these end effects usually leads to a distortion in the experimental results (Kaštánek et al., 1993) and inaccurate RTD measurements, resulting in findings and correlations limited to the experimental conditions of the particular studies.

The gas tracer technique (Han, 2007) involves two injecting ports and three sampling ports, as shown in Figure 4.2. The tracer was injected at the center of the inlet gas line (I1) and at the gas-liquid disengagement surface (I2), while the sampling was done at: 1) the gas inlet (S1, view A, Figure 4.1) close to port I1, 2) the pores of the gas distributor (S2), and 3) the neck of the collecting cone above the disengagement surface (S3). The collecting cone covered about half the cross-sectional area of the column to get a radially averaged response at the column exit. The RTD was measured at different radial positions at the disengagement level (by moving the cone radially) in both the homogenous and heterogeneous regimes. However, there were negligible differences in the responses obtained at different radial positions, confirming that a cup mixing average sample was always achieved.

The pulse input of the tracer was introduced to the plenum using a solenoid valve controlled by digital timers (injecting time 0.1 s). Gas was sampled continuously at the indicated sampling ports through thin nylon tubes (1/16" inner diameter) under a vacuum generated by a vacuum pump. Using the pre-mentioned injection and sampling ports, four measurements (i-iv) were conducted at each experimental condition. Table 4.2 shows the different ports of tracer injection and gas sampling used for the four measurements and the gas dispersion effects associated with each measurement (Han, 2007). Finally, gas phase axial dispersion was determined by model fitting and a convolution method, as discussed in the next section.

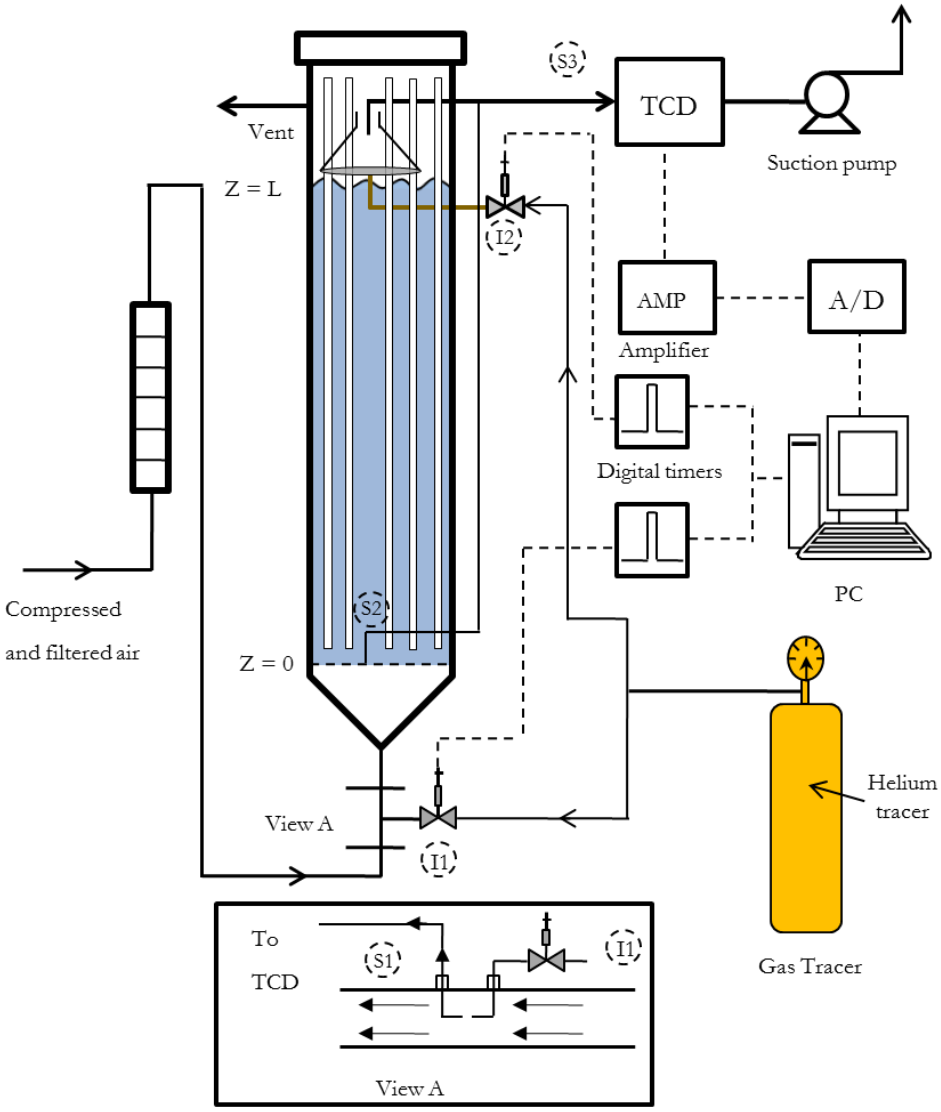

Figure 4.2 - Schematic diagram of the gas tracer experiment

Table 4.2 - Different ports used for tracer injection and gas sampling

Measurement	Tracer injection	Sampling	Dispersion zones measured
C(i)	I1	S1	Sampling/analytical system
C(ii)	I1	S2	Plenum + sampling analytical system
C(iii)	I2	S3	Sampling/analytical system
C(iv)	I1	S3	Plenum + reactor + sampling/analytical system

I1, I2: Injection ports; S1, S2, S3: sampling ports. All locations indicated in Figure 4.2
* Table from Han (2007)

It is important to note that the application of the convolution method is valid only when the sub systems are completely independent, which means that there is practically no back-mixing between them (i.e. convective unidirectional flow dominates at the boundaries between the sub systems). This assumption was checked at the entrance boundary between

the plenum and the reactor by calculating the orifice Reynolds number. The orifice Reynolds numbers in the 8-inch and the 18-inch columns ranged from 3,600 to 126,000 which means that the distributor operates in the jetting regime (Degaleesan, 1997). This indicates that the flow through the distributor holes is unidirectional and there is no possibility of back-mixing of the tracer to the plenum. This argument was also investigated experimentally by injecting the tracer, at different experimental conditions, just above the plenum and measuring the tracer concentration inside the plenum (Figure 4.3(a)). These experiments showed that there was no back-mixing of the tracer through the distributor holes. The same experiments were repeated at the column exit to ensure the validity of the convolution method at the exit boundary. This was done by injecting the tracer at the sampling point and measuring the tracer concentration at the liquid surface (Figure 3.4 (b)). Similar to the entrance boundary, no tracer was detected at the liquid surface, which indicates the absence of back-mixing between the two convoluted systems. This was made possible because the collecting cone was designed to be open at the top to keep a high gas flow rate passing through it, preventing any back-mixing of the tracer.

In this work, some modifications were implemented to improve the accuracy of the gas tracer technique. Firstly, the gas-liquid separator used by Han (2007) to prevent the liquid traces in the sampling line to the detection system was removed because there was significant mixing in this separator due to the low flow rate of the tracer through the separator. This mixing in the gas-liquid separator causes uncertainties in the parameter estimation since the variance of the RTD of the separator is comparable to the variance of the RTD of the bubble column itself. The flow of liquid to the detection system was prevented by carefully monitoring the sampling lines visually during the experiment. The vacuum pump was stopped momentarily if any liquid trace was observed in the sampling lines. The second modification was to place the detection system close to the column exit. This insured that the mean residence time and variance of the tracer in the sampling lines were as small as possible. The implementation of these modifications caused a significant reduction in the mean residence time and the variance of the sampling and analytical systems. In all of the gas tracer experiments carried out in this work, the variance of the RTD of the plenum, sampling lines and analytical system (measurement C(ii)) was always

less than 20% of the variance of the RTD of the whole system (measurement C(iv)) which allows more accurate estimation of the extent of gas mixing in the column.

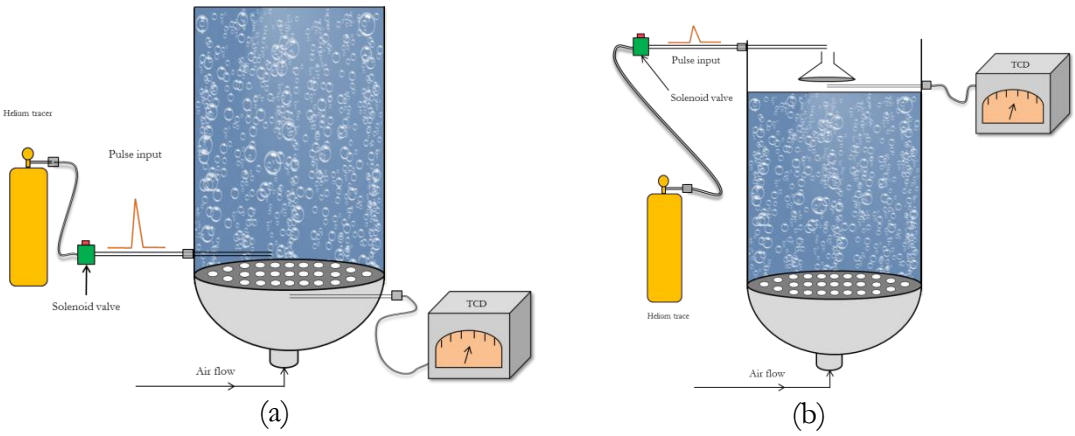

Figure 4.3 - Validation experiments for the gas tracer technique

4.3.3 Data analysis

The experimentally measured RTD was analyzed using a 1-D, axial dispersion model to estimate the value of the axial dispersion coefficient (D_g). The obtained value of D_g and the corresponding axial gas Péclet number provided the quantification of the extent of the overall axial gas dispersion at that particular operating condition.

In this work, the tracer input to the column was not modeled as a delta function. The input to the axial dispersion model, at the gas distributor boundary, was rather modeled as the output response of the plenum to the pulse input of the tracer at the plenum boundary. The details of the model formulation are shown below.

a) Plenum:

The gas distributor plenum was modeled as a CSTR. The output response of the plenum,$C_{g,p}$, was used as the input concentration to the bubble column. Pulse injection to the plenum can be represented by:

$$\frac{dC_{g,p}}{dt} = -\frac{1}{\tau_p} C_{g,p} \tag{4.2}$$

where τ_p is the residence time of the gas phase in the plenum and is obtained by regression. The solution of equation (4.2) is shown in equation (4.3), with initial condition $C_{g,p}(0) = C_{inj}$ used as the input to the reactor model.

$$C_{g,p} = C_{inj} e^{-(\frac{t}{\tau_p})}. \quad (4.3)$$

Measurements (i) (I1-S1) and (ii) (I1-S2) in Table 4.2 represent the dispersion in the injection lines and analytical systems and the dispersion in the plenum section plus the injection lines and analytical systems, respectively. In measurement (i) (I1-S1), the tracer input profile can be considered as an ideal pulse because the sampling tube S1 was placed very close to the injection nozzle (Figure 4.2, view A). Figure 4.4 shows an example of measurements (i) (I1-S1) and (ii) (I1-S2), indicating that measurement (i) (I1-S1) has some apparent spreading which confirms that some dispersion occurs in the sampling lines and analytical system. Sampling lines from S1 and S2 had the same length and inner diameter and the gas velocity in both lines was fixed using a Rotameter in the analytical device. Hence, the dispersion in the sampling line from S1 can be considered identical to that of S2. The impulse response obtained from measurement (i) (*C(i)*) was convoluted with the CSTR model and the model prediction (C^*_{in}) was compared against measurement (ii) (*C(ii)*), where τ_p was optimized by minimizing the mean squared error in the time domain. The estimated values of τ_p ranged from 0.4-2 seconds and were always slightly higher (~5-15% higher) than the actual residence time of the gas phase inside the plenum which was calculated from the gas volumetric flow rate and the volume of the plenum. This indicates that the plenum deviates from the ideal CSTR performance. However, the CSTR assumption is considered the best approximation available for the mixing pattern in the plenum. Other models like PFR or ADM may introduce more significant errors if used and are not able to predict the RTD of the plenum. As shown in Figure 4.4, there is an acceptable fit between *C(ii)* and C^*_{in}, confirming that the CSTR approximation is able to predict the extent of gas mixing in the plenum.

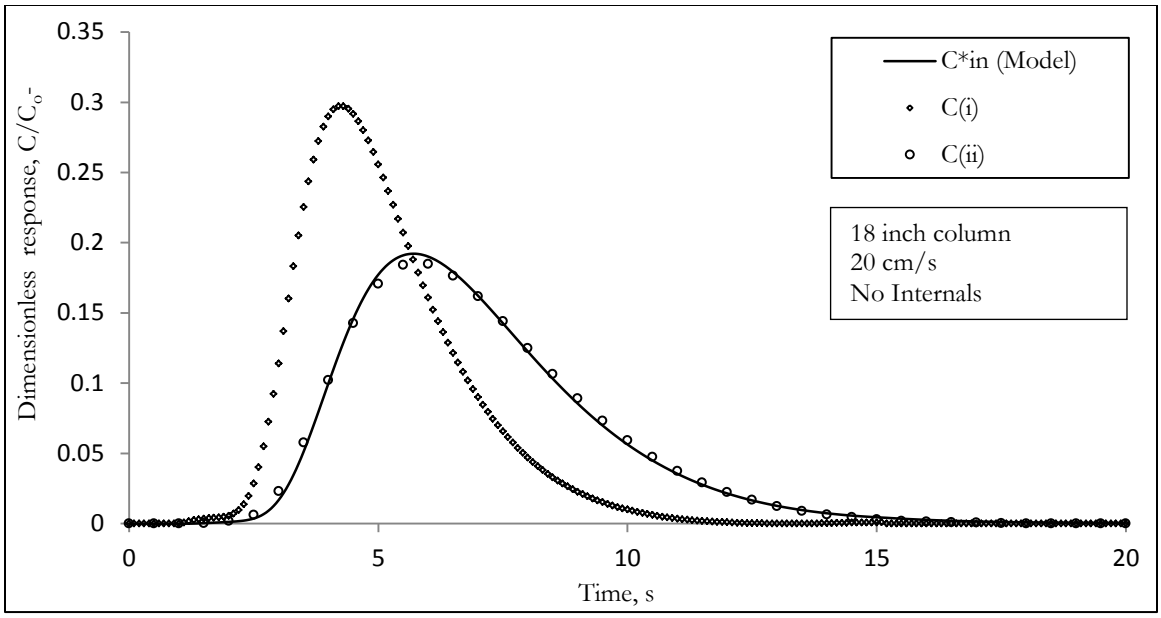

Figure 4.4 - Normalized gas tracer concentration at the distributor with the CSTR model fit for the plenum

b) Bubble column:

A mass balance around a differential segment of the column, in the absence of chemical reaction and radial variations, yields the 1-D axial dispersion model, represented by:

$$\frac{\partial C_g}{\partial t} = D_g \frac{\partial C_g}{\partial z^2} - U_g \frac{\partial C_g}{\partial z} \tag{4.4}$$

where the effect of mass transfer can be neglected under the conditions of this experimental study (Appendix 1). Danckwerts boundary conditions were used for the closed-closed boundaries, since there was a sufficient pressure drop across the gas distributor, and the cone covered most of the reactor cross-section at the outlet.

$$Z = 0: U_g C_{g,p} = U_g C_g\big|_{Z=0} - D_g \frac{\partial C_g}{\partial z}\Big|_{Z=0}, \text{ and} \tag{4.5}$$

$$Z = L: \frac{\partial C_g}{\partial z}\Big|_{Z=L} = 0 \tag{4.6}$$

where $C_{g,p}$ in equation (4.5) was obtained from equation (4.3) using the fitted τ_P. The initial condition is given by: $t=0,\ C_g=0$. The superficial gas velocity, U_g, was known from the controlled flow rate, and the overall gas holdup, ε_g, was measured by observing the overall dynamic bed expansion. Measurement (iii) (I2-S3) represents the dispersion in the sampling lines and analytical system at the column exit, and measurement (iv) (I1-S3) represents the dispersion in the bubble column plus all the sampling line and the analytical system. Using

$C_{g,p}$ from equation (4.3), as the input tracer concentration, the reactor model yields an output profile $C_{out}(t)$ at the disengagement level. The reactor response ($C_{out}(t)$) is then convoluted with *C(iii)* yielding the overall reactor model convoluted response (C_{out}*) :

$$C^*_{out}(t) = \int_0^t C_{out}(t').C_{iii}(t-t')dt' \tag{4.7}$$

C_{out}* is the compared against the measured response of the whole system (*C(iv)*), where D_g was fitted by minimizing the mean squared error in the time domain, defined as:

$$Error = \frac{1}{n}\sum_{i=1}^{n}[C^*_{out}(t_i) - C_{(iv)}(t_i)]^2 \tag{4.8}$$

The convolution of *C(iii)* and $C_{out}(t)$ is valid since both systems can be assumed 'closed' (independent) due to the high flow rate of the tracer at the cone neck, which eliminates the opportunity for back-mixing between the two convoluted systems as shown earlier in this chapter. Figure 4.5 shows the model fits of C_{out}* and *C(iv)* in both the 8-inch and the 18-inch columns, respectively.

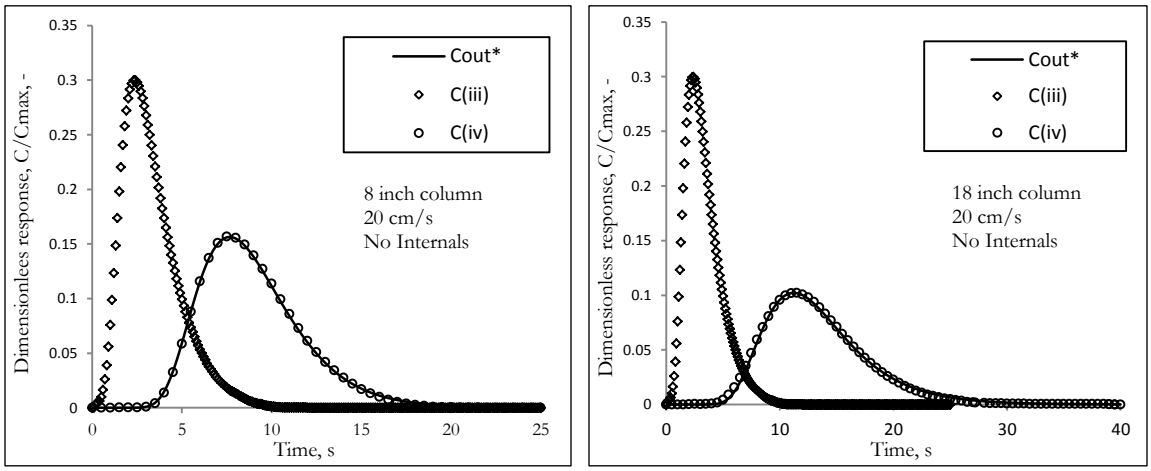

Figure 4.5 - Gas tracer response curves at the column outlet with ADM fit

4.3.4 Effect of Internals on the Overall Axial Dispersion on the Gas Phase

The major thrust of the gas tracer experiments is to illustrate the effect of U_g and internals on the extent of the overall axial mixing of the gas phase. In addition, some results related to the measurement of ε_g are also presented. In this study, ε_g was measured by recording the

dynamic bed expansion ($\varepsilon_g = (H_D - H_S)/H_D$). Figure 4.6 shows the gas holdup measurements at different superficial gas velocities covering both the homogenous and churn turbulent flow regimes in the presence and absence of internals. On the basis of repeated measurements and uncertainties in the establishment of aerated dispersion column height, an average uncertainty of ± 5% is assigned to ε_g values. The average gas holdup was found to increase with the increase in U_g both in the presence and absence of internals. The presence of internals was found to increase the average gas holdup compared to columns with no internals. This result is similar to the findings obtained by other researchers (Roy et al., 1989, Pradhan et al., 1993, and Youssef, 2010) who carried-out their investigation in bubble columns using vertical tubes as internals. The presence of internals increases the rate of breakup of bubbles, leading to the formation of smaller bubbles which have a high residence time in the column, causing an increase in ε_g (Pradhan et al., 1993 and Youssef, 2010).

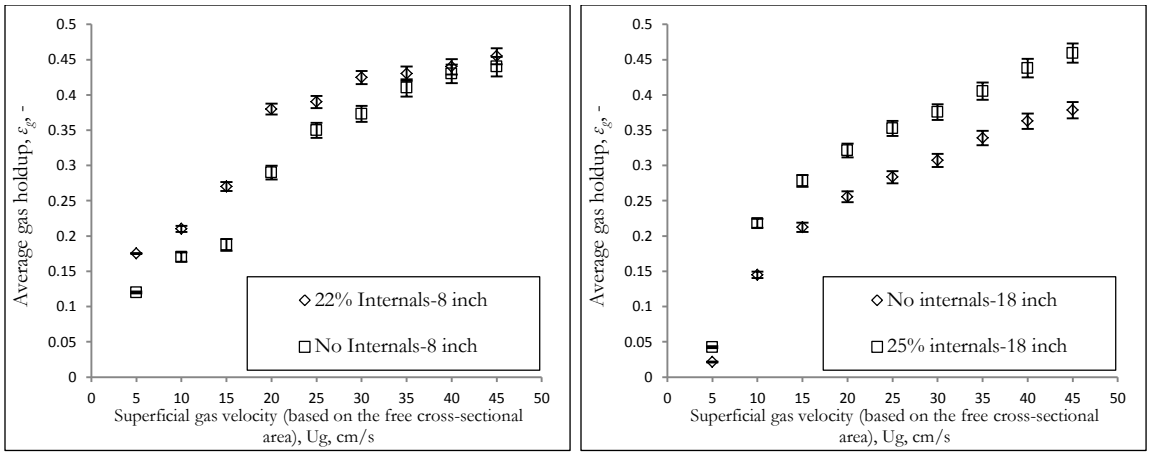

Figure 4.6 - Average gas holdup at different superficial gas velocities (based on free cross-sectional area) and different column diameters in absence and presence of internals

Figure 4.7 shows the effect of U_g and internals on the gas phase axial dispersion coefficient in the 8-inch and the 18-inch columns. D_g increased with increasing U_g in both columns in the presence and absence of internals, which is the same trend observed by other investigators (Towell and Ackerman, 1972, Field and Davidson, 1980, and Kantak et al., 1995) in bubble columns without internals and reflected by different D_g correlations. The increase in D_g with increasing superficial gas velocity can be explained by investigating the causes of the overall axial gas dispersion, which lumps two distinct physical processes: large scale circulation and turbulent dispersion. The increase in U_g causes an increase in the large

scale gas circulation (just as it causes the increase in liquid circulation), leading to a further increase in the residence times of small bubbles in the column due to their longer entrainment by the circulating liquid (Kaštánek et al., 1993). In addition, the increase in U_g leads to an increase in the power input to the column, thus increasing turbulence, which causes the enhancement of turbulent dispersion in the column.

Figure 4.7 also shows that the presence of internals reduces D_g significantly especially at higher superficial gas velocities in both the lab-scale (8-inch) column and the pilot scale (18-inch) column. Such an effect has never been reported in the open literature. Furthermore, the increase in the Péclet number (Pe) values in the presence of internals suggests that the overall axial gas mixing is reduced in their presence as shown in Figure 4.7.

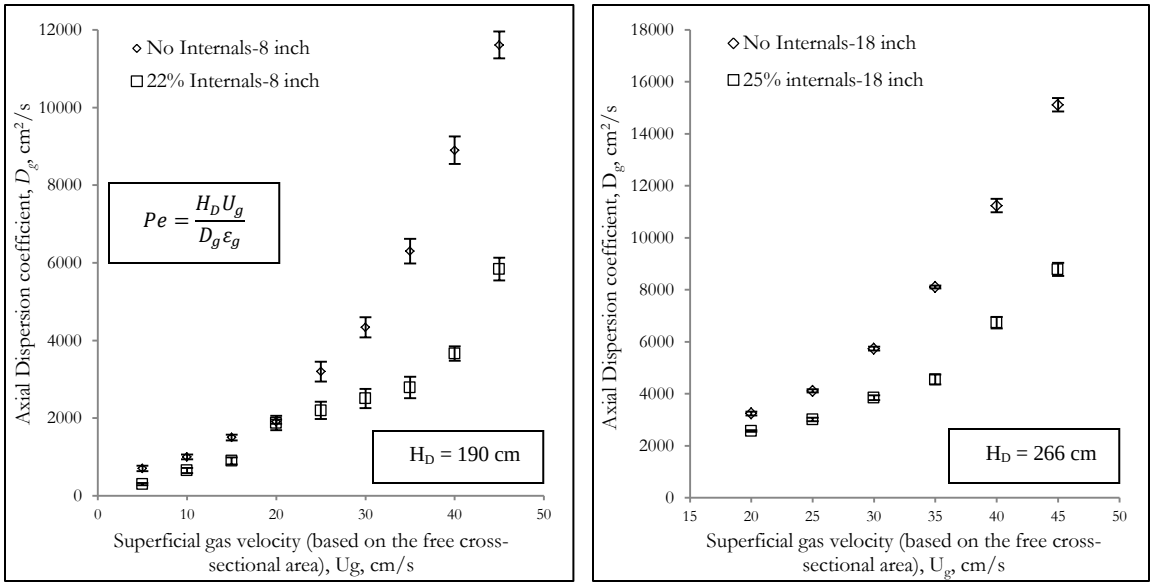

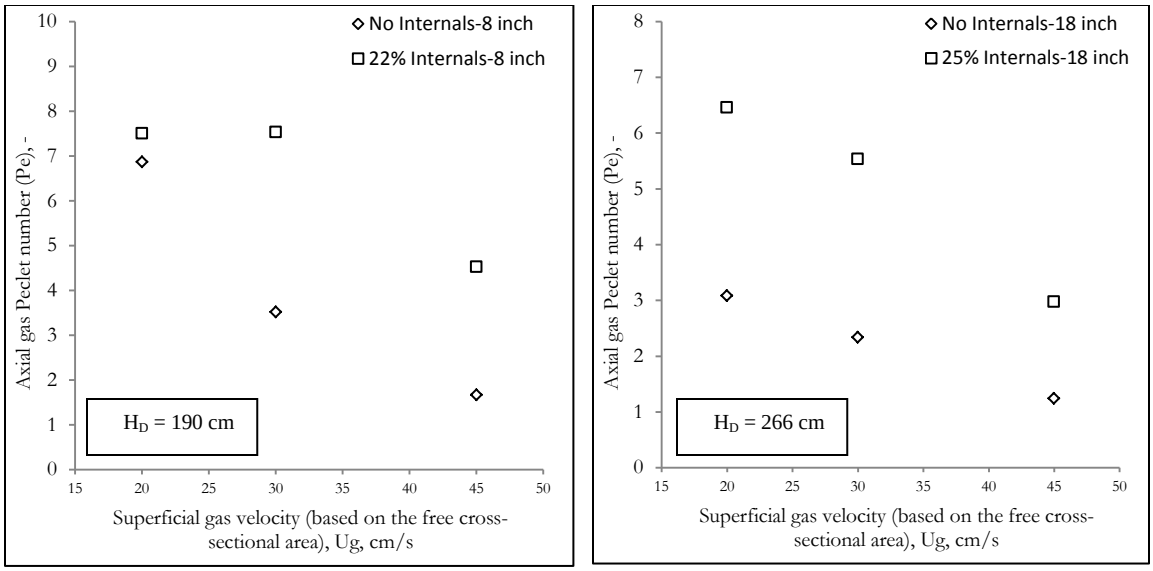

Figure 4.7 - Effect of superficial gas velocity (based on the cross-sectional area) on D_g and axial gas Pe values in the 8-inch and 18-inch columns with/without internals

In order to interpret the effect of internals on the gas phase mixing, one needs to understand their effect on the hydrodynamic and turbulent parameters which affect the overall axial gas mixing. An analysis of the different mechanisms causing axial gas mixing is shown below, followed by a discussion of the effect of internals on each mechanism.

Axial gas mixing on the macro-scale is a resultant of:

- Global convective recirculation of both liquid and gas phase, which is induced by the non-uniform radial gas holdup distribution.
- Turbulent dispersion due to eddies generated by the moving bubbles. This is an overall contribution due to turbulence which consists of:
    - Large-scale fluctuations caused by large-scale eddies
    - Small-scale fluctuations arising from the entrainment of the liquid in the wakes of the fast rising bubbles
- Molecular diffusion, which is negligible compared to the other factors especially in the churn turbulent flow regime

In the axial dispersion model used to analyze the measured RTD data, all of the above mentioned mechanisms, which lead to macro-scale gas mixing, are lumped into a single parameter, D_g. Therefore, it is important to understand the effect of internals on each of

these mechanisms to comprehend their effect on the overall axial mixing. On one hand, earlier work showed that the presence of internals will cause an increase in the global liquid circulation (Chen et al., 1999, Forret et al., 2003, and Berneman, 1989). The enhancement of the circulation of the liquid phase suggests that there will be an increase in the overall axial mixing of the gas phase. On the other hand, the presence of internals was found to generally decrease the turbulence in the system including liquid turbulent dispersion coefficients (Chen et al., 1999), fluctuating velocity (Chen et al., 1999 and Forret et al., 2003), and turbulent kinetic energy (Larachi et al., 2006). The dampening of turbulence in the presence of internals suggests that there will be a decrease in turbulent dispersion and hence less overall axial mixing. The experimental results indicate that the second effect (decrease in turbulent dispersion) is more dominant than the increase in the circulation in presence of internals, leading to an overall decrease in the axial gas mixing as evident from the observed increase in the axial gas Pe values in the presence of internals. This result suggests that the overall axial gas mixing is mainly caused by turbulent dispersion. Section 4.4.4 analyzes this argument in details based on the 2-D model results.

4.3.5 Effect of Scale on the Overall Axial Dispersion in the Gas Phase

Figure 4.8 shows the effect of column diameter on the extent of the overall axial gas mixing in the absence and presence of internals. The increase in column diameter from 8 inch to 18 inch causes a significant increase in D_g (~20-40% increase in the absence of internals and ~35-75% in the presence of internals)) and a decrease in the Pe values, indicating an increase in the overall axial gas mixing. The same trend of dependence of D_g on the bubble column diameter was also reported by other investigators (Towell and Ackerman, 1972, Field and Davidson 1980, Mangartz et al., 1981, Joshi et al., 1982, and Wachi and Nojima, 1990) and is reflected by different D_g correlations. However, the quantitative dependence of D_g on the column diameter is different from the previous studies, mainly due to the experimental technique used for D_g measurements in this work which considered the extra mixing in the plenum. The increase in D_g is due to the increase in the gas circulation and the turbulent dispersion caused by the increase in the column diameter within the range of studied column diameters.

In order to support these arguments theoretically and have a more fundamental understanding of the dominant mixing mechanisms at different conditions, a 2-D convection-diffusion model was employed to quantify the effects of different mixing mechanisms on the overall axial mixing in bubble columns. This model allows us to determine the contribution of each mixing mode on the overall axial mixing. Although this model is used in this work for the gas phase mixing, it is also applicable to simulate the liquid phase mixing, provided that the correct parameters are used (Degaleesan and Dudukovic, 1998). The derivation of this model is shown in section 4.4.4.

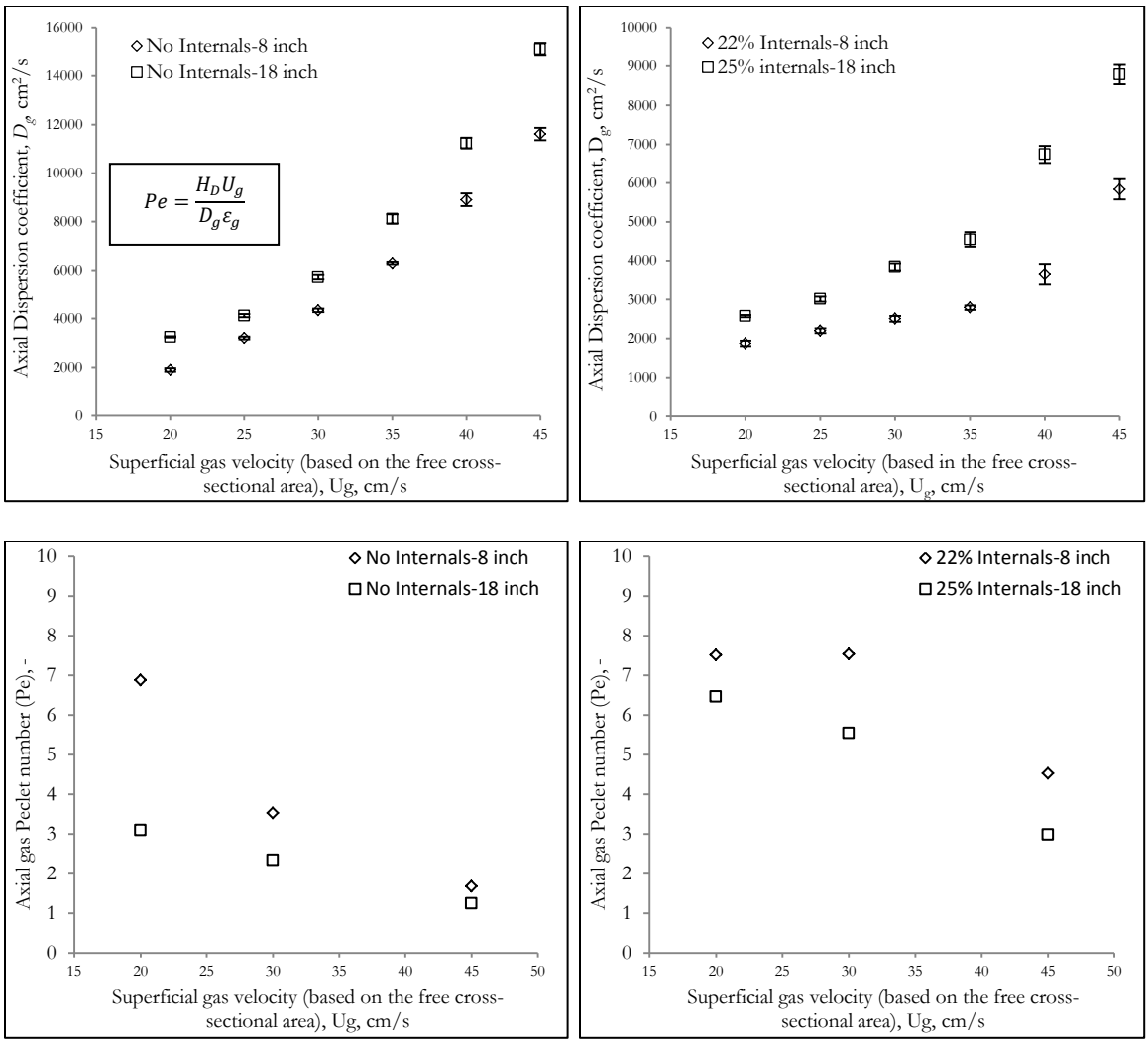

Figure 4.8 - Effect of column diameter on D_g at different superficial gas velocities (based on free cross-sectional area) in the absence and the presence of internals

4.4 Modeling of Gas Phase Mixing in Bubble Columns

In this section a 2-D model for gas phase mixing in bubble columns is presented based on a fundamental description of mixing as dictated by the fluid dynamics in the column. The main motivation behind such a model is the absence of fundamentally based gas phase mixing models that can simulate the contribution of the convective mixing and turbulent dispersion to the overall axial gas phase mixing. The development and evaluation of such a model was made possible due to the availability of experimental data for the necessary input fluid dynamic parameters from the 4-point optical probe.

The derivation of the model equations for a 2-D axisymmetric flow field is presented in the following section. The ability of the model to fit the experimental data at different operating conditions is then illustrated at two column scales in the presence and absence of internals.

4.4.1 A 2-D Convective-Diffusion Model for Gas Mixing in Bubble Columns

The fundamental two-fluid model mass balance equation for a local instantaneous species in phase *k*, is given by the following equation (Degaleesan 1997):

$$\frac{\partial \rho_k C_k}{\partial t} + \nabla . \rho_k C_k \boldsymbol{u_k} = D_m \nabla^2 C_k. \tag{4.9}$$

In the above equation, the phase density, ρ_k, for incompressible flows such as in bubble columns, can be considered constant. D_m is the molecular diffusivity, which is small compared to the turbulent diffusivity, especially in highly turbulent flows and will be neglected hereafter. Phasic averaging of the above equation in an axisymmetric system, for an inert, non-volatile or insoluble species, yields:

$$\frac{\partial}{\partial t}\left(\rho_k \varepsilon_k \overline{C_k}\right) + \frac{\partial}{\partial z}\rho_k \varepsilon_k \left(\overline{u_{z,k}}\,\overline{C_k} + \overline{u'_{z,k}C'_k}\right) + \frac{1}{r}\frac{\partial}{\partial r} r \rho_k \varepsilon_k \left(\overline{u_{r,k}}\,\overline{C_k} + \overline{u'_{r,k}C'_k}\right) = \Gamma. \tag{4.10}$$

Additional source terms can be added in Γ to account for reaction or mass transfer. Since the model is primarily concerned with the gas phase, the subscript "*g*" will be used instead of "*k*". In addition, all symbols denoting the averaging are dropped, in order to simplify notation. For the present situation, where the gas tracer experiment described earlier is

simulated, an insoluble and inert gas tracer was used, and hence, the right hand side of equation (4.10) is set to zero.

The cross-correlation terms between the fluctuating velocity and tracer concentration are closed using a standard gradient diffusion model (Hinze 1975, Tennekes and Lumly, 1971, Sienfield 1986), as:

$$\overline{u'_{z,g}C'_g} = -D_{zr}\frac{\partial C_g}{\partial r} - D_{zz}\frac{\partial C_g}{\partial z} \tag{4.11}$$

and

$$\overline{u'_{r,g}C'_g} = -D_{rr}\frac{\partial C_g}{\partial r} - D_{rz}\frac{\partial C_g}{\partial z} \tag{4.12}$$

Previous Computer Automated Radioactive Particle Tracking (CARPT) experiments showed that for the liquid phase, the non-principal diagonal terms are zero (Degaleesan, 1997):

$$D_{zr} = D_{rz} \sim 0 \tag{4.13}$$

In this work, the same will be assumed for the gas phase. Therefore:

$$\overline{u'_{z,g}C'_g} = -D_{zz}\frac{\partial C_g}{\partial z} \tag{4.14}$$

$$\overline{u'_{r,g}C'_g} = -D_{rr}\frac{\partial C_g}{\partial r} \tag{4.15}$$

where D_{zz} and D_{rr} are the local axial and radial turbulent diffusivities, respectively. This assumption is valid since the turbulent intensity in the gas and liquid phases are closely related because most of the turbulence in the liquid phase is induced by the wakes of the rising bubbles (Cui, 2005 and Qi and Shuli, 2008). This assumption was further validated from the turbulent intensity data of the gas and liquid phases as shown in section 4.4.5. Unfortunately, no experimental data are available for D_{zz} and D_{rr} for the gas phase. One would expect that there would be a radial dependence of D_{zz} and D_{rr} due to the non-uniform radial distribution of turbulent intensity and relevant turbulent parameters. However, this claim has neither been confirmed experimentally nor quantified theoretically. Therefore, as a first step in checking the ability of the 2-D model to simulate gas phase mixing, the values of D_{zz} and D_{rr} are assumed constant over the cross-sectional area of the column and will be referred to as $\overline{D_{zz}}$ and $\overline{D_{rr}}$. The 4-point optical probe data also showed that the ensemble-averaged radial bubble velocities, $u_{g,r}$ are negligible, and hence all the terms

containing $u_{g,r}$ can be dropped. Therefore the final form of the model equation for the distribution of the gas phase tracer is:

$$\frac{\partial}{\partial t}(\varepsilon_g(r)C_g(t,r,z)) + \frac{\partial}{\partial z}(\varepsilon_g(r)u_z(r)C_g(t,r,z)) = \frac{1}{r}\frac{\partial}{\partial r}\left(r\varepsilon_g(r)\overline{D_{rr}}\frac{\partial C_g(t,r,z)}{\partial r}\right) + \frac{\partial}{\partial z}\left(\varepsilon_g(r)\overline{D_{zz}}\frac{\partial C_g(t,r,z)}{\partial z}\right) \quad (4.16)$$

Danckwerts boundary conditions were used at the inlet, standard zero flux boundary conditions were used at the wall and the center and a zero gradient were assumed at the outlet boundary. This final form represents the averaged transient 2-D convection-diffusion balance equation for an inert and insoluble gas species in the fully developed section of the column, which is the correct form to represent the gas tracer experiment described earlier. The various averaged hydrodynamic and turbulent quantities in the above model equation refer to long time-averaged quantities. The model inputs include the time-averaged radial gas holdup profile and the time-averaged gas velocity profile which were obtained from the 4-point optical probe data as shown in Chapter 3.

There is considerable experimental evidence in the literature, including results from CARPT and the 4-point optical probe, showing that in columns of high aspect ratios (L/D) the time-averaged flow pattern is axisymmetric with global liquid and gas recirculation. This long time-averaged circulation exists in the form of a circulation cell that occupies most of the column, in which gas and liquid flow upwards in the core region and downwards in the wall region. In this circulation cell, a single 1-D velocity profile is always identified occupying the middle part of the column (fully developed flow region) in which all the hydrodynamic parameters are not a function of the axial position. However, axial variations are evident in the distributor and free surface region. Therefore, the computation domain was divided axially into three regions: a distributor zone at the bottom, a fully developed region in the middle, and a disengagement zone at the top. Based on experimental evidence (Degaleesan, 1997 and Gupta, 2002), the distributor and disengagement zones in churn turbulent regime are assumed to extend over a height approximately equal to one column diameter. In these regions, the gas phase is assumed to be completely mixed. Varying the height of these zones from 0 to 2 times the column diameter does not affect the results significantly as long as the outlet concentration was adequately averaged (Equation 4.20).

The 2-D model was used to analyze the tracer responses for different cases in which experimental data are available to investigate the effect of superficial gas velocity, internals, and column scale on the axial and radial diffusivities in the gas phase. Based on the fitted values of $\overline{D_{zz}}$ and $\overline{D_{rr}}$, and using fundamental mixing concepts, the contribution of different mixing mechanisms is assessed.

4.4.2 Effect of Superficial Velocity and Internals on Gas Turbulent Diffusivities

In this section, we assess the effect of superficial gas velocity on the radial and axial turbulent diffusivities of the gas phase. This is accomplished by changing the values of the axial and radial diffusivities to fit the model predictions to the experimentally measured tracer responses.

In all experiments, the mode of operation was continuous with respect to the gas phase and batch with respect to the liquid phase. The appropriate boundary conditions for the model are:

$$r = 0 \; and \; r = R: \frac{\partial C_g}{\partial r} = 0, \tag{4.17}$$

$$z = 0: U_g C_g - \overline{D_{zz}} \frac{\partial C_g}{\partial z} = U_g C_{in}, \tag{4.18}$$

where C_{in} is the exit concentration from the plenum as shown in equation (4.3), and

$$z = L : \frac{\partial C_g}{\partial z} = 0. \tag{4.19}$$

A time step of 0.1 seconds, a radial grid size of 0.1 cm, and an axial grid size of 0.1 cm were found to be the acceptable discretizations. The model was solved to predict the radial and axial tracer concentration. The values of $\overline{D_{zz}}$ and $\overline{D_{rr}}$ were estimated by fitting the experimental RTD data to the predicted normalized exit mixing cup concentration, calculated as follows:

$$C_{g,CM}(\mathrm{t}) = \frac{\int_0^R C_g(t,r,L)\varepsilon_g(r)u_{g,z}(r)rdr}{\int_0^R \varepsilon_g(r)u_{g,z}(r)rd\,r} \tag{4.20}$$

Figure 4.9 shows a typical comparison between the fitted exit mixing cup concentration profile and the measured RTD of the gas phase at U_g of 20 cm/s in the 8-inch column with

no internals. Figure 4.10 shows the effect of the superficial gas velocity on the axial and radial turbulent diffusivities in the presence and absence of internals.

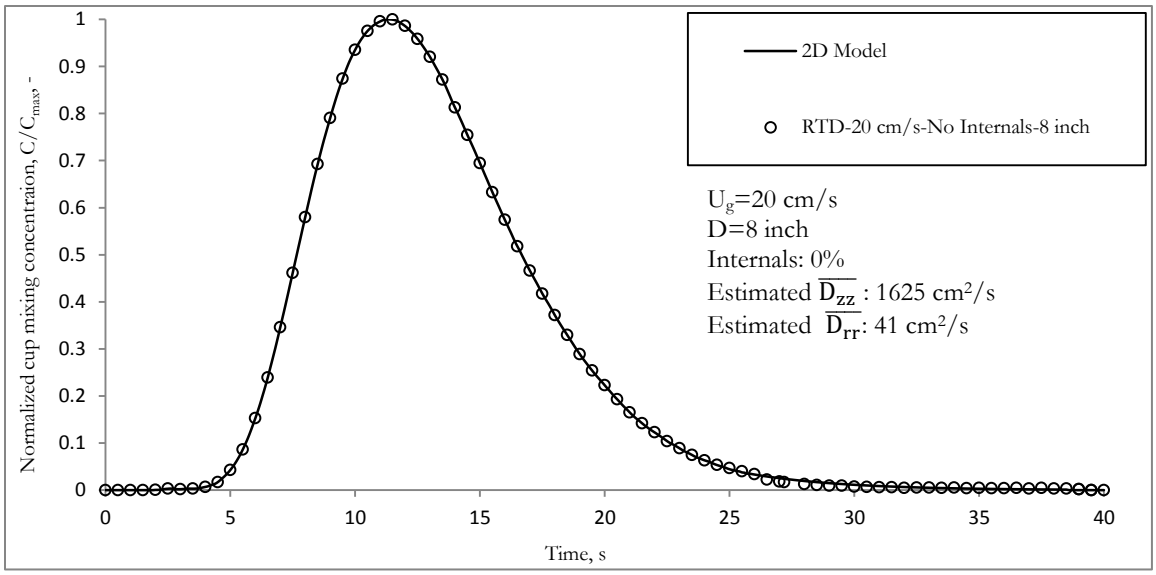

Figure 4.9 - Gas tracer response with 2-D model fit

As can be seen from Figure 4.10, the values of the axial and radial diffusivities increase with increasing the superficial gas velocity and decrease in the presence of internals. It should be noted that, to the best of the author's knowledge, such results have not been previously reported in the literature either quantitatively or qualitatively.

The turbulent eddy diffusivity can be expressed in terms of a turbulent length scale and a mean fluctuating velocity as shown by Franz et al. (1984):

$$D_{zz} = \ell_z \sqrt{\overline{u_z'^2}} \tag{4.21}$$

$$D_{rr} = \ell_r \sqrt{\overline{u_r'^2}} \tag{4.22}$$

The significant increase of the axial turbulent diffusivities with the increase in the superficial gas velocities especially in the column with no internal is due to the increase in turbulence at higher superficial gas velocities. This causes an increase in the root means squared (RMS) axial fluctuating velocities and possibly in the axial mixing length scale. The radial turbulent diffusivities in columns with no internals are much smaller and tend to an asymptotic value with increased superficial gas velocity. Clearly, the turbulence is not isotropic and mixing

length in the radial direction are much smaller than in axial. The same result was shown by Degaleesan (1997) for the liquid turbulent diffusivities using CARPT data.

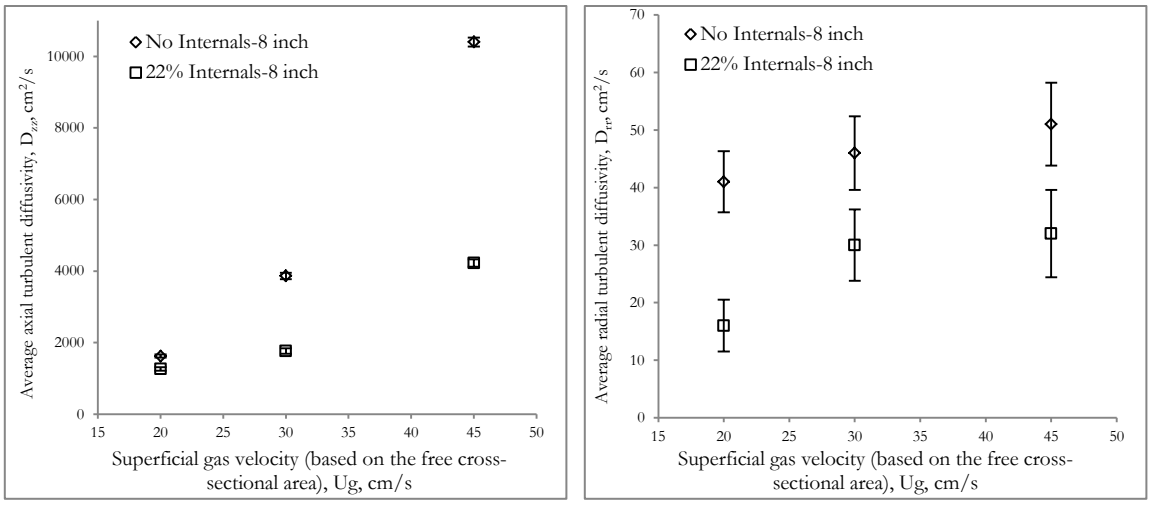

Figure 4.10 - Effect of superficial gas velocity and internals on the cross section average axial and radial turbulent diffusivities

The decrease in both axial and radial the turbulent diffusivities in the presence of internals is evident from Figure 4.10 and can be attributed to the fact that internals dampen turbulence, as shown in the work of Chen et al. (1999) and Larachi et al (2006). Chen et al. (1999) also found that the presence of internals causes a decrease in the liquid turbulent diffusivities and a decrease in the fluctuating velocity (also noted by Forret et al., 2003). This result is supported by fundamental arguments since the presence of vertical internals will bound the maximum bubble size, decreasing the bubble-induced turbulence. In addition, the physical presence of internals breaks the large turbulent wakes, causing them to be less energetic, and dampens large turbulent eddies. Moreover, the presence of internals presents additional restrictions to the bubble-induced eddies in the radial direction, causing a significant decrease in the radial mixing length scale. All these effects lead to a decrease in turbulence and turbulent-related parameters in presence of internals including the turbulent gas diffusivities.

4.4.3 Effect of Scale on Gas Turbulent Diffusivities

The confident scale-up of bubble columns requires good understanding of the effect of the column diameter on turbulent mixing parameters. In this work, the effect of column diameter on the turbulent gas mixing parameters was studied using the 2-D gas mixing

model coupled with the RTD data measured in two different column scales. Figure 4.11 illustrates the effect of column diameter on the axial and radial turbulent diffusivities of the gas phase.

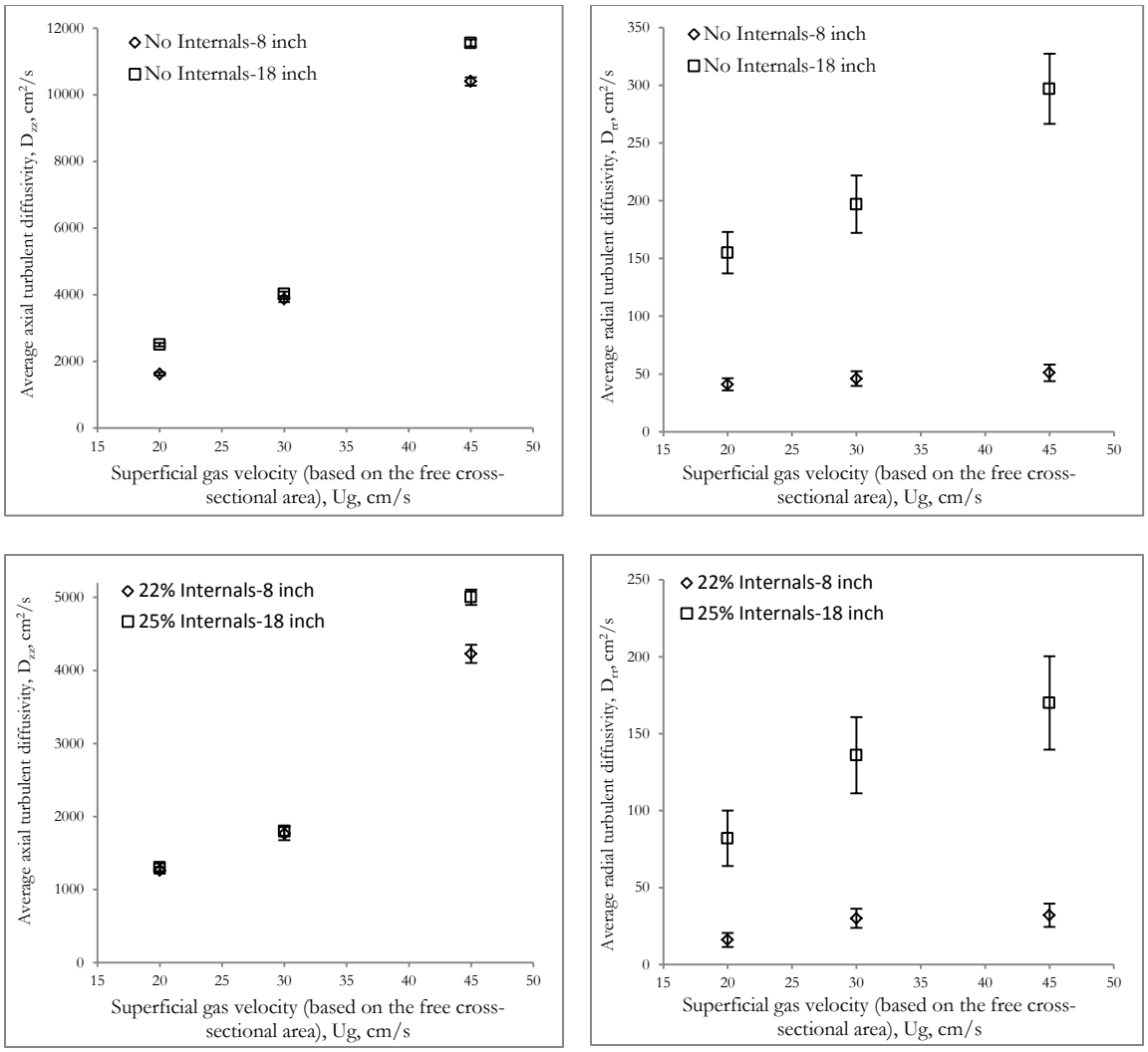

Figure 4.11 - Effect of superficial gas velocity and column diameter on the cross section average axial and radial turbulent diffusivities

The increase in column diameter was found to increase the radial turbulent diffusivity significantly in bubble columns with and without internals; however, it only slightly affects the axial turbulent diffusivity. These results suggest that only the radial mixing length scale is affected by the increase in column diameter, which implies that the turbulent eddies generated at high superficial velocities, are of the same order of magnitude of the column diameters used in this study. Therefore, in smaller columns, the column walls dampen these eddies, causing a decrease in the radial turbulent diffusivities.

The next section discusses these results using the model developed by Degaleesan and Dudukovic (1998) to analyze the contribution of different mixing mechanisms to the overall axial gas phase mixing.

4.4.4 Gas Mixing Mechanism in Bubble Columns

The most common model used in simulating gas mixing is the 1-D axial dispersion model (ADM). In the ADM, all the mechanisms leading to the overall axial gas mixing are lumped into a single coefficient: the axial dispersion coefficient (D_g). This causes D_g to become sensitive to the reactor scale and operating conditions, and hence very difficult to scale up. The popularity of the model stems from its simplicity and ease of use, although its ability to describe two-phase flows with large degrees of back-mixing, such as those in bubble columns, is questionable. It is the lack of better alternatives that makes the ADM predominantly used to describe back mixing in bubble columns.

Despite the various attempts to develop theoretical or semi-theoretical expressions for D_g, there still exists no relationship that quantifies the contributions of the different mixing mechanisms to the overall axial gas mixing in bubble columns. The present work attempts such quantification. The main objective is to better understand the relation between the axial dispersion coefficient and the key fluid dynamic parameters and turbulent dispersion coefficients. In the light of the development of such an expression, one should be able to:

1. Better understand the effects of different process conditions and column scale on D_g.
2. Define the key parameters that should be used to predict D_g.

It is not the objective of this work to develop a correlation to predict D_g, rather, our goal is to develop an approach by which one can understand the effects of different mechanisms on the overall mixing and use this approach to explain the experimental results developed in this work.

The contribution of the turbulent dispersion and convective mixing to the overall axial mixing of the liquid phase was analyzed by Wilkinson (1991) and Degalesaan and Dudukovic

(1998). Wilkinson (1991) developed a mechanistic model and used it to calculate the axial liquid dispersion coefficient from the average axial turbulent diffusivity, recirculation velocity (u_{rec}), overall gas holdup (ε_g) and a radial exchange term (k).

$$D_{ADM} = \overline{D_{zz}} + \frac{u_{rec} D\sqrt{2}}{16k(1-\varepsilon_g)^2}. \tag{4.23}$$

Degaleesan and Dudukovic (1998) developed a 2-D convection diffusion model for the liquid phase and reduced it to a 1-D model, from which the axial liquid dispersion coefficient was calculated from the recirculation liquid velocity, cross-sectionally averaged turbulent axial diffusivities, and cross-sectionally averaged radial diffusivities (equation 4.24).

$$D_{ADM} = \overline{D_{zz}} + \frac{1}{K_T}\frac{\overline{u_{rec}^2} R^2}{\overline{D_{rr}}} \tag{4.24}$$

where K_T is an empirical constant. Both of the above models indicate that the overall axial dispersion coefficient conceptually can be divided into two parts: a turbulent diffusivity term which accounts for the contribution of the turbulent dispersion in the axial direction, and a Taylor-type 'diffusivity' term which accounts for the contribution of convection to the overall axial mixing and of radial turbulent diffusivity. Both studies showed that the turbulent diffusivity term is equal to the cross-sectional averaged axial turbulent diffusivity ($\overline{D_{zz}}$), while the Taylor diffusivity term ($\overline{D_{Taylor}}$), given by the second term of equation (4.24), is a function of the recirculation phase velocity and the cross sectional averaged radial turbulent diffusivity ($\overline{D_{rr}}$). Based on these models, it is evident that the overall axial mixing will increase with an increase in the axial turbulent diffusivity and the recirculation velocity, and will decrease with an increase in the radial turbulent diffusivity. It is also evident that the contribution of convection (recirculation velocity) to the overall axial mixing decreases at higher values of radial turbulent diffusivities.

The predicted values of $\overline{D_{zz}}$ and $\overline{D_{rr}}$ were analyzed using this concept where the contribution of the axial mixing was quantified by dividing the axial turbulent diffusivity by the overall axial mixing coefficient (D_g) determined from the gas tracer studies described in Section 4.3.3. Figure 4.12 shows the variation of the ratio of $\overline{D_{zz}}$ to D_g with the superficial gas velocities in the 8-inch and 18-inch bubble columns with and without internals. Figure 4.13 shows the variation of D_g, $\overline{D_{zz}}$, and $\overline{D_{Taylor}}$ with the superficial gas velocity in the 8-

inch and 18-inch columns with and without internals. $\overline{D_{Tylor}}$ values were calculated from Equation (4.24) by subtracting $\overline{D_{zz}}$ from D_g.

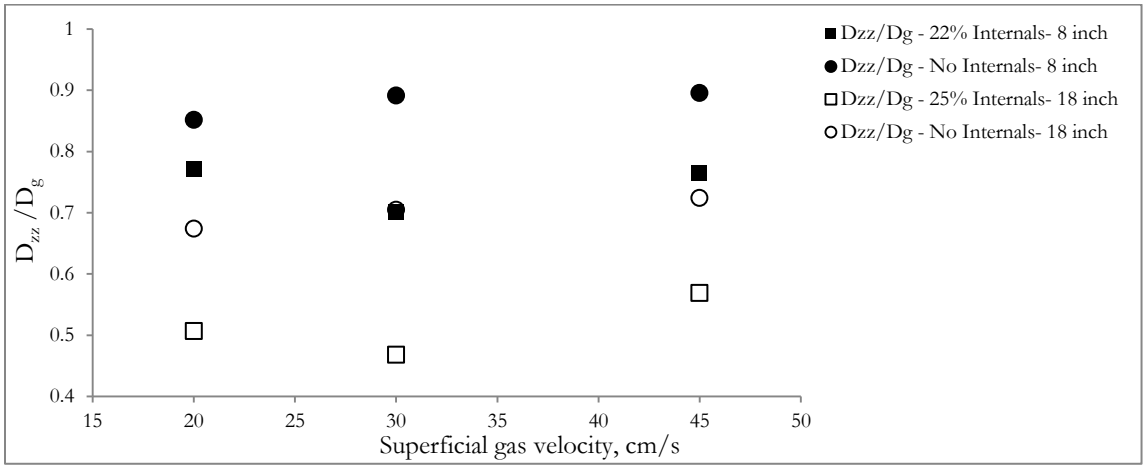

Figure 4.12 - The ratio the axial turbulent diffusivity to the axial dispersion coefficient (D_{zz}/D_g) at different superficial gas velocities in the presence and absence of internals in the 8-inch and 18-inch columns

The data shows that in the lab-scale 8-inch diameter column, the overall axial gas mixing is mainly controlled by the axial turbulent dispersion, since it accounts for ~85% of the total axial mixing.

In the presence of internals, the contribution of the convective mixing starts to increase due to the increase in the centerline gas velocity (as shown in chapter 3) and the decrease in the radial turbulent diffusivity. Both these effects cause the influence of convective mixing to be more significant. Although there is a considerable contribution of the convective mixing in the presence of internals, turbulent dispersion remains the more dominant mode of mixing, which explains why the dampening of turbulence in the presence of internals leads to an overall decrease in the overall axial gas mixing.

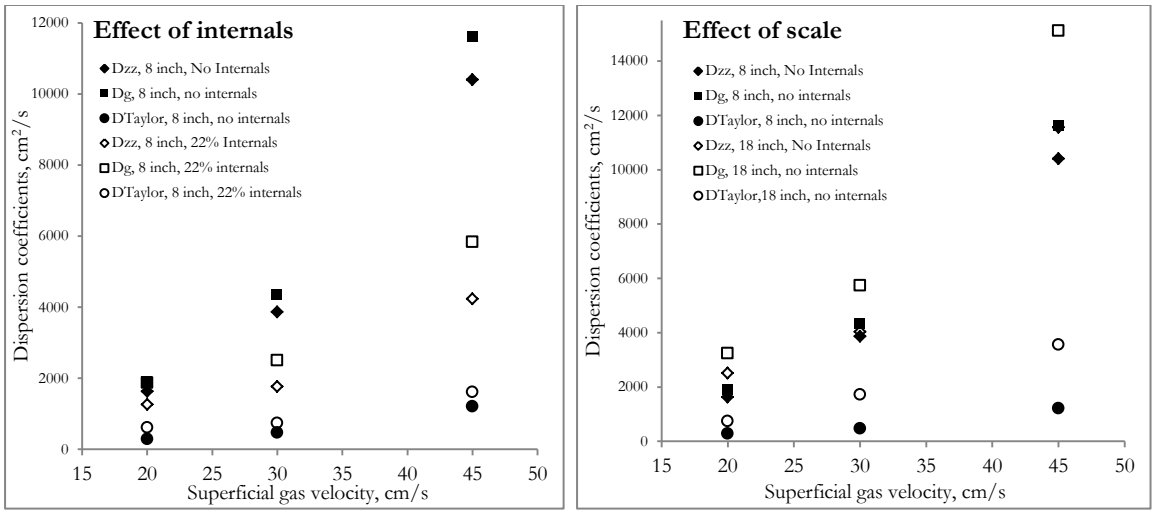

Figure 4.13 - Effect of internals and column scale on the axial turbulent diffusivity and Taylor-type diffusivity

Figure 4.12 also shows that the contribution of the convective mixing increases with increase in the column diameter, mainly due to the significant increase in the gas circulation with the increase in column diameter. This was also reflected in the values of the Taylor diffusivities in the 18-inch column, shown in Figure 4.13, which were larger than those in the 8-inch column, in spite of the increase in the radial turbulent diffusivities.

4.4.5 Turbulent Gas Mixing Length Scales

Turbulent dispersion in bubble columns is caused by turbulent eddies of different sizes which carry forward fluid particles at different rates causing fluctuations in the fluid concentration. The concentration fluctuation generated by these eddies is proportional to their length scale and the mean concentration gradient: $|C'| \sim L_{eddies} \frac{\partial \bar{C}}{\partial z}$. Following the analogy between turbulent flux and diffusion flux, the turbulent flux can be closed in terms of a turbulent diffusivity term as show in equation (4.11). As shown equation (4.21), the turbulent diffusivity can be defined as the product of a characteristic turbulence velocity scale and a characteristic turbulent length scale. Therefore, estimating the turbulent length scales is important to predicting turbulent diffusivities. In fact, many length scales co-exist in a turbulent flow, so it is important to choose the length scale that affects turbulent dispersion the most. It is fair to assume that the largest eddies are the most effective in distributing momentum, mass, and heat in a turbulent system. As a result, the geometric configuration of a certain system becomes an important indication of the scale of eddy sizes

in that system, since it dictates the maximum eddy size. In addition, in anisotropic turbulent systems like bubble columns, the turbulent length scales will be direction dependent.

Very little is known regarding the characteristic mixing length scales in bubble columns, due to the absence of experimental data that quantifies both the turbulent diffusivities and the fluctuating velocities. In bubble columns, the mixing length scales in the axial direction are expected to be larger than those in the radial direction, since there is lesser restriction in the axial direction to the passage of large eddies than in the radial direction, due to column diameter or the presence of vertical internals. This postulate was confirmed by Degaleesan (1997), who found that the ratio between the axial and radial length scales in a 6 inch diameter column is 7:1. Moreover, if one follows the two-fluid approach, where the phases are treated separately, each phase should have its own turbulent length scale based on the turbulent diffusivity and the turbulent intensity in that specific phase.

In this section, we attempt to estimate the turbulent mixing length scales based on the gas phase turbulent diffusivity data. In order to estimate the mixing length scales, the eddy diffusivities and turbulent intensities are needed as evident from equation (4.21). The eddy diffusivities of the gas phase were obtained as shown in section 4.2. The turbulent intensities of the gas phase can be obtained from the 4-point optical probe data, since the probe records the instantaneous bubble velocities. It should be noted, however, that the fluctuations in the gas phase velocity are not merely due to the turbulence, but also due to the variation of bubble sizes. Recent experimental data showed that the ratio of the dispersed (gas) to continuous (liquid) phase fluctuations approaches a constant value close to unity after the gas holdup increases beyond a certain limit, which could be as small as 6% (Garnier et al., 2001, Larue de Tournemine et al., 2001, and Deen et al., 2002). This indicates that contribution of the variation of bubble sizes to the gas phase velocity fluctuations is negligible especially at high gas holdups. These experimental data were further supported in this work by comparing the gas velocity fluctuations and liquid velocity fluctuations at the same conditions. This was possible due to the availability of data for a limited set of conditions in a 6-inch bubble column at 30 and 45 cm/s. At these conditions, Ong (2003) reported the cross-sectional averaged mean fluctuating liquid velocity based on CARPT data, while Xue (2004) measured the instantaneous gas velocities from which the cross-sectional

averaged mean fluctuating gas velocity can be calculated. The data of Xue (2004) was re-processed and the local mean fluctuating gas velocity was calculated from:

$$\sqrt{\overline{u'_{z,g}(r)^2}} = \sqrt{(\overline{u_{z,g}(r)} - u_{z,g}(r))^2} \tag{4.25}$$

where $\sqrt{\overline{u'_{z,g}(r)}}$ is the local mean fluctuating gas velocity, $\overline{u_{z,g}(r)}$ is the local mean gas velocity and $u_{z,g}(r)$ is the instantaneous local gas velocity. After calculating the local mean fluctuating gas velocity, the cross-sectional averaged mean fluctuating gas velocity was calculated from:

$$\sqrt{\overline{u'_{z,g}{}^2}} = \frac{\int_0^R \sqrt{\overline{u'_{z,g}(r)^2}}\, r\, dr}{\int_0^R r\, dr} \tag{4.26}$$

Table 4.3 shows the mean liquid and gas fluctuating velocities in a 6-inch column at 30 cm/s and 45 cm/s for an air-water system. The table shows that the mean fluctuating gas velocity is always larger than the mean fluctuating liquid velocity, as expected. The difference between the gas and liquid fluctuating velocities is negligible (less than 10%), indicating that the fluctuations in the gas phase velocity caused by the bubble size distribution are insignificant compared to those created by turbulence. This presents strong evidence that the use of the mean fluctuating velocities of the gas phase to calculate the mixing length scales gives a reasonable order of magnitude estimation of mixing length scales.

Table 4.3 - The relation between the mean liquid fluctuating velocity and mean gas fluctuating velocity

Ug (cm/s)	$\sqrt{\overline{u'_{z,l}}}$ (Ong, 2003), cm/s	$\sqrt{\overline{u'_{z,g}}}$ (Xue, 2004), cm/s	% increase
30	48.98	49.41	0.87
45	52.4	55.72	6.01

The availability of the fluctuating gas velocity data can serve as an indicator of the turbulent intensity at different conditions. Figure 4.14 displays the effect of column diameter and internals on the fluctuating gas velocity and turbulent intensity at different superficial gas velocities. This figure shows that the mean fluctuating gas velocity increases with increasing column scale, reflecting the increase in turbulence intensity with the increase in the column scale. It is evident from Figure 4.14 that the presence of internals decreases the mean fluctuating gas velocity, confirming the earlier findings of Forret et al (2003), who showed

that the presence of internals decreased the fluctuating liquid velocity, and the findings of Chen et al. (1999), who showed that the presence of internals decrease all the turbulent related parameters. Another important result shown by these studies is that the turbulence in the gas and liquid phases are closely related, which validates the earlier assumptions made in this chapter. Based on these results, one would expect that the radial turbulent fluctuations are similar in the gas and liquid phases. Unfortunately, insufficient experimental data is available to support this claim.

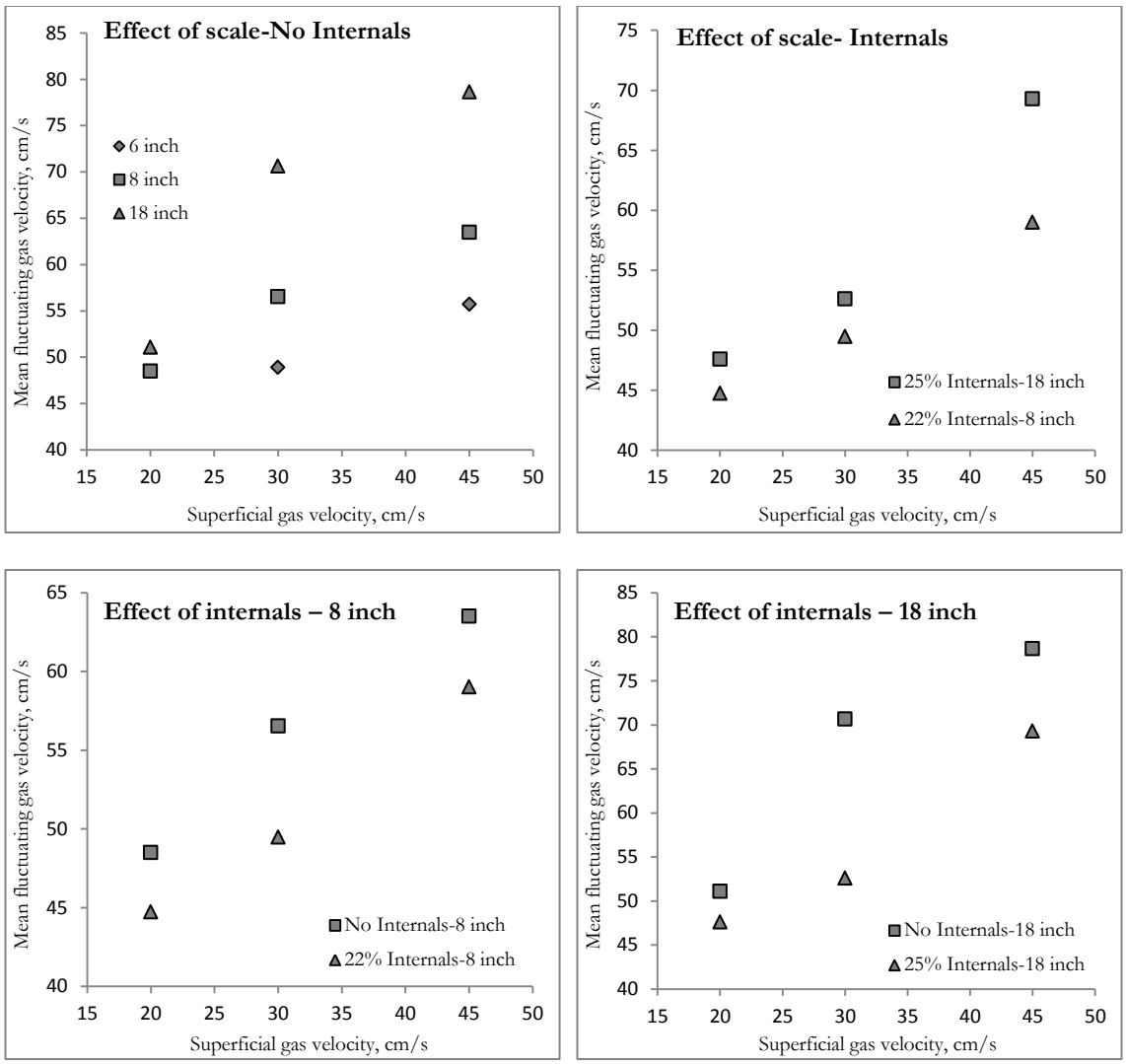

Figure 4.14 - Effect of scale and internals on the mean gas fluctuating velocity

Table 4.4 displays the cross-sectional averaged length scales for all the operating conditions investigated in this work. As can be seen from Table 4.4, the mixing turbulent length scale of

the gas phase increases with increasing superficial gas velocity and decreases in the presence of internals. These results present further evidence that the presence of internals dampens large eddies.

Table 4.4 also shows the characteristic length scales in the liquid, reported by Degaleesan (1997) and Ong (2003), in a 6-inch column at different operating pressures. It can be seen that the trends observed for the turbulent mixing length scale of the gas phase qualitatively match the dependence of the mixing turbulent length scale of the liquid phase. An important observation is that the presence of internals and the increase in pressure cause a decrease in the mixing lengths of the gas and liquid phases.

Table 4.4 - The effect of superficial gas velocity, column diameter, internals, and pressure on the gas and liquid turbulent length scales

Ug, cm/s	Column diameter, cm	Internals/Pressure	$\bar{l}_{z,g}$, cm	$\bar{l}_{z,l}$, cm
20.0	19	No Internals/1 atm	33.5	-
30.0	19	No Internals/1 atm	68.4	-
45.0	19	No Internals/1 atm	163.8	-
20.0	19	22% Internals/1 atm	28.2	-
30.0	19	22% Internals/1 atm	35.7	-
45.0	19	22% Internals/1 atm	71.6	-
20.0	45	No Internals/1 atm	49.0	-
30.0	45	No Internals/1 atm	56.9	-
45.0	45	No Internals/1 atm	146.9	-
20.0	45	25% Internals/1 atm	27.4	-
30.0	45	25% Internals/1 atm	34.3	-
45.0	45	25% Internals/1 atm	72.2	-
30.0	14 (Ong, 2003)	No Internals/1 atm	-	~ 7
45.0	14 (Ong, 2003)	No Internals/1 atm	-	~ 7.39
30.0	14 (Ong, 2003)	No Internals/4 atm	-	~ 6.5
45.0	14 (Ong, 2003)	No Internals/4 atm	-	~ 6.98
30.0	14 (Ong, 2003)	No Internals/10 atm	-	~ 5.85

Table 4.4 also shows that the values of the characteristic mixing length scales of the gas phase are much higher than the characteristic mixing length scales calculated based on the liquid phase. This result is expected since the superficial gas velocity is much higher than the superficial liquid velocity, causing the dispersion coefficients (D_g, $\overline{D_{zz}}$, and $\overline{D_{rr}}$) of the gas phase to be higher than those of the liquid phase. The increase in these dispersion

coefficients at the same magnitude of the fluctuating velocities of both phases, as shown earlier in this section, can only be caused by the increase in the characteristic mixing length scale, as evident from equation (4.21). It should be noted that, physically, the characteristic mixing length scale denotes the size of the largest eddies, which are the most efficient in transporting momentum, mass and heat. Based on this argument, it seems unreasonable that the largest eddy sizes will be different in both phases. This is an interesting subject of research that has not been explored in the literature either experimentally or theoretically. One way to validate this finding is through Large Eddy Simulations (LES) simulations that are able to compute the spectrum of all the large eddies in both phases. Although the transfer of turbulence back and forth between the gas and liquid phases is still poorly understood, it seems realistic that eddies of the same size will affect both phases differently due to the differences in the physical properties for the two phases, especially the phase densities. These differences causes the eddies of the same size to be more effective in transporting momentum, mass and heat through the gas phase compared to the liquid phase, which can partially explain the prediction of larger characteristic mixing lengths for the gas phase.

4.5 Remarks

In this chapter, the effect of different operating conditions on the overall axial gas mixing was studied. The gas tracer experiments showed that the increase in the superficial gas velocity increases D_g in the presence and absence of internals. The presence of internals caused a significant decrease in D_g due to the decrease in the axial turbulent gas diffusivity. The increase in column diameter enhanced the overall axial gas mixing due to the increase in gas recirculation and the increase in the axial turbulent gas diffusivity.

A 2-D convection-diffusion gas mixing model was used to predict the RTD of the gas phase by fitting the axial and radial turbulent gas diffusivities. The 2-D model results showed that both the axial and radial turbulent diffusivities decreased in the presence of internals due to the dampening of turbulence and turbulent related parameters caused by the presence of internals. In contrast, the increase in column diameter caused an increase in the radial and axial turbulent gas diffusivities due to the increase in turbulent intensity. This work provided, for the first time, values for the axial and radial turbulent diffusivities of the gas phase in

bubble columns with and without internals. Further studies are needed to predict with more confidence the values for the radial turbulent diffusivities of the gas phase by measuring the radial gas phase concentration.

The model developed by Degaleesan and Dudukovic (1998) was used to determine the contribution of different mixing mechanisms to the overall axial gas mixing. The analysis showed that the main contributing factors to the overall gas mixing in bubble columns are gas recirculation (convective mixing) and turbulent dispersion. The extent of the effect of different mechanisms at different conditions is complex which may partly explain why a universal correlation for the axial gas dispersion coefficient has not been developed. The analysis presented in this chapter, however, allowed us to examine the effect of changes in the fundamental fluid dynamic parameters, namely, the gas holdup profile, the gas velocity profile, the axial turbulent diffusivity, and the radial turbulent diffusivity on the axial gas dispersion coefficient. Experimental measurements of the radial gas holdup and radial gas velocity profiles, using the 4-point optical probe, and the RTD of the gas phase, using the developed gas tracer technique, coupled with the 2-D convection diffusion model have been used to illustrate the expected trends in the axial dispersion coefficient.

Generally, the overall axial gas mixing is mainly controlled by turbulent dispersion; however, the increase in column diameter increases the contribution of convective mixing due to the increase in gas circulation. In addition, the presence of internals increases the contribution of convective mixing by decreasing the radial turbulent diffusion. It is therefore important to consider the contribution of both the convective mixing and turbulent dispersion in the modeling of gas mixing or the development of axial gas dispersion coefficient correlations.

Chapter 5 - Mass Transfer in Bubble Columns with Internals

This chapter addresses the effect of internals on the overall volumetric mass transfer coefficient (k_La) in a pilot-scale bubble column. The experimentally measured k_La values were coupled with the data for the interfacial area obtained using a 4-point optical probe to calculate the gas-liquid side mass transfer coefficient (k_L) in the presence and absence of internals.

5.1 Introduction

The overall volumetric gas-liquid mass transfer coefficient (k_La) is an important design parameter for bubble columns, especially in processes involving the absorption of gases in organic liquids such as methanol synthesis and the F-T process. Accordingly, mass transfer has been extensively studied in the last 50 years, resulting in a large body of experimental data and correlations for k_La under a wide range of operating conditions. Despite all these efforts, none of these studies addressed the effect of the presence of vertical cooling internals on k_La. Previous work has revealed that the presence of internals affects the flow field including the liquid velocity profile (Bernemann, 1989, Chen et al, 1999, and Forret et al., 2003), gas velocity profile (Chapter 3 of this work), bubble dynamics (Youssef, 2010), and turbulent intensities (Chen et al., 1999 and Forret et al, 2003). These changes are expected to affect k_La based on different developed mass transfer theories.

k_La depends on two interrelated factors, namely: the gas-liquid side mass transfer (k_L) and gas liquid interfacial are per unit volume of gas-liquid dispersion (a). It is very important to separate both factors to understand how k_La changes with different conditions. It is widely accepted that Higbie's theory is adequate to describe mass transfer in bubble columns based

on experimental data covering a wide range of conditions (Deckwer, 1992). This theory suggests that k_L is directly proportional to the average bubble size. The work of Youssef (2010) showed that internals decrease the average bubble chord length, indicating that k_L will most likely decrease in the presence of internals. Other mass transfer theories (Fortescue and Pearson, 1967, and Lamont and Scott, 1970) advocate that k_L is a function of the turbulent intensity of the system, which suggests that the presence of internals decreases k_L due to the decrease in the turbulent intensity. On one hand, k_La is expected to decrease in the presence of internals due to the likely decrease in k_L. On the other hand, the increase in the interfacial area in the presence of internals (Youssef, 2010) is expected to significantly enhance k_La. Some authors have claimed that the observed variations of k_La with different operating conditions are mainly attributed to the difference in the interfacial area at these conditions (Fan, 1989, Patel et al., 1990, and Behkish et al., 2002). This suggests that the increase in the interfacial area in the presence of internals most likely enhances k_La in spite of the decrease in k_L.

This work has investigated the hydrodynamics and gas phase back-mixing at different operating conditions in the presence and absence of internals. If the mass transfer is studied at the same conditions, this knowledge will greatly help in understanding the effects of key fluid dynamic and mixing parameters on k_La and k_L. The phase dispersion parameters estimated in other parts of this work, in addition to the bubble dynamics measured by the 4-point optical probe, help us to implement better models to quantify mass transfer since they provide the necessary inputs to these models. In addition, the data of interfacial area available from the 4-point optical probe coupled with the measured k_La values allow the estimation of k_L under different operating conditions. All these reasons motivated the extension of this work to investigate the effect of internals on k_La.

5.2 Research Objectives

This work aims to provide a better understanding of the effect of superficial gas velocity on the gas-liquid mass transfer in bubble columns in the presence and absence of internals. Particularly, the following objectives were set for this study:

- Investigate the effect of superficial gas velocity and internals on the overall volumetric mass transfer in a pilot-scale bubble column.
- Assess the effect of superficial velocities and internals on the gas-liquid side mass transfer coefficient (k_L) by combining the values of the interfacial area, calculated at the same conditions using the 4-point optical probe, with the values of k_La obtained in this work.

5.3 Gas-Liquid Mass Transfer Experiments

In this work, the k_La values of oxygen were measured using the optical oxygen probe technique and an oxygen-enriched air dynamic method (Han, 2007). The experimental details, reactor models used, and results are shown below.

5.3.1 Reactor Setup and Experimental Conditions

Mass transfer experiments were conducted in an 18-inch bubble column, as shown in Figure 5.1. Various ports in the column were used for mounting the optical oxygen probe for local axial measurements of the oxygen tracer. The experimental conditions for the oxygen mass transfer measurements were designed to cover a wide range of superficial gas velocities in the churn turbulent regime, in the presence and absence of internals (Table 5-1) using an air-water system.

Table 5.1 - Experimental conditions of the mass transfer experiment

D_c (cm)	Internals (%CSA)	U_g (cm/s)	Axial positions
45	0 %	20	x/L = 0.05, 0.3, 0.5, 0.65
45	0 %	30	x/L = 0.05, 0.3, 0.5, 0.65

45	0 %	45	x/L = 0.05, 0.3, 0.5, 0.65
45	25%	20	x/L = 0.05, 0.3, 0.5, 0.65
45	25 %	30	x/L = 0.05, 0.3, 0.5, 0.65
45	25 %	45	x/L = 0.05, 0.3, 0.5, 0.65

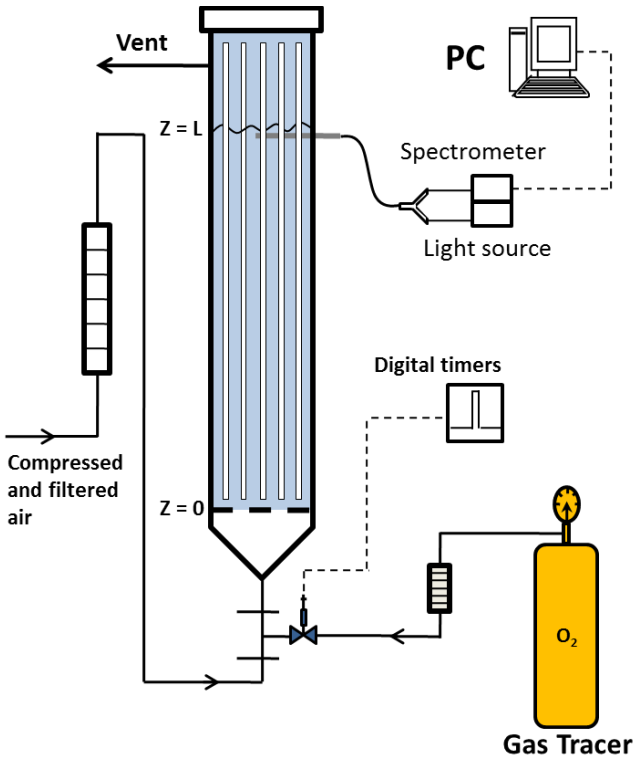

Figure 5.1 - Experimental Setup

5.3.2 Oxygen-Enriched Air Dynamic Method

Generally, mass transfer experiments involve the generation of a driving force, which triggers the transport of a partially soluble tracer from the gas phase to the liquid phase. The concentration of this tracer is then monitored in the liquid or gas phase at the required measurement locations. The measured tracer concentration can then be analyzed using a suitable model to quantify the rate of mass transfer.

Different experimental methods were developed to measure k_La in bubble columns. The main difference among these methods is the way the needed transport driving force is generated. In this work, the oxygen-enriched method was implemented to quantify k_La by measuring the concentration of the oxygen tracer in the liquid phase. This method was first introduced in fermentation systems by Chang et al. (1989), then Linek et al. (1991) validated its application on coalescent liquid systems such as the air-water system. The idea is to add a small oxygen flow, while maintaining the main air flow, as a step change to achieve a switch between air and oxygen-enriched air. In this work, this was done by raising and lowering the oxygen concentration in the main gas flow by a small oxygen flow (measured as 3% of the overall flow rate) which was started and stopped by a solenoid valve and a digital timer. The oxygen-enriched method was chosen over other mass transfer measurement techniques since it does not cause significant flow fluctuations during the tracer input. It also does not require the use of inconveniently large quantities of the tracer compared to other mass transfer methods.

The optical oxygen probe was used to monitor the transient oxygen concentration in the liquid phase at the desired axial positions. The experiments were repeated for sufficiently long time intervals to insure that the new dissolved oxygen equilibrium was achieved. The obtained concentration curves can be considered as the response of the system to a typical step-up experiment, and were used for the quantification of k_La.

5.3.3 Optical Oxygen Probe Technique

The optical oxygen probe, used in this work to measure the dissolved oxygen (DO) concentration, is a fluorescence-type sensor first developed at TU-Hannover, Germany (Comte et al., 1995). Due to their fast response, stability, and long life, these probes are used in transient mass transfer experiments. The measurement system in Figure 5.2 consists of an oxygen optical probe, optic fiber, light source, spectrometer, USB A/D converter, PC, and software. As shown in Figure 5-3, when irradiated at 470 nm by the light source, a thin film

coated on the probe tip emits fluorescence at about 600 nm. The increase in the dissolved oxygen (DO) concentration quenches the 600-nm fluorescence linearly. Thus, DO concentration data can be obtained by measuring the fluorescence intensity with the spectrometer. The characteristic response frequency constant (reciprocal of the characteristic probe time) of the probe used in this study is 1.1 s^{-1}, which is about one magnitude larger than typical k_La values in bubble columns. This indicates that the time scale of the probe delay is small enough for the mass transfer measurements to be accurate.

1. Optical oxygen probe
2. Optical fiber
3. Light source
4. Spectrometer
5. Integrated A/D converter+ USB interface
6. PC and software

Figure 5.2 - Optical oxygen probe

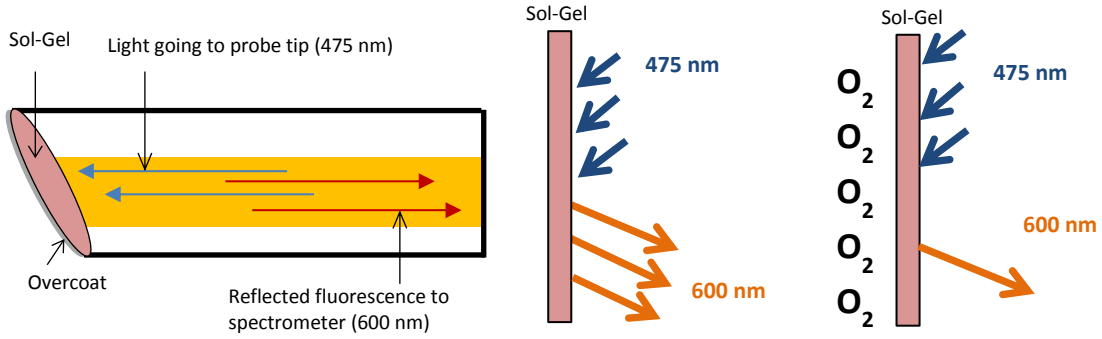

(a) Probe tip (b) Fluorescence emitting

Figure 5.3 - Mechanism of the optical oxygen probe

5.3.4 Reactors Models

The measured transient responses of the dissolved oxygen tracer in the mass transfer experiment include information on the extent of the gas-liquid mass transfer in addition to gas and liquid mixing. The commonly used models to quantify mixing of the two phases are usually based on one of the following assumptions:

a. CSTR-CSTR: complete mixing of gas/liquid phases,
b. PF-PF: plug-flow of gas/liquid phases,
c. PF-CSTR: plug flow of gas and complete mixing of the liquid phase, and
d. ADM-ADM: dispersed plug flow (axial dispersion model) for the gas/liquid phases.

The assumption of ideal mixing patterns for the gas and liquid phase leads inaccurate k_La values. Hence, a reactor model is needed to accurately quantify the extent of the liquid and gas phase mixing in order to estimate accurate k_La values.

Although the applicability of the PF-CSTR model (which assumes complete back-mixing for the liquid phase and constant gas concentration in the gas phase) is only restricted to columns which have small length to diameter ratios, it has been used in most of the reported k_La measurements due to its simplicity. Some authors (Deckwer et al., 1974, Deckwer et al., 1983 and Lau et al., 2004) criticized the use of this model since the gas and liquid mixing patterns in bubble columns significantly deviate from perfect mixing patterns. Deckwer et al., 1983 and Lau et al., 2004 showed that there are differences between the estimated k_la values using ADM and those obtained using CSTR or PF models. In addition to the estimation of inaccurate k_La values, they also showed that using the CSTR or PF models for the analysis of mass transfer experiments can lead to the prediction of incorrect dependencies of k_La on the axial position and the superficial liquid velocity. Therefore, the ADM is used in this work to estimate k_La from the transient dissolved oxygen response curves.

It should be emphasized that the ADM (which assumes partial mixing of the gas and liquid phases) is only used for comparative purposes since it is the simplest available model that can account to a certain extent for the effects of mixing in both phases and hence should allow the estimation of more accurate k_La values. The main drawback of the ADM lies in the difficulty of estimating the axial dispersion coefficients of the gas and liquid phases; however, these difficulties were overcome in this work as follows:

- The axial dispersion coefficient of the gas phase (D_g) was experimentally measured at the same experimental conditions of the mass transfer experiment as shown in chapter 4. This provides a proper estimate of the extent of the dispersion of the gas phase which can be accounted for using the ADM. The extent of dispersion of tracers of different solubilities (insoluble helium used in gas tracer experiments and partially soluble oxygen used in mass transfer experiments) can be assumed to be equal since the extent of mixing of the gas phase is not affected by the physical properties of the gas phase as shown by Kantak et al. (1995) and Towell and Ackerman (1972).

- The axial dispersion coefficient of the liquid phase was estimated from correlations developed at similar operating conditions. A sensitivity analysis of the effect of the value of the estimated D_L has been performed and the estimated k_La values were found to be affected by less than 2% when increasing or decreasing the value of D_L by 100%. This indicates that the fitted k_La values using the ADM are not sensitive to the estimated D_L values under the operating conditions used in this study. Deckwer et al. (1983) reached the same conclusion and suggested that the three parameter optimization mass transfer problem can often be reduced to a two parameter problem by estimating the value of D_L from correlations given in literature. Although the model is insensitive to the variations of D_L, it is still advisable not to assume a perfect mixing pattern for the liquid since this will result in the misinterpretation of experimental data. For instance, assuming a plug flow model for liquid will misinterpret the concentration jump near the column inlet (entrance region) as an

increase in mass transfer where it is simply a result of liquid back-mixing. It should be noted that, under conditions when the extent of the gas phase mixing approaches complete back mixing, the mass transfer model becomes also insensitive to the value of D_g, however this is not the case since the gas tracer experiments in chapter 4 showed that the gas phase cannot be modeled as completely mixed.

The axial Dispersion Model: Two equations are required, one for the liquid and one for the gas phase:

$$\frac{\partial C_L}{\partial t} = D_L \frac{\partial^2 C_L}{\partial z^2} + \frac{k_L a}{\varepsilon_L}(HC_g - C_L) \tag{5.1}$$

$$\frac{\partial C_g}{\partial t} = D_g \frac{\partial^2 C_g}{\partial z^2} - \frac{U_g}{\varepsilon_g}\frac{\partial C_g}{\partial z} - \frac{k_L a}{\varepsilon_g}(HC_g - C_L) \tag{5.2}$$

Danckwerts boundary conditions are used for both the gas and liquid:

$$z = 0, \left.\frac{\partial C_L}{\partial z}\right|_{z=0} 0 \qquad \text{and} \qquad U_g C_{g,in} = U_g C_g\big|_{z=0} - D_g \left.\frac{\partial C_g}{\partial z}\right|_{z=0} \tag{5.3}$$

$$z = L, \left.\frac{\partial C_L}{\partial z}\right|_{z=L} 0 \qquad \text{and} \qquad \left.\frac{\partial C_g}{\partial z}\right|_{z=L} = 0 \tag{5.4}$$

The initial conditions are given as: t=0, $C_L = C_g = 0$.

The unknown k_La term was determined by a minimum squared error fit between $C_L(t,z)$ and the measured transient concentration of the tracer (dissolved oxygen) in the liquid phase. The overall gas holdup, ε_g, was measured by observing the bed expansion. The values of D_g were obtained experimentally at the same conditions using the gas tracer technique as shown in Chapter 4. The values of D_L were estimated from the correlation presented by Baird and Rice (1975) which was based on experimental data developed at similar conditions to this work. Figure 5.4 shows the fitting of the axial dispersion and PF-CSTR models to the experimental data. It is clear from the figure that the PF-CSTR model, commonly used by researchers, is inappropriate to represent the experimental data even close to the reactor inlet.

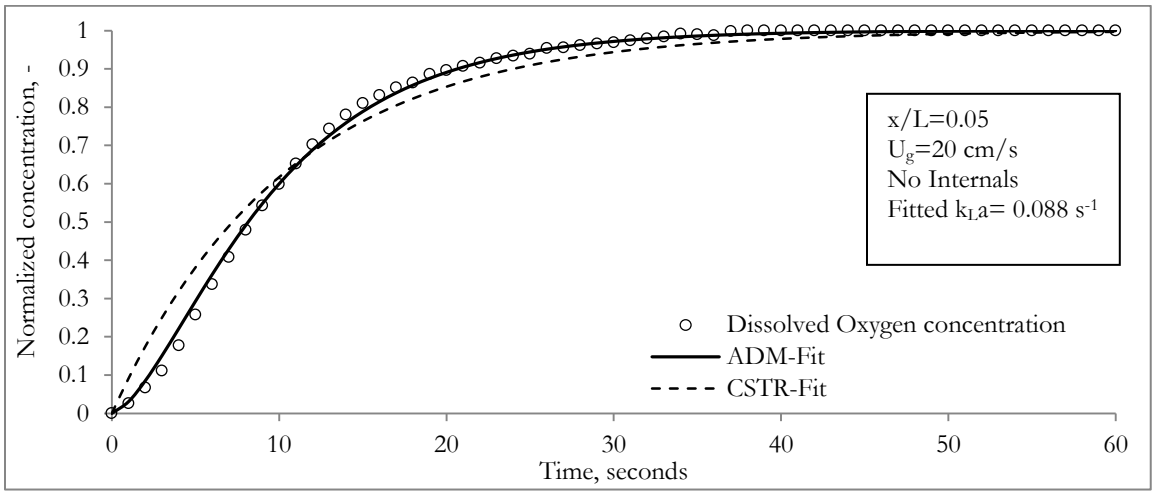

Figure 5.4 - Dissolved oxygen concentration fitted by the ADM and CSTR models

5.4 Results

5.4.1 The Effect of the Axial Position

The experimental conditions used to study the effect of internals on k_La at different axial positions are listed in Table 5.1. Figure 5.5 shows that the estimated k_La values are constant along the column height. These finding agree with those of Deckwer et al. (1983) and Han (2007) who showed that using the ADM, which correctly accounts for the superficial gas velocity, sampling position, and the extent of the gas phase mixing, the estimated values of k_La are independent of the axial position. This result is expected since all the key variables that control k_La including the bubble dynamics and the turbulent intensity are almost constant in the fully developed region of the column.

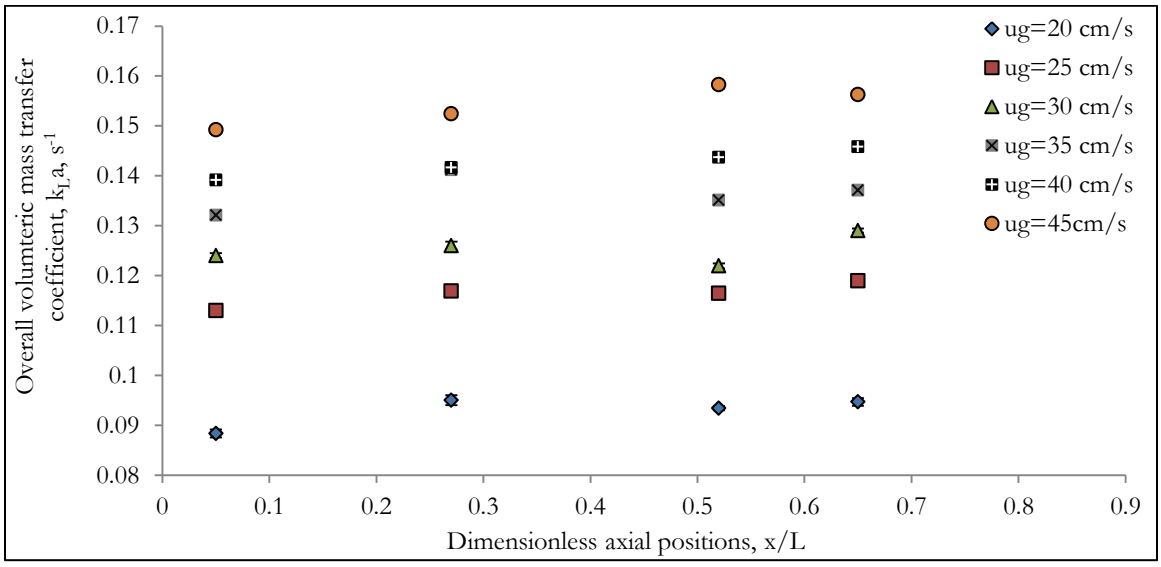

Figure 5.5 - The variation of k_La with the axial position

5.4.2 Effect of Superficial Gas Velocity and Internals on k_L and k_La

Figure 5.6 shows the effect of U_g on k_La measured at different axial positions. The increase in the superficial gas velocity was found to increase k_La, which is in line with the findings of almost all of the published mass transfer studies in bubble columns (e.g: Akita and Yoshida 1973, Deckwer et al., 1983, Letzel et al., 1999, Han, 2006, and Nedeltchev et al., 2010). The effect of U_g on the interfacial area and k_L values in the absence and presence of internals is shown in Figure 5.7. The interfacial area increases with the increase in the superficial gas velocity, while k_L was found to be insensitive to the changes in U_g. This suggests that the observed increase in k_La with the increase in U_g is merely due to the increase in the interfacial area.

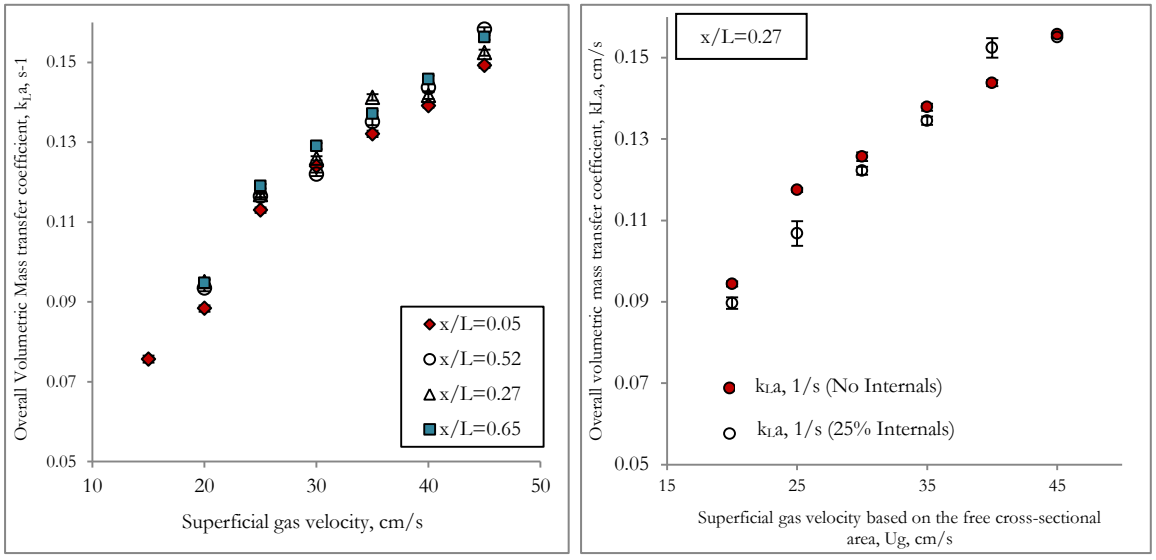

Figure 5.6 - Effect of superficial gas velocity based on the free cross-sectional area on the overall volumetric mass transfer coefficient at different axial locations

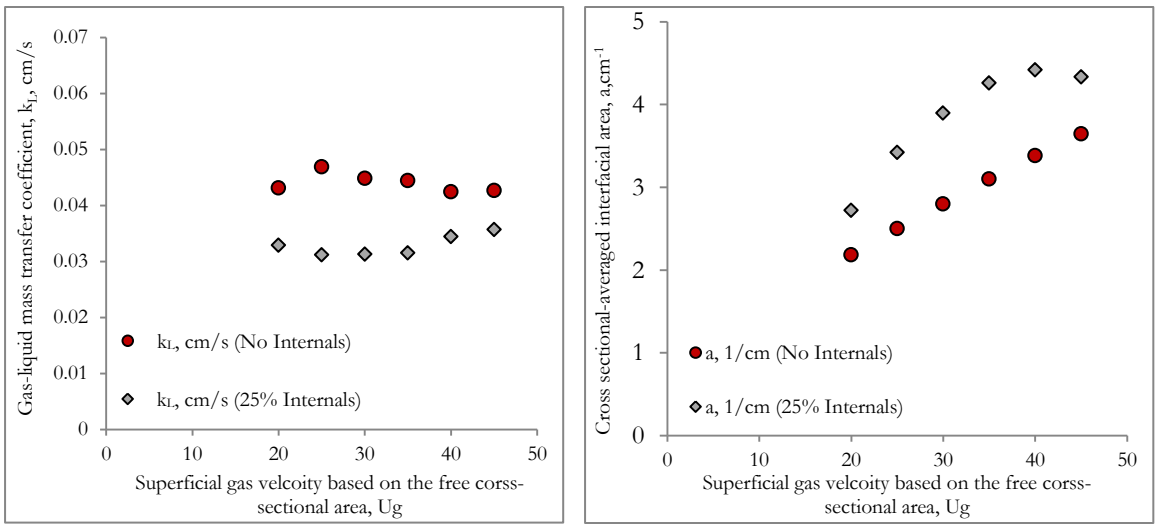

Figure 5.7 - Effect of superficial gas velocity and internals on k_L and interfacial area

The presence of internals did not affect k_La values as evident from Figure 5.6. Although the presence of internals is expected to increase k_La due to the increase in the interfacial area, this effect was balanced by the decrease in k_L in the presence of internals as seen in Figure 5.7. The next section discusses these results in the light of the developed fundamental theories for k_L.

5.5 Discussion

Over several decades, many approaches have been developed to predict the mas transfer coefficient (k_L). A brief survey of some of these approaches is given in Table 5.2. Generally, the developed theories assume one of two approaches:

1. **The penetration theory and its variants:** assume that the mass transfer process can be modeled as an unsteady state diffusion process at the gas-liquid interface. Thus, the rate of mass transfer is mainly related to the exposure time of bubbles to the liquid or the refreshment rate of liquid around the bubbles. The exposure time is the time span for surface renewal which can be approximated as the time needed for the bubble to move a distance equal to its own characteristic length scale:

   $$t_e = \frac{d_b}{u_b} \tag{5.5}$$

   where d_b is a characteristic bubble length scale and u_b is a characteristic bubble velocity scale. Based on this approach, the decrease in the exposure time or the increase in the surface renewal rate causes an increase in k_L. It is evident that, based on this formulation, k_L is largely dependent on the relationship between bubble size and its velocity which differs for various bubble shapes. Finally this approach does not consider the complete flow field in the vicinity of the bubble and hence it fails to explain the increase in k_L with increase in the bubble characteristic length scale due to the increase in the turbulence induced by larger bubbles.
2. **The turbulent theory:** assumes that the rate of mass transfer at the interface is mainly caused by the convective turbulent eddies. Hence, the rate of mass transfer becomes strongly affected by the turbulent intensity (mean fluctuating velocity) and the turbulent eddy sizes. On the other extreme, it is clear that this approach does not take into account the effect of the bubble size on the mass transfer rate.

Several other models were proposed to simulate k_L that were based on the combination of these two approaches (Toor and Marchello, 1958, Harriot, 1962, Bullin and Dukler, 1972,

Balasubraniyam, 1996, and Jajuee et al., 2006), however these models result in more hard-to-predict variables. In this section, the penetration and turbulent theories will be used for the analysis of our experimental data.

Table 5.2 - Developed mass transfer theories

Model or Theory	Description	Equation
Higbie (penetration) theory (Higbie, 1935)	Assumes unsteady state across the gas-liquid interface. The liquid is refreshed continuously and all the fluid elements have the same exposure times	$k_L = \sqrt{\frac{4D_m}{\pi t_e}}$
Danckwerts (Surface renewal) theory (Danckwerts, 1951)	Assumes unsteady state diffusion across the gas-liquid interface. The fluid elements can be randomly replaced by fresh ones	$k_L = \sqrt{4D_m S}$
Large-Eddy model (Fortescue and Pearson, 1967)	Large eddies dominate the mass transfer at the interfaces by the convective effect of turbulence	$k_L = 1.46\sqrt{\frac{D_m\sqrt{\overline{u^2}}}{\overline{l_{eddy}}}}$
Small-Eddy model (Lamont and Scott, 1970)	The mass transfer is mainly controlled by highly mobile small eddies	$k_L = 0.4\sqrt{\frac{D_m}{(\nu_m/\epsilon)^{0.5}}}$

The increase in k_La with increasing U_g was reported in almost all mass transfer studies in bubble columns. At low superficial gas velocities, the increase in the energy input and the consequent increase in the turbulent intensity cause the enhancement of k_L. In addition, the increase in the turbulent intensity increases the interfacial area due to the increased rate of bubble break-up. Hence, both factors contribute to the increase in k_La at low gas velocities. In this study, our results showed that at higher superficial gas velocities, k_L is unaffected by the increase in U_g in the presence and absence of internals. This may be due to the balance between the rates of coalescence and break-up at higher superficial gas velocities which leads to the stabilization of the average bubble size which mainly controls k_L. At these high superficial gas velocities, the increase in k_La is only due to the increase in the interfacial area caused by the generation of more bubbles at higher gas velocities. These findings concur with different researchers, who did their mass transfer experiments at high superficial gas velocities in bubble columns without internals, and were reflected by their correlations as shown in Figure 5.8.

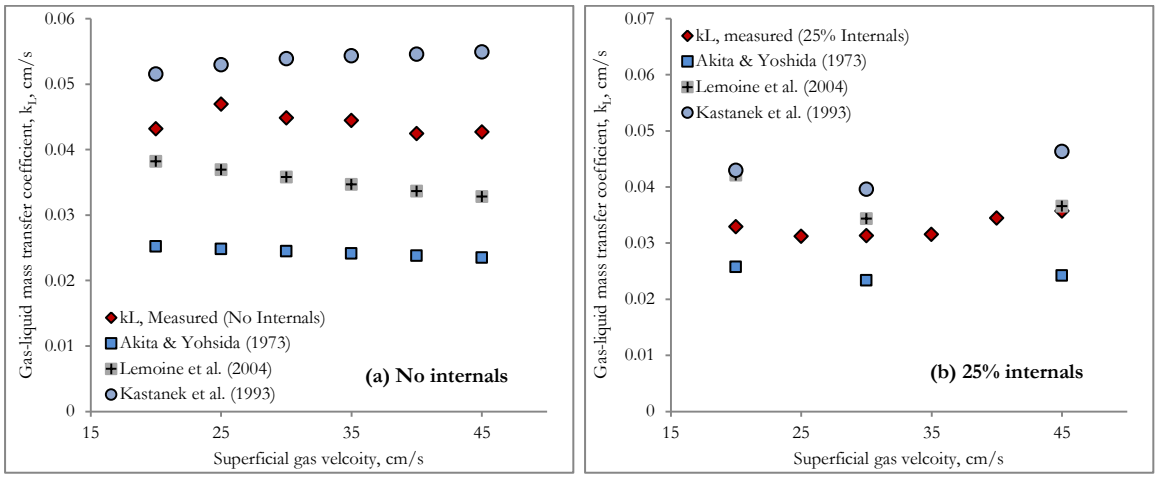

Figure 5.8 - Effect of the superficial gas velocity based on the free cross-sectional area on k_L: experimental data vs. correlations for (a) No internals and (b) with 25% internals

Figure 5.6 and 5.7 showed that the internals did not significantly affect k_La due to the balance between the increase in the interfacial area and the decrease in k_L in their presence. The increase in the interfacial area of bubbles in the presence of internals is caused by the enhancement of the rate of bubble break-up which leads to the formation of smaller bubbles that have high surface area. The decrease in the average bubble size coupled with the physical presence of internals leads to the decrease in the turbulent intensity of the liquid phase as shown by (Chen et al., 1999, Forret et al., 2003, and Larachi et al., 2006) which mainly caused the observed decrease in k_L in the presence of internals.

5.6 Remarks

This chapter investigated the effect of superficial gas velocity and internals on k_La and k_L in a pilot scale 18-inch column. The oxygen-enriched method was used to measure the concentration of the soluble oxygen tracer and the axial dispersion model was used to quantify the value of k_La in the presence and absence of internals at different axial positions. The data of the interfacial area available from the 4-point optical probe was used to estimate the values of k_L at different operating conditions.

The estimated k_La values were found to be independent on the axial and radial position when the axial dispersion model was used. The k_La values increased with increasing the superficial gas velocity in the presence and absence of internals based on the estimates of the ADM, while the k_L values were independent on the superficial gas velocities within the range used in this study. This suggests that the increase of k_La at higher superficial gas velocities may be merely due to the increase in the interfacial area. These findings qualitatively agree with the reported k_L correlations in the literature.

The presence of internals did not affect the values of k_La in spite of the increase in the interfacial area. This can be attributed to the fact that internals dampen the turbulence causing a decrease in the k_L values which consequently balances the increase in the interfacial area.

Chapter 6 – Summary of Findings and Recommendations

This work investigated the gas hydrodynamics, gas phase mixing, and mass transfer in bubble columns with and without internals. One of the distinct features of this work is that it utilized columns of different scales to assess the effect of column diameter in the presence of internals. In addition, two models were presented for the modeling of gas phase velocity and gas phase mixing in bubble columns with and without internals. Finally, this work presents a methodology by which the effect of different variables mixing and mass transfer can be studied in bubble columns. The essence of this methodology is to relate the macro-scale mixing and mass transfer phenomena to the local fluid dynamic parameters in both phases. This allows the prediction of the effect of different variables on the mixing and mass transfer characteristics in bubble columns if their effect on the local hydrodynamics is known. This section presents a summary of the findings of this work along with recommendations for future work in bubble columns with and without internals.

6.1 Gas Velocity Profiles

The effect of the occluded CSA by internals on the gas velocity profiles was investigated and quantified over a wide range of superficial gas velocities in lab-scale and pilot-scale bubble columns in the presence and absence of internals using the 4-point optical probe. The increase in the superficial gas velocity was found to increase the steepness of the gas velocity profile (increase in the center-line gas velocity and a decrease in the near-wall gas velocity) and an enhancement of the gas circulation. This result is in agreement with the earlier work of Xue (2004). The same trend was observed in the presence of internals in the 8-inch and the 18-inch bubble columns. The presence of internals caused an increase in the center-line gas velocity due to the dampening of turbulence caused by their presence. The increase in

the column diameter enhanced the gas circulation significantly due to the increase in turbulence in larger columns.

The experimental data generated in this work was used to validate the 1-D gas velocity model develop by Gupta (2002). The model simulations indicated that the mixing length correlations were able to better predict the gas velocity profile, where Kumar's mixing length was found to be the best mixing length correlation to fit the gas velocity profile data in this study. The gas velocity model was capable of simulating the gas velocity profile under different operating conditions and different column diameters in the presence and absence of internals provided that the dampening of turbulence in the presence of internals is accounted for.

It should be emphasized that the 1-D gas velocity model used in this study, is not fully predictive since the gas holdup profile is still used as an input to the model. Although some empirical correlations have been developed to predict the radial gas holdup profile in bubble columns (Wu et al., 2001), the extrapolation of these correlations to a wide range of conditions is still questionable. Notably, the radial gas holdup profile remains the most difficult hydrodynamic parameter to predict and the main obstacle in closing the modeling dilemma. If one takes a close look at the different phenomenological and compartmental models developed by various workers in the field, it can be realized that these models have a good potential to confidently scale up bubble columns (Wilkinson, 1991, Degaleesan 1997, Gupta et al., 2001, and Gupta 2002); however they all require the gas holdup profile as an input. As a result, it is recommended that more research should be directed to address this issue and develop models that predict the radial gas holdup profile in bubble columns. In view of the available approaches to predict the radial gas holdup profile, the solution of the 1-D radial force balance on the gas phase seems to be the most practical one. The radial force equation will typically include the balance between the lift (due to the presence of bubble in a shear flow field), Magnus (due to bubble rotation), turbulent dispersion (due to bubble diffusion), and wall lubrication forces on the gas phase. This equation has to be

coupled with the gas and liquid momentum equations and solved simultaneously for the gas holdup, gas velocity, and liquid velocity profiles.

6.2 Gas Phase Mixing

The axial gas phase mixing was measured using a gas tracer technique and analyzed using 1-D and 2-D mixing models. The effects of the superficial gas velocity, internals, and column diameter were investigated. The axial gas mixing was found to significantly decrease in the presence of internals due to the decrease in the turbulent intensity caused by their presence. The increase in column diameter enhanced the axial gas mixing due to the increase in gas circulation and turbulent dispersion in larger columns.

The 2-D model was used to estimate the axial and radial turbulent diffusivities in the gas phase, which were shown to qualitatively match the turbulent dispersion diffusivities in the liquid phase. The model developed by Degaleesan and Dudukovic (1998) was coupled with the fitted values of the axial and radial diffusivities to determine the dominant gas mixing mechanism. It was shown that under the operating conditions used in this study, the gas mixing is mainly controlled by turbulent dispersion, and hence, any effect that leads to the dampening of turbulence will lead to the decrease in the axial mixing. This finding can also be used to explain the effect of pressure and solids loading (Han 2007) on the axial gas phase mixing.

Although this work presented a detailed description of the mechanism of gas phase mixing in bubble columns, more research is needed to enhance this understanding at different operating conditions. This requires the implementation of novel experimental techniques to measure the gas concentration locally. The absence of axial and radial gas concentration data hinders our ability to estimate the local turbulent parameters of the gas phase. Such techniques can be coupled with a 2-D model, similar to the one used in this study, to achieve more confident estimation of the axial and radial profiles of D_{zz} and D_{rr}. In addition, these

techniques will help us to understand how the relative magnitudes of different mixing mechanisms change with the column height. This can lead to a better prediction of the developing axial profile of the lumped axial gas dispersion coefficient.

6.3 Mass Transfer

The volumetric gas-liquid mass transfer coefficient, k_La and the gas-liquid mass transfer, k_L, of oxygen were measured in a pilot-scale bubble column in the absence and presence of internals using the oxygen-enriched technique. The increase in k_La with increasing the superficial gas velocity at the high gas velocities used in this study may be attributed to the increase in the interfacial area at higher gas velocities. The presence of internals did not affect k_La significantly due to the balance between the increase in the interfacial area on the one hand, and the decrease in k_L on the other hand. The decrease in k_L was due to the decrease in the turbulent intensity in the presence of internals, while the increase in the interfacial area was due to enhancement of the rate of bubble break-up in their presence.

The key finding of internals and column diameter obtained in this study are summarized in table 6.1.

Table 6.1 - Effects of key variables studied in this work

Variable	Effect	Supporting data
↑ U_g (In the presence and absence of internals)	↑ Overall ε_g ↑ Gas circulation ↑ D_g ↑ D_{zz} of gas phase ↑ D_{rr} of gas phase ↑ k_La ↑ Interfacial area Insignificant effect on k_L	Figure 4.6 Figure 3.2 Figures 4.7 & 4.8 Figures 4.11 & 4.12 Figures 4.11 & 4.12 Figure 5.7 Figure 5.8 Figure 5.8
↑ Column diameter (D) (At any given U_g and % occluded CSA by internals)	↑ Overall ε_g ↑ Gas circulation ↑ D_g ↑ D_{zz} of gas phase ↑ D_{rr} of gas phase	Figure 4.6 Figure 3.4 Figure 4.8 Figure 4.11 Figure 4.11

Presence of internals (For any given U_g and D)	↑ Overall ε_g	Figure 4.6
	↑ Center-line gas velocity	Figure 3.3
	↓ D_g	Figure 4.7
	↓on D_{zz} of gas phase	Figure 4.10
	↓ D_{rr} of gas phase	Figure 4.10
	Insignifanct effect on k_La	Figure 5.7
	↑ Interfacial area	Figure 5.8
	↑ Interfacial area	Figure 5.8
	↓k_L	Figure 5.8

6.4 Internals

In this work, only the effect of the occluded CSA by internals was studied. It was assumed that this is the most important parameter that can simulate the effect of internals. The effect of other parameters that are considered in the design of internals as discussed in Chapter 1 should be studied at constant occluded CSA by internals. This includes the effect of tube diameter and tube configurations. In addition, the study of different shapes of vertical internals such as the U-shaped vertical internals and internals that are totally immersed in the liquid is of great interest to the industry. Finally, the validation of these finding in mimicked process conditions is important to assess the effect of pressure, solids loading, and the physical properties of different phases.

Appendix A – Effect of Gas Tracer Solubility on the RTD of the Gas Phase

A mass balance on a tracer species in the gas phase and in the liquid phase of a bubble column are, respectively, described by the axial dispersion model yields:

$$\frac{dC_g}{dt} = D_g \frac{d^2C_g}{dz^2} - \frac{u_g}{\varepsilon_g}\frac{dC_g}{dz} - \frac{k_l a}{\varepsilon_g}\left(\frac{C_g}{H} - C_L\right) \tag{A.1}$$

$$\frac{dC_L}{dt} = D_L \frac{d^2C_L}{dz^2} + \frac{k_l a}{(1-\varepsilon_g)}\left(\frac{C_g}{H} - C_L\right) \tag{A.2}$$

with initial conditions: t = 0, $c_g = 0$, $c_L = 0$ and boundary conditions:

$$z = 0: C_g - C_{in} = \frac{D_g}{u_g}\frac{\partial C_g}{\partial z}, and\ \frac{\partial C_L}{\partial z} = 0 \tag{A.3}$$

$$z = L: \frac{\partial C_g}{\partial z} = 0, and\ \frac{\partial C_L}{\partial z} = 0\ . \tag{A.4}$$

Using the above equations, simulations were run at typical experimental conditions used in this study at different values of Henry's constant. Figure A1 shows the effect of the tracer gas solubility (Henry's constant) on the residence time distribution of the gas phase at the column exit. At Henry's solubility values greater than 50, the effect of overall volumetric gas-liquid mass transfer is negligibly small at the experimental conditions of the current study as shown in Figure A.1. Therefore, since the Henry's solubility constant of Helium at 298 K is 110 (Green and Perry 2008), the interface term can be omitted in the gas tracer experiments. The solubility of the oxygen tracer used in the mass transfer experiments at 298 K is 32 (Green and Perry 2008), indicating that the mass transfer term cannot be neglected.

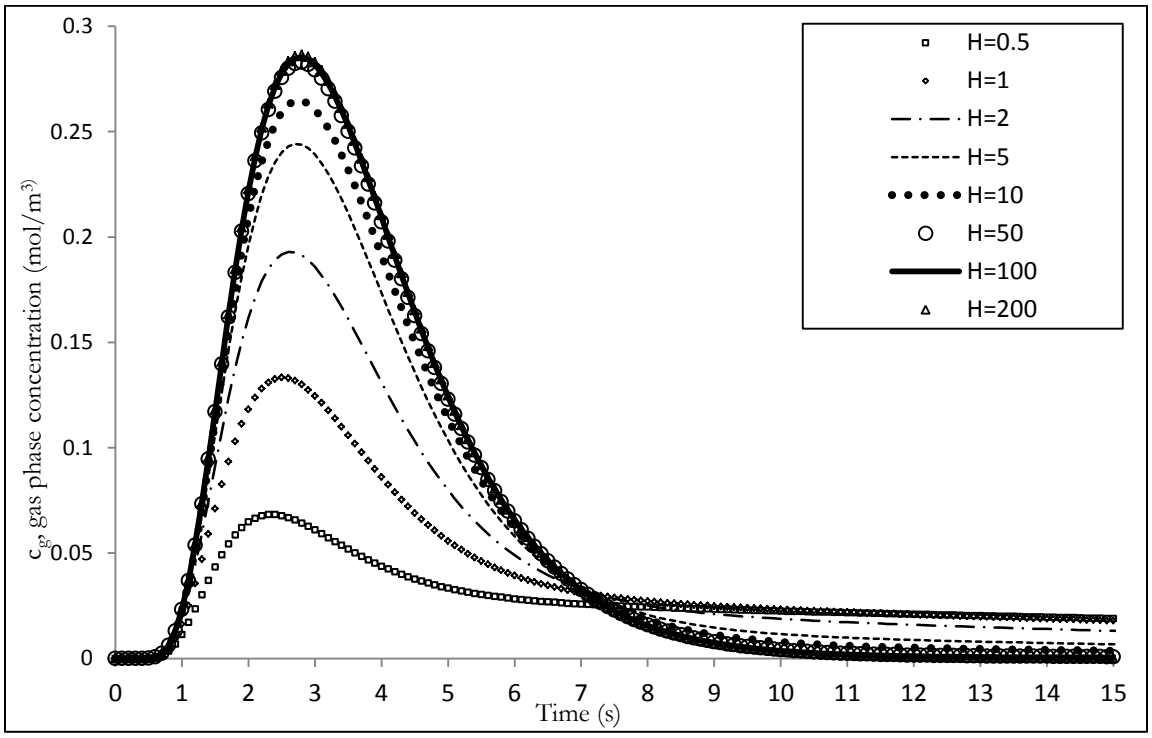

Figure A.1 - Effect of gas tracer solubility on the gas tracer concentration at the outlet

References

Akita, K. and Yoshida, F., 1973. Gas holdup and volumetric mass transfer coefficient in bubble columns: Effects of liquid properties, Industrial & Engineering Chemistry Process Design and Development, 12 (1), 76-80.

Alper, E., 1979. Measurement of effective interfacial area in a packed-column absorber by chemical methods, Trans. Instn. Chem. Engrs., 57, 64.

Alvare, J. and Al-Dahhan, M. H., 2006. Gas Holdup in Trayed Bubble Column Reactors, Industrial & Engineering Chemistry Research, 45(9), 3320-3326.

Baird, M. I. and Rice, R. G., 1975. Axial dispersion in large un-baffled columns, Chemical Engineering Journal, 9, 171-174.

Balasubraniyam, J., 1996. Transport Phenomena at the Interface, M.Sc. Thesis, Mumbai University, India.

Bandyopadhyay, B., Humphrey, A. E., Taguchi, H., 1967. Dynamic measurement of the volumetric oxygen transfer coefficient in fermentation systems. Biotechnology and Bioengineering, 9 (4), 533-544.

Bartholomew, W. H., Karow, E. O., Sfat, M. R., Wilhelm, R. H., 1950. Oxygen transfer and agitation in submerged fermentations: Mass transfer of oxygen in submerged fermentation by Streptomyces griseus, Journal of Industrial and Engineering Chemistry, 42, 1801-1809.

Behkish, A., 2004. Hydrodynamic and mass transfer parameters in large-scale slurry bubble column reactors, Ph.D. Thesis, University of Pittsburgh, Pittsburgh, Pa, USA.

Bernemann, K., 1989. On the hydrodynamics and mixing of the liquid phase in bubble columns with longitudinal tube bundles, Ph.D. Thesis, University of Dortmund, Germany.

Bullin, J. A. and Dukler, A. E., 1972. Random Eddy Models for Surface Renewal: Formulation as a Stochastic Process, Chem. Eng. Sci., 27 (2), 439-442.

Calderbank, P. H. and Moo-Young, M. B., 1961. Continuous phase heat and mass transfer properties of dispersions, Chemical Engineering Science, 16 39-54.

Carleton, J., Flain, R., and Valentin, F., 1976. Some properties of packed bubble column, Chemical Engineering Science, 22, 1839-1845.

Carra, S. and Morbidelli, M., 1987. Gas-liquid reactors, Chemical Industries, 26, 545.

Chang, H. N., Halard, B., and Moo-Young, M., 1989. Measurement of KLa by a gassing-in method with oxygen-enriched air, Biotechnology and Bioengineering, 34 (9), 1147- 1157.

Chen, J., Li, F., Degaleesan, S., Gupta, P., Al-Dahhan, M. H., Dudukovic, M. P. and Toseland, B. A., 1999. Fluid Dynamic Parameters in Bubble Columns with Internals, Chemical Engineering Science, 54 (13-14), 2187-2197.

Clark, N. N., Atkinson, C. M., and Flemmer, R. C., 1987. Turbulent circulation in bubble columns, American Institute of Chemical Engineers Journal, 33(3), 515–518.

Comte, A., Kohls, O., and Scheper, T., 1995. Fiber optical chemosensors and biosensors, CLB Chemie in Labor und Biotechnik, 46 (1), 18-22.

Cui, Z., 2005. Hydrodynamics in a bubble column at elevated pressures and turbulence energy distribution in bubbling gas-liquid and gas-liquid-solid flow systems, M.Sc. Thesis, The Ohio State University, Columbus, OH, USA.

Danckwerts, P. V., 1951. Significance of Liquid-Film Coefficients in Gas Absorption, Ind. Eng. Chem., 43, 1460.

Danckwerts, P. V., 1970. Gas–Liquid Reaction, New York: McGraw-Hill, 239–50.

Deckwer, W. D., Bubble Column Reactors, John Wiley & Sons, 1992.

Deckwer, W. D., 1976, Non-isobaric bubble columns with variable gas velocity, Chemical Engineering Science, 31, 309-317.

Deckwer, W. D., Burckhart, R., and Zoll, G., 1974. Mixing and mass transfer in tall bubble columns, Chemical Engineering Science, 29 (11), 2177-2188.

Deckwer, W. D., Nguyen-Tien, K., Kelkar, B. G., and Shah, Y. T., 1983. Applicability of axial dispersion model to analyze mass-transfer measurements in bubble columns, AIChE Journal, 29 (6), 915-922.

Deen, N., G., Hjertager, B., H. and Solberg, T., 2000. Comparison of PIV and LDA measurements methods applied to the gas-liquid flow in bubble columns, 10th international symposium on applications of laser techniques to fluid mechanics, Lisbon, Portugal.

Deen, N. G., Solberg, T., and Hjertager, B. H., 2001. Large eddy simulation of the Gas–Liquid flow in a square cross-sectioned bubble column, Chemical Engineering Science, 56, 6341–6349.

Degaleesan, S., 1997. Turbulence and Liquid Mixing in Bubble Columns, D.Sc. Thesis, Washington University in St. Louis, Saint Louis, Missouri, USA.

Degaleesan, S. and Duduković, M. P., 1998. Liquid back-mixing in bubble columns and the axial dispersion coefficient, AIChE Journal, 44, 2369–2378.

Delnoij, E., Lammers, F. A., Kuipers, J. M. and van Swaaij, W. M., 1997. Dynamic Simulation of Dispersed Gas-Liquid Two-Phase Flow Using a Discrete Bubble Model, Chern. Eng. Sci., 52, 1429-1458.

Devanathan, N., 1991. Investigation of Liquid Hydrodynamics in Bubble Columns via a Computer Automated Radioactive Particle Tracking (CARPT) Facility, D.Sc. Thesis, Washington University in St. Louis, Saint Louis, Mo, USA.

Drew, D. A. and Passman, S. L., 1998. Theory of Multicomponent Fluids, Springer, New York.

Duduković, M. P., 2007. Relevance of Multiphase Reaction Engineering to Modern Technological Challenges, Ind. Eng. Chem. Res., 46(25), 8674–8686.

Fair, J. R., Lambright, A. J., and Anderson, J. W., 1962. Heat transfer and gas holdup in a sparged contactor. I & EC Process Design and Development, 1, 33-36.

Fan, L. S., 1989. Gas-Liquid-Solid Fluidization Engineering, Butterworth Series in Chemical Engineering, Boston, MA.

Field, R. W. and Davidson, J. F., 1980. Axial dispersion in bubble columns, Transactions of the Institution of Chemical Engineers, 58 (4), 228-236.

Forret, A., Schweitzer, J. M., Gauthier, T., Krishna, R. and Schweich, D., 2003. Liquid dispersion in large diameter bubble columns with and without internals, The Canadian Journal of Chemical Engineering, 81, 360–366.

Fortescue, G. E. and Pearson, J. A., 1967. On gas absorption into a turbulent liquid, Chem. Eng. Sci., 22, 1163-1176.

Franz, K., Borner, T., Kantorek, H. J., and Buchholz, R., 1984. Flow structures in bubble columns, German Chemical Engineering, 7, 365-374.

Garnier, C., Lance, M., and Marié, J.L., 2001. Measurements of local flow characteristics in buoyancy-driven bubbly flow at high void fraction. Proceedings of the Fourth International Conference on Multiphase Flow, New Orleans, LA, USA, May 27–June 1.

Geary, N. W. and Rice, R. G., 1992. Circulation and Scale-up in Bubble Columns, AIChE J., 38(1), 76-81.

Grienberger, J. and Hoffman, H., 1992. Investigations and Modeling of Bubble Columns, Chem. Eng. Sci., 47(9-11), 2215-2220.

Gupta, P., 2002. Churn-turbulent bubble columns - experiments and modeling, D.Sc. Thesis, Washington University in St. Louis, Saint Louis, Mo, USA.

Han, L., 2007. Hydrodynamics, back-mixing, and mass transfer in a slurry bubble column reactor for Fischer-Tropsch alternative fuels, D.Sc. Thesis, Washington University in St. Louis, Saint Louis, Mo, USA.

Han, L. and Al-Dahhan, M.H., 2007. Gas-liquid mass transfer in a high pressure bubble column reactor with different sparger designs, Chemical Engineering Science, 62 (1-2), 131-139.

Harriot, P., 1962. A Random Eddy Modification of the Penetration Theory, Chem. Eng. Sci., 17, 149-154.

Hawthorne W. H., Ibsen M. D., Pedersen P. S., and Bohn M. S., 2006. Fischer-Tropsch slurry reactor cooling arrangement, US Patent 7,108,835.

Herbolzheimer, E., and Iglesia, E., 1994. Slurry bubble column, U.S. Patent 5348982.

Higbie, R., 1935. The Rate of Absorption of a Pure Gas into a Still Liquid During Short Period of Exposure, Trans. Am. Inst. Chem. Eng., 31, 365-389.

Hinze, J. O., 1975. Turbulence. McGraw-Hill, New York.

Hyndman, C. and Guy, C., 1995. Gas phase hydrodynamics in bubble columns, Chemical Engineering Research and Design, 73, 426-434.

Ishii, M., 1975. Thermo-Fluid dynamic theory of two phase flows, Eyrolles, Paris, 142-201.

Jajuee, B., Margaritis, A., Karamanev, D., and Bergougnou, M. A., 2006. Application of Surface-Renewal-Stretch Model for Interface Mass Transfer, Chem. Eng. Sci, 61, 3917-3929.

Jakobsen, H. A., Lindborg, H., and Dorao, C. A., 2005. Modeling of bubble column reactors: Progress and Limitations, Ind. Eng. Chem. Res., 44, 5107-5151.

Joseph, S., Shah, Y. T., and Kelkar, B. G., 1984. A simple experimental technique to measure gas phase dispersion in bubble columns, Chemical Engineering Communications, 28 (4-6), 223-230.

Joshi, J. B., 1982. Gas phase dispersion in bubble columns, Chemical Engineering Journal (Amsterdam, Netherlands), 24 (2), 213-216.

Kantak, M. V., Hesketh, R. P. and Kelkar, B. G., 1995. Effect of gas and liquid properties on gas phase dispersion in bubble columns, Chemical Engineering Journal (Lausanne), 59 (2), 91-100.

Kaštánek, F., Zahradnik, J., Kratochvil, J., and Cermak, J., 1993. Chemical reactors for gas liquid systems, New York, Ellis Horwood.

Kawagoe, M., Otake, T., and Robinson, C., W. 1989. Gas-phase mixing in bubble columns, Journal of Chemical Engineering Japan, 136-142.

Kawasaki, H., Hirano, H., and Tanaka, H., 1994. Effects of multiple draft tubes with perforated plates on gas holdup and volumetric mass transfer coefficient in a bubble column, Journal of Chemical Engineering of Japan, 27(5), 669-670.

Kawase, Y., Halard, B., and Moo-Young, M., 1987. Theoretical prediction of volumetric mass transfer coefficients in bubble columns for Newtonian and non-Newtonian fluids, Chemical Engineering Science, 42 (7), 1609-1617.

Kawase, Y. and Moo-Young, M., 1989. Turbulence Intensity in Bubble Columns, Chem. Eng. J., 40 (1), 55-58.

Korte, H., 1987. Heat transfer in bubble columns with and without internals, Ph.D. Thesis, University of Dortmund, Germany.

Krishna, R., van Baten, J. M. and Urseanu, M. I., 2000. Three-phase Eulerian simulations of bubble column reactors operating in the churn-turbulent regime: a scale up strategy, Chern. Eng. Sci., 55, 3275-3286.

Kulkarni, A. and Shah, Y. T., 1984. Gas phase dispersion in a down-flow bubble column, Chemical Engineering Communications, 28 (4-6), 311-326.

Kumar, S. B., 1994. Computed tomographic measurements of void fraction and modeling of the flow in bubble columns, Ph.D. Thesis, Florida Atlantic University.

Lamont, J. C. and Scott, D. S., 1970. An Eddy Cell Model of Mass Transfer into the Surface of a Turbulent Liquid, AIChE J., 16, 513-519.

Lapin, A. and Lubbert, A., 1994. Numerical simulation of the dynamics of two-phase gas-liquid flows in bubble columns, Chern. Engng. Sci., 49, 3661-3674.

Larachi, F., Desvigne, D., Donnat, L., and Schweich, D., 2006. Simulating the effects of liquid circulation in bubble columns with internals, Chemical Engineering Science, 61(13), 4195-4206.

Larue de Tournemine, A., Roig, V., Suzanne, C., 2001. Experimental study of the turbulence in bubbly flows at high void fraction. Proceedings of the Fourth International Conference on Multiphase Flow, New Orleans, LA, USA, May 27–June 1.

Lau, R., Peng, W., Velazquez-Vargas, L. G., Yang, G. Q., and Fan, L. S., 2004. Gas-Liquid Mass Transfer in High-Pressure Bubble Columns, Industrial & Engineering Chemistry Research, 43 (5), 1302-1311.

Lefevbre, S., Chaouki, J., and Guy, C., 2004. Phase Modeling in Multiphase Reactors Containing Gas Bubble: a Review, International Journal of Chemical Reactor Engineering, 2, R2.

Letzel, H. M., Schouten, J. C., Krishna, R., and Van den Bleek, C. M., 1999. Gas holdup and mass transfer in bubble column reactors operated at elevated pressure, Chemical Engineering Science, 54 (13-14), 2237-2246.

Lehman, J. and Hammer, J., 1978. Continuous fermentation in tower fermentor I. European congress on biotechnology, Interlaken, Part 1, 1.

Levenspiel, O., 1972. Chemical reaction engineering, New York, Wiley Eastern Press.

Levenspiel, O. and Fitzgerald, T., J., 1983. A warning in the misuse of the dispersion model, Chem Engng. Sci., 38, 489-491.

Linek, V., Sinkule, J., and Benes, P., 1991. Critical assessment of gassing-in methods for measuring kLa in fermenters, Biotechnology and Bioengineering, 38 (4), 323-330.

Luo, H. and Svendsen, H. F., 1991. Turbulent circulation in bubble columns from eddy viscosity distributions of single-phase pipe flow, Canadian Journal of Chemical Engineering, 69(6), 1389-1394.

Mashelkar, R. A. and Sharma, M. M., 1970. Mass transfer in bubble and packed bubble columns, Transactions of the Institution of Chemical Engineers, 48(4-6), 162-172.

Mangartz, K. H. and Pilhofer, T., 1981. Interpretation of mass transfer measurements in bubble columns considering dispersion of both phases, Chemical Engineering Science, 36 (6), 1069-1077.

Miyauchi, T. and Shyu, C. N., 1970. Flow of fluid in gas bubble columns, Kagaku Kogaku, 34, 958-964.

Miyauchi, T., Furusaki, S., Morooka, S., and Ikeda, Y., 1981. Transport Phenomena and Reaction in Fluidized Catalysts Beds, Advances in Chemical Engineering, 11, 275-448.

Modak, S., Juvekar, V., and Rane, V., 1993. Dynamics of the gas phase in bubble columns, Chemical Engineering & Technology, 16, 303-306.

Molerus, O. and M. Kurtin, 1986. Modeling of residence time distributions of the gas phase in bubble columns in the liquid circulation regime, Chemical Engineering Science, 41, 2693-2698.

Motarjemi, M. J. and Jameison G. J., 1978. Mass transfer from very small bubbles: the optimum bubble size for aeration, Chem. Eng. Sci., 33, 1415-1423.

Myers, K. J., Dudukovic, M. P. and Ramachandran, P. A., 1987. Modeling churn turbulent bubble columns-I, Liquid-phase mixing, Chemical Engineering Science, 42 (10), 2301-2311.

Nedeltchev, S., Jordan, U., and Schumpe, A., 2010. Semi-theoretical prediction of volumetric mass transfer coefficients in bubble columns with organic liquids at ambient and elevated temperatures, The Canadian Journal of Chemical Engineering, 88, 523–532.

Nosier, S. A., 2003. Solid-liquid mass transfer at gas sparged tube bundles, Chemical Engineering & Technology, 26(11), 1151-1154.

Ong, B. C., 2003. Experimental Investigation of Bubble Column Hydrodynamics: Effect of Elevated Pressure and Superficial Gas Velocity, D.Sc. Thesis, Washington University in St. Louis, Saint Louis, Mo, USA.

Palaskar, S. N., De, J. K., Pandit, A. B., 2000. Liquid phase RTD studies in sectionalized bubble column, Chemical Engineering & Technology, 23(1), 61-69.

Patel, S. A., Daly, J. G., and Bukur, D.B., 1989. Holdup and Interfacial Area Measurements Using Dynamic Gas Disengagement, AIChE Journal, 35, 931-942.

Perry, R. and Green, W., 2008. Perry's Chemical Engineer's Handbook, Mc-Graw Hill.

Pilhofer, T., Bach, H. F., Mangartz, K. H., 1978. Determination of fluid dynamic parameters in bubble column design. ACS Symposium Series, 65 372-383.

Pradhan, A., Parichia, and De, P., 1993. Gas hold-up in non-Newtonian solutions in a bubble column with internals, The Canadian journal of chemical engineering, 71, 468-471.

Qi, S. and Shuli, W., 2008. Measurement of turbulent of gas-liquid two-phase flow in a bubble column with a laser velocity meter, Advances in Natural Science, 1, 89-96.

Rados, N., 2003. Slurry bubble column hydrodynamics: experimentation and modeling, D.Sc. thesis, Washington University in St. Louis, Saint Louis, Mo, USA.

Rice, R. G. and Geary, N. W., 1990. Prediction of liquid recirculation in viscous bubble columns, AIChE Journal, 36, 1339-1348.

Riquarts, H. P., Strömungsmechanische, Impulsaustausch und Durchmischung der Flüssigen Phase in Blasensäulen, Chem. Ing. Tech., 53, 60-61 (1981).

Roy, S., Parichha, R. K., Ray, P., and Barman, B., 1989. Gas hold-up in bubble columns with immersed tubes, Proceedings of the Indian Chemical Engineering Congress 1, 72-77.

Schlichting, H., 1979. Boundary Layer Theory, McGraw Hill, New York, 602-609.

Schlüter, S., Steiff, A., and Weinspach, P. M., 1995. Heat transfer in two- and three-phase bubble column reactors with internals, Chemical Engineering and Processing, 34(3), 157-172.

Seinfeld, J., H., 1986. Atmospheric chemistry and physics of air pollution, Wiley publications, New York.

Sekizawa, T., Kubota, H., and Chung, W. C., 1983. Apparent Slip Velocity with Recirculating Turbulent Flow in Bubble Columns, J. Chem. Eng. Japan, 16 (4), 327-330.

Shah, Y. T., S. Joseph, D. N. Smith and A. J. Ruether, 1985. Two-bubble class model for churn-turbulent bubble-column reactors, Industrial and Engineering Chemistry, Process Design and Development, Vol. 24, 1096-1104.

Shetty, S. A., Kantak, M. V. and Kelkar, B. G., 1992. Gas-phase back-mixing in bubble column reactors, AIChE Journal, 38 (7), 1013-1026.

Sokolichin, A. and G., Eigenberger, 1994. Gas-Liquid Flow in Bubble Columns and Loop Reactors: Part 1. Detailed Modeling Numerical Simulation, Chern. Eng. Sci., 24, 5735-5746.

Sokolichin, A., Eigenberger, G., Lapin, A. and Lubbert, A., 1997. Dynamic numerical simulation of gas–liquid two-phase flows: Euler-Euler versus Euler-Lagrange, Chemical Engineering Science, 52(4), 611–626.

Steiff, A. and Weinspach, P. M., 1987. Heat transfer in stirred and non-stirred gas liquid reactors, Ger Chem Eng, 150.

Stern, D., Bell, A. T., and Heinemann, H., 1983. Effects of mass transfer on the performance of slurry reactors used for Fischer-Tropsch synthesis, Chemical Engineering Science, 38 (4), 597-605.

Rafique, M., Chen, P., and Dudukovic, M. P., 2004. Computational, Modeling of Gas-Liquid Flow in Bubble Columns, Rev. Chem. Eng., 20, 225-375.

Tennekes, H. and Lumely, J. L., 1972. A first course in turbulence., The MIT press, Cambridge.

Tomiyama, A., Kataoka, I. and Sakaguchi, T., 1995. Drag Coefficients of Bubbles (1st report, Drag Coefficients of a Single Bubble in a Stagnant Liquid), Trans. JSME Part B, 61(587), 2357-2364.

Toor, H. L. and Marchello, I. M., 1958. Film-penetration Model for Mass and Heat Transfer, AIChE J., 4, 97.

Towell, G. D. and Ackermann, G. H., 1972. Axial mixing of liquid and gas in large bubble reactors, Proc. 5th European-2nd International Symposium on Chemical Reaction Engineering, Amsterdam.

Ueyama, K. and Miyauchi, T., 1979. Properties of recirculating turbulent two-phase flow in gas bubble columns, AIChE J., 25, 258.

van Vuuren, D. S. and Heydenrych, M. D., 1985. Multicomponent modeling of Fischer-Tropsch slurry reactors, Chemical Engineering Research Group (CSIR) Report CENG 581. Pretoria, South Africa.

Vandu, C. O. and Krishna, R., 2003. Gas holdup and volumetric mass transfer coefficient in a slurry bubble column, Chemical Engineering & Technology, 26 (7), 779-782.

Wachi, S. and Nojima, Y., 1990. Gas-phase dispersion in bubble columns, Chemical Engineering Science, 45 (4), 901-905.

Wender, I., 1996. Reactions of Synthesis Gas, Fuel Processing Technology, 48, 189.

Westerterp, K. R., van Swaaij, W. P., and Beenackers, A. A., 1987. Chemical reactor design and operation, Chicester: Wiley.

Wilkinson, P. M., 1991. Physical aspects and scale-up of high pressure bubble columns, Ph.D. Thesis, University of Groningen, Rijksuniversiteit Groningen, the Netherlands.

Wu, C., 2007. Heat Transfer and Bubble Dynamics in Slurry Bubble Columns for Fischer-Tropsch Clean Alternative Energy, Ph.D. Thesis, Washington University in St. Louis, Saint Louis, Mo, USA.

Wu, Y., Ong, B., and Al-Dahhan, M. H., 2001. Predictions of Radial Gas Holdup Profiles in Bubble Column Reactors, Chemical Engineering Science, 1207-1210.

Xue, J., 2004. Bubble velocity, size and interfacial area measurements in bubble columns, D.Sc. Thesis, Washington University in St. Louis, Saint Louis, Mo, USA.

Yamashita F., 1987. Effects of vertical pipe and rod internals on gas .g holdup in bubble columns, Journal of Chemical Engineering of Japan, 20(2), 204-206.

Youssef, A. A. and Al-Dahhan, M. H., 2009. Impact of Internals on the Gas Holdup and Bubble Properties of a Bubble Column, Industrial & Engineering Chemistry Research, 48(17), 8007-8013.

Youssef, A. A., 2010. Fluid Dynamics and Bubble Columns with Internals, Ph.D. Thesis, Washington University in St. Louis, Saint Louis, Mo, USA.